FLUORESCENCE LIFETIMES OF FREE AND INTRACELLULAR FLUORESCEIN AS MEASURED AT THE CELLULAR LEVEL IN SACCHAROMYCES CEREVISIAE

by

Steven Joseph Page

B.S., Southwest Missouri State College, 1972

A MASTER'S THESIS

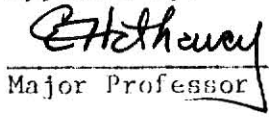
submitted in partial fulfillment of the
requirements for the degree

Master of Science

Department of Physics
Kansas State University
Manhattan, Kansas

1975

Approved by:



Major Professor

LD
2668
T4
1975
P34
C.2
Document

DEDICATION

To . . .

My parents

Jim and Beth Europa

Jess and Liz Randall

. . .

May God bless them for their love,

friendship, strength and understanding

in my times of need.

TABLE OF CONTENTS

Chapter		Page
I.	INTRODUCTION	1
	A. Previous Research	1
	B. Models for Fluorescence in Biological Samples	6
	1. Fluorescence Spectra: A Simple Model	7
	2. Experimental Plausibility: A Realistic Approach	13
II.	EXPERIMENT	21
	A. Experimental Methodology	21
	B. Instrumental Consideration	35
	1. Illumination Sources	35
	2. Sample Illumination Techniques	37
	3. Condensers	54
	4. Field-Limiting Aperture	61
	C. Sample Preparation Methodology	64
III.	DATA ANALYSIS	74
	A. Formulation and Theory	74
	B. Statistics and Errors	85

Page

IV. DATA PRESENTATION 95

A. Deconvolution 95

B. Concentration-Decay Lifetime Relationship in Pure Fluorescein Solution 97

C. Cell Culture Age-Decay Lifetime Relationship 98

D. Cell/FDA Mixture Duration-Lifetime Relationship . . . 103

V. SUMMARY OF CONCLUSIONS 182

Appendix

I. SAMPLE PREPARATION PROCEDURE 184

II. DATA DECONVOLUTION AND FITTING PROGRAM 192

A. Program Functions 192

B. Program Execution 200

III. EQUIPMENT SPECIFICATIONS 231

ACKNOWLEDGEMENTS 236

REFERENCES 233

ABSTRACT 238

LIST OF PLATES

Page

PLATE I 9

Bonding structures of fluorescein and fluorescein diacetate.

PLATE II 11

Representation of the potential energy curves for a simple diatomic molecule, in terms of the internuclear separation.

PLATE III 16

A basic model for cellular uptake and hydrolysis of FDA.

PLATE IV 26

Electronics schematic.

PLATE V 28

General electro-optical schematic.

PLATE VI 30

Optics schematic.

PLATE VII 40

Transmitted illumination schematic.

PLATE VIII 42

Incident illumination schematic.

PLATE IX 46

Ploem Illuminator barrier filter transmission curves.

PLATE X 48

Baird-Atomic barrier filter transmission curve.

PLATE XI 50

Typical fluorescein absorption and emission spectra.

Page

PLATE XII 52

Ploem Illuminator construction schematic.

PLATE XIII 58

Typical cardiod darkground condenser.

PLATE XIV 60

Typical brightfield condenser.

PLATE XV 63

Field-limiting aperture schematic.

PLATE XVI 78

Idealized model for convolution.

PLATE XVII 80

A model for channel-decay superposition.

PLATE XVIII 111

Channel-shift corrected plots of an instrument function and an observed 10^{-4} M fluorescein solution decay spectrum.

PLATE XIX 113

Channel-shift corrected plots of an instrument function and an observed 10^{-4} M fluorescein solution decay spectrum.

PLATE XX 115

Channel-shift corrected plots of an instrument function and an observed 10^{-4} M fluorescein solution decay spectrum.

PLATE XXI 117

Channel-shift corrected plots of an instrument function and an observed 10^{-4} M fluorescein solution decay spectrum.

PLATE XXII 119

Channel-shift corrected plots of an instrument function and an observed intracellular fluorescein decay spectrum.

Page

PLATE XXIII 121

Channel-shift corrected plots of an instrument function and an observed intracellular fluorescein decay spectrum.

PLATE XXIV 123

Channel-shift corrected plots of an instrument function and an observed cell/FDA solution background fluorescence decay spectrum.

PLATE XXV 125

Channel-shift corrected plots of an instrument function and an observed cell/FDA solution background fluorescence decay spectrum.

PLATE XXVI 127

Least squares fit of an instrument function-exponential decay convolution to a 10^{-4} M fluorescein solution decay spectrum.

PLATE XXVII 129

Least squares fit of an instrument function-exponential decay convolution to a 10^{-4} M fluorescein solution decay spectrum.

PLATE XXVIII 131

Least squares fit of an instrument function-exponential decay convolution to a 10^{-4} M fluorescein solution decay spectrum.

PLATE XXIX 133

Least squares fit of an instrument function-exponential decay convolution to a 10^{-4} M fluorescein solution decay spectrum.

PLATE XXX 135

Least squares fit of an instrument function-exponential decay convolution to an intracellular fluorescein decay spectrum.

Page

PLATE XXXI 137

Least squares fit of an instrument function-exponential decay spectrum convolution to an intracellular fluorescein decay spectrum.

PLATE XXXII 139

Least squares fit of an instrument function-exponential decay convolution to a cell/FDA solution background fluorescence decay spectrum.

PLATE XXXIII 141

Least squares fit of an instrument function-exponential decay convolution to a cell/FDA solution background fluorescence decay spectrum.

PLATE XXXIV 145

Linear least squares fit of lifetime vs. concentration for pure fluorescein solution.

PLATE XXXV 149

Linear least squares fit of lifetime vs. concentration for pure fluorescein solution.

PLATE XXXVI 153

Linear least squares fit of lifetime vs. cell culture age for intracellular fluorescein.

PLATE XXXVII 157

Linear least squares fit of lifetime vs. cell culture age for intracellular fluorescein.

PLATE XXXVIII 161

Linear least squares fit of lifetime vs. cell culture age for cell/FDA background fluorescence.

Page

PLATE XXXIX 165

Linear least squares fit of lifetime vs. cell culture age for cell/FDA background fluorescence.

PLATE XL 169

Linear least squares fit of lifetime vs. mixing time of cells and FDA for intracellular fluorescein.

PLATE XLI 173

Linear least squares fit of lifetime vs. mixing time of cells and FDA for intracellular fluorescein.

PLATE XLII 177

Linear least squares fit of lifetime vs. mixing time of cells and FDA for cell/FDA background fluorescence.

PLATE XLIII 181

Linear least squares fit of lifetime vs. mixing time of cells and FDA for cell/FDA background fluorescence.

LIST OF TABLES

Page

TABLE I 32

Parts description for Plate VI.

TABLE II 34

Time-PHA channel calibration values.

TABLE III 44

Parts description of Plates VII and VIII.

TABLE IV. 69

FDA dilutions from stock solution of 10^4 μM FDA in acetone.

TABLE V 71

A listing of samples prepared in order that lifetime spectra could be made and compared.

TABLE VI 73

Cell count for samples used in Spectra J-Series, K-Series, and L-Series.

TABLE VII 88

Computer-calculated output of a representative sample of collected data.

TABLE VIII 91

Statistics of a representative sample of collected data.

TABLE IX 105

Specifications of samples used for data deconvolution, calculated lifetimes included.

Page

TABLE X 107

Specifications of samples used for data deconvolution, calculated lifetimes included.

TABLE XI 109

Computer-calculated output of a representative sample of collected data.

TABLE XII 143

Statistics of Plate XXXIV.

TABLE XIII 147

Statistics of Plate XXXV.

TABLE XIV 151

Statistics of Plate XXXVI.

TABLE XV 155

Statistics of Plate XXXVII.

TABLE XVI 159

Statistics of Plate XXXVIII.

TABLE XVII 163

Statistics of Plate XXXIX.

TABLE XVIII 167

Statistics of Plate XL.

TABLE XIX 171

Statistics of Plate XLI.

TABLE XX 175

Statistics of Plate XLII.

Page

TABLE XXI 179

Statistics of Plate XLIII.

TABLE XXII 188

Qualitative scoring of fluorescence for various solutions of FDA.

TABLE XXIII 190

Qualitative scoring of fluorescence for various cell/FDA solutions.

I. INTRODUCTION

A. Previous Research

Since 1941 when Coons et al.[1] introduced the fluorescent antibody (FA) technique as a means of microscopical analysis, fluorescence microscopy has found widespread application. Although this date is credited with the first use of fluorescent dyes as biological labels, it is by no means the date when fluorescence microscopy originated. On the contrary, fluorescent techniques had been employed as early as 1904 by August Köhler and in 1911 by Lehmann with rather successful results, considering the infantile stage of development of fluorescence microscopy. However, it has been only within the last decade that, through significant technological achievements, fluorescence analysis has progressed from essentially exclusive use as a research tool to applications as a routine diagnostic procedure.

Perhaps the single most important reason for the success of the original fluorescent antibody method is the observable specificity. By using immune serum globulin labeled with a fluorescent dye to locate the corresponding antigen, direct cytological examination locates the trace dye, and hence the desired antigen. Obviously, since fluorescent dyes are easily detected in minute quantities under microscopical observation, this method generally is preferred over the indirect histological techniques. However, it must be noted that the technique of radiological tracing has progressed within the last decade from a stage of rather indirect tracing to a highly specific tracing technique, comparable in many cases to the advantages of fluorescence tracing methods.

There are also other advantages to using fluorochromes as tracers. Proteins, including serum antibodies, can be effectively labeled, chemically, with fluorochromes without any noticeable effect, biologically or immunologically. Properly illuminated, these labeled proteins will fluoresce with substantial intensity and distinguishability so that they may be detected in much smaller concentrations more directly than non-fluorescent labeling techniques allow.

Originally, the only fluorochrome with suitable labeling properties was fluorescein isocyanate[2,3]. However, even though this particular dyestuff had good labeling properties, the chemical techniques required for proper conjugation became overwhelming and it was not until 1958 when Riggs[4] et al. developed fluorescein isothiocyanate (FITC) that another important advantage was gained. The dye FITC allowed conjugation of fluorochrome and protein to be performed easily and efficiently. At present, the number of fluorochromes developed and made commercially available since the introduction of fluorescein isocyanate is nearly inexhaustable. Obviously, the rather large number of fluorochromes is mandatory since no one fluorochrome is suitable as a universal label. To be both adequate and brief in a description of fluorochrome is impossible and for this reason reference is made to texts by R. C. Nairn[5], A. A. Thaer and M. Sernetz[6], and others[7,8] for extensive descriptions of various fluorochromes and their derivatives as well as the fluorescence, a chemical and biological properties.

For direct conjugation of fluorochrome and protein the most widely used dyes are as follows:

1) FITC

2) 1-Dimethylaminonaphthalene-5-sulphonic acid (DANS[9])

3) lissamine rhodamine B (RB200[10]).

FITC and DANS both exhibit strong green fluorescence as distinct from the bright orange fluorescence of RB200. These particular dyes are the most commonly used primarily because of their strong fluorescence, fluorescence-background contrast and conjugation simplicity. Other fluorochromes are chosen on these same general criterion for applicability. Nairn cites Chadwick[7] et al. and Pearse[11] with a list of criteria describing the suitability of fluorochromes for labeling and, in general, nearly all fluorochromes used exhibit these properties although ultimately the application decides which criteria the fluorochromes must meet.

Although the reactive group in the protein determines which label is appropriate, it must be pointed out that these fluorochromes enjoy various different applications outside of direct protein conjugation. Foremost among these is the intracellular analysis[12,13,14] by means of studying the fluorescence characteristics of the absorbed fluorochrome. To mention briefly now and to expound later on, the particular fluorescence properties of significant importance are

1) polarization,
2) excited state decay laws,
3) emission spectra
    a) steady-state and
    b) time-resolved.

The addition of fluorochrome to the precision of microscopy has not only facilitated the qualitative identification of bacterial, viral, protozoal, helminthic, fungal and animal tissue antigens as well as serum antibody characteristics since the technique was first introduced, but has in recent years proved to be an invaluable and extremely sensitive tool for quantificatic

Quantitative advances have been in the areas of diagnostic syphilis serology[15] and of fluorescence polarization characteristics of normal and malignant mammalian lymphocytes[13], both of which employ steady state conditions with respect to the fluorescence kinetics. The next level of technical achievement was in the ability to extract the time dependency of fluorescent processes, namely, time-resolved fluorescence spectroscopy in the nanosecond to subnanosecond domain.

Undoubtedly the most significant advances in quantitative fluorescence analysis have had their origins in the recent electro-optical detection system developments[16,17]. Perhaps the technique enjoying the largest success, and which will be used in this presentation, is the time-correlated single photon counting method. The single largest reason for the use of this method is that it provides a means of direct contact with, and analysis of, the excited state while maintaining high sensitivity.

Adding to this, the introduction of the laser to fluorescence analysis has amply demonstrated its ability to replace and surpass conventional illumination sources[15,18], such as the mercury-or zenon-arc lamp. The reasons for this are fairly obvious. Lasers are very monochromatic, stable and directional light sources as opposed to the conventional sources which provide a broad spectrum of unwanted emission. Consequently, arc sources must be filtered strongly in order that only the radiation suitable for stimulating fluorescence be transmitted to the sample. This results in very little effective stimulation as compared with much higher power per band width values found in lasers. Reported comparisons[18] have found increases in fluorescence intensities up to one hundred times between laser and arc lamp-induced fluorescence. Another difficulty associated with conventional light

sources is that the primary emission lines seldom coincide with the absorption maxima of the fluorochrome and one is often forced to assume a further excitation deficit. However, this problem is completely eliminated with the advent of the tunable, pulsed dye laser. To date, dye lasers are available which are capable of continual tuning from the far red to violet[19] region of the visible spectrum and frequency-doubling into the ultraviolet. This ability has the clear advantage of excitation at any desired preferential wavelength. Obviously, this is only a superficial description of the applications and developments in fluorescence analysis and a much more inclusive description is given by A. A. Thaer and M. Sernetz[6], which also includes extensive references to the literature.

However, the majority of quantitative fluorescence analysis has been for the most part limited to the study of solutions, suspensions and homogenates rather than of individual cells at the microscopical level. This is especially true of fluorescence lifetime and polarization characteristics of the individual "fluorochromated" cells. Once this has been thoroughly investigated and tested, fluorescence analysis standardization will have reached a much higher level of development. It is thus the intent of this thesis to demonstrate the feasibility and practicality of applying laser and electro-optic technology directly to microscopical observation with anticipation of a higher specificity of cellular behavior. In particular, recent investigations[12,13,14,20,22] of the polarization characteristics of fluorescence emission due to intracellular fluorescein produced by cellular enzymatic hydrolysis of fluorescein diacetate (FDA), a non-fluorescent compound, in mammalian blood lymphocytes and yeast cells have based all theoretical and interpreted results on the assumption that the fluorescence

lifetime of the excited state is constant with respect to environment. As is well known, all polarization characteristics are directly related to lifetime behavior and any assumption as to this behavior, whether the fluorochrome be in the free state or in vivo, must be well justified. For this particular reason, the intent of this thesis is to develop the techniques and investigate this assumption.

B. Models for Fluorescence in Biological Samples

Under nearly all circumstances, a practical working model of an actual physical entity is a very involved and complex concept, if adequate descriptive detail is sought. Quite often it is impossible to depict the actual model and one must be content to extract the physically important characteristics and properties from a not-too-over-simplified model. Although molecular fluorescence spectra is such an entity, the nature of these processes and their association with biochemical reactions at the intracellular level is essentially an entirely different, and undetermined, entity.

A great deal of theoretical and empirical knowledge has been formulated for fluorescence decay spectra, transition rates and lifetimes of molecular systems. But as far as the processes involved with intracellular fluorescence kinetics is concerned, little qualitative understanding and even less quantitative understanding is to be found. This is true because of the complexity of the cellular structure and behavior, both of which are fundamentally unknown.

Being that the fundamental process dealt with is fluorescence emission and understanding that the nature of this investigation is experimental rather

than theoretical, a brief description as to the origins of fluorescence emission follows. Thereafter, will follow a model description assumed to be adequate and fully consistent with experimental aspects of sample preparation and behavior. Detailed within this descriptive model will be other possible variations on the intermediate reaction kinetics that are likewise consistent with experiment and, where necessary, attention will be drawn to the consistency. For more detailed description, reference is made to LaMolla[20] and Steinfeld[21] for a rather in-depth treatise on molecular spectra.

1. Fluorescence Spectra: A Simple Model

According to Plate I, it is seen that the fluorescein chromophore is a complicated structure of aromatic benzene rings, carboxyl and hydroxide groups. In order to interpret the fluorescence emission spectrum of fluorescein in terms of potential energy curves would require a multi-dimensional coordinate system with m x n dimensions where

$m = 2,3,4, \ldots$ number of interacting atoms, and

$n = 1,2,3, \ldots m-1$.

Thus, it is impossible to graphically illustrate the potential interactions simultaneously of such a complicated molecule as fluorescein. However, it is very fortunate indeed that nearly all of the salient spectroscopic features of fluorescence can be understood in terms of the simple diatomic molecule which requires only two generalized coordinates: (1) the internuclear separation and (2) the potential interaction between the two nuclei. Plate II illustrates the potential energy curves as a function of internuclear distance which is appropriate for the diatomic molecule.

Because electronic transitions take place on a time scale much faster than molecular vibrations, the Franck-Condon principle states that absorption

THIS BOOK CONTAINS NUMEROUS PAGES WITH ILLEGIBLE PAGE NUMBERS THAT ARE CUT OFF, MISSING OR OF POOR QUALITY TEXT.

THIS IS AS RECEIVED FROM THE CUSTOMER.

PLATE I

Typical bonding structures of fluorescein and fluorescein diacetate (FDA).

THIS BOOK CONTAINS NUMEROUS PAGES WITH DIAGRAMS THAT ARE CROOKED COMPARED TO THE REST OF THE INFORMATION ON THE PAGE.

THIS IS AS RECEIVED FROM CUSTOMER.

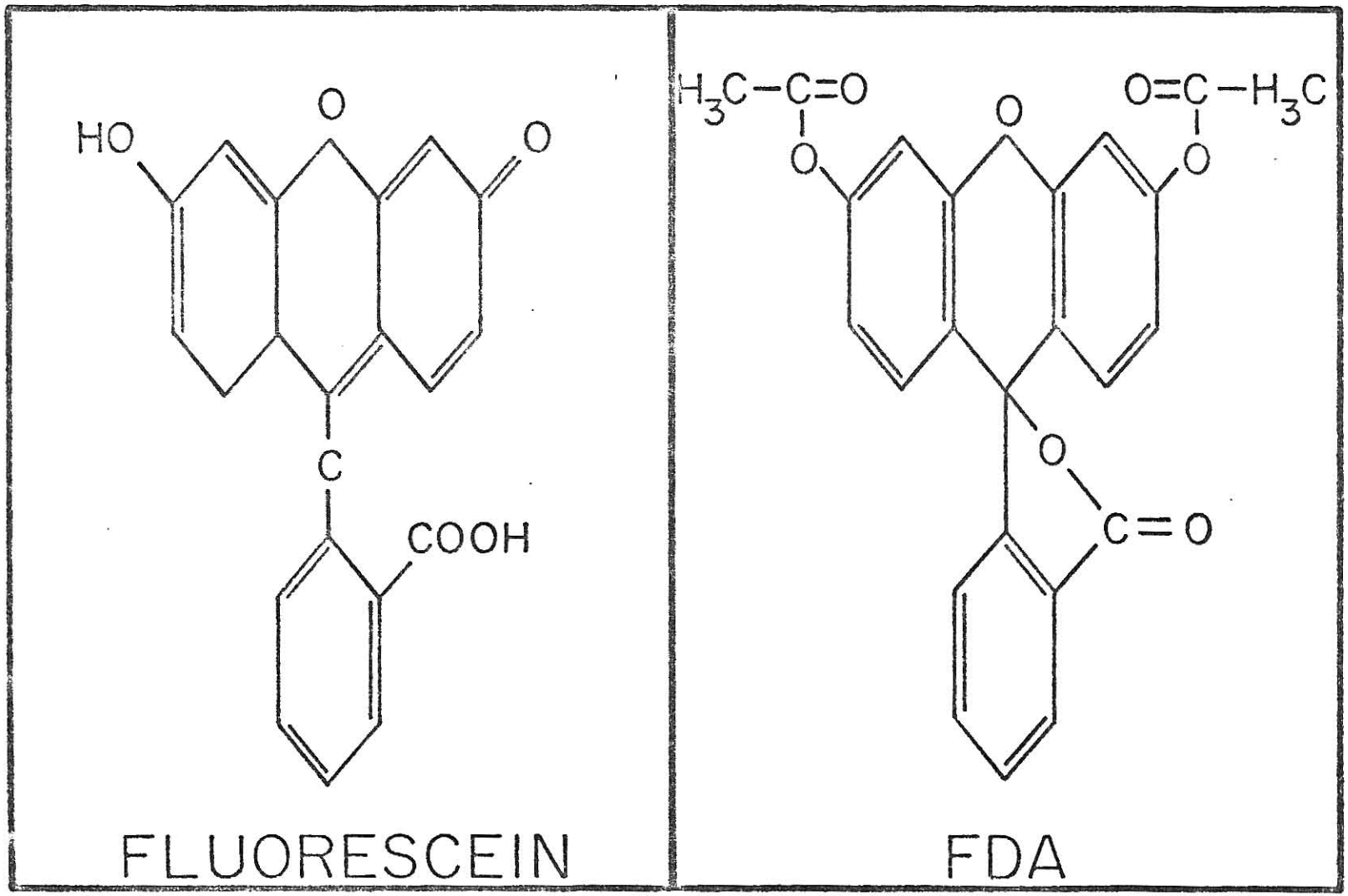
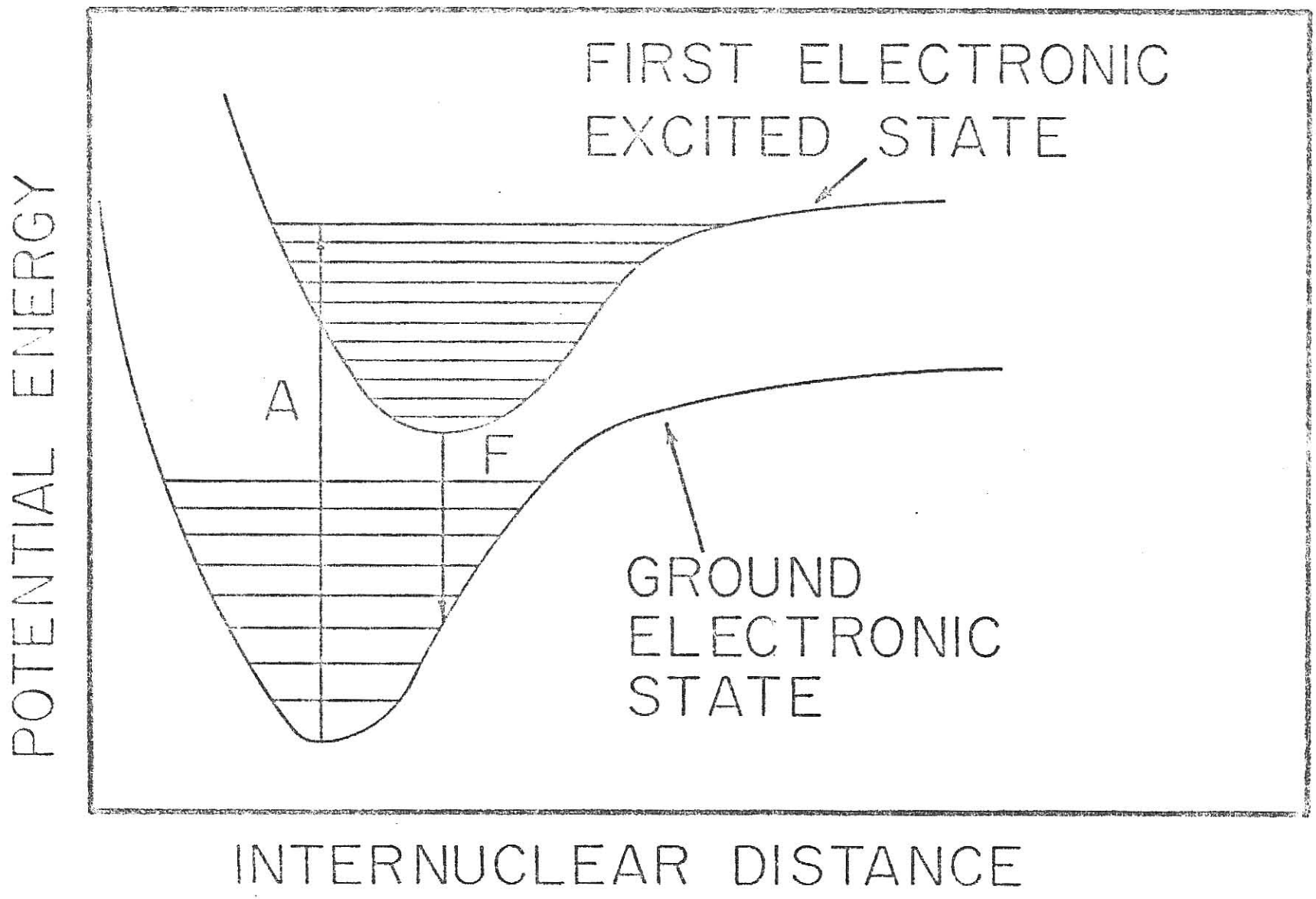

HO
O
O
C
COOH
FLUORESCEIN
H3C–C=O
O
O=C–H3C
O
O
O
C=O
FDA

PLATE II

Representation of the potential energy curves, in terms of the internuclear separation, for a simple diatomic molecule. Shown are the ground electronic and first excited electronic states and typical vibrational levels.


FIRST ELECTRONIC
EXCITED STATE
A
F
GROUND
ELECTRONIC
STATE
POTENTIAL ENERGY
INTERNUCLEAR DISTANCE

processes invariably occur with no change in the internuclear separation and within a period of approximately 10^{-15} seconds. Implicit in this principle is the effect due to the nuclear mass, which are much more massive in comparison with the electrons involved in the transitions. This means, graphically, that the transition may be represented by a vertical line from the ground state to the first excited state, as represented in Plate II. To make note, absorption transitions are possible not only to the first excited states but also to the higher excited electronic states which are not shown in Plate II for reasons of clarity. To each of these states is associated a continuum of vibrational-rotational energy levels to which absorption transitions may occur. In all molecules the energy gained through photon absorption is quickly lost (10^{-12} seconds), either totally or substantially in part, through the vibrational modes of the molecule and in molecular collisions. Such processes are definitely non-radiative and are manifested in processes termed internal conversion and intersystem crossing. However, should the molecule be sufficiently stable, i.e., rigid, against vibrational decay, energy may be lost through a transition other than vibrational-rotational modes. Plate II depicts the transition to an upper vibrational level of the first excited state. As mentioned, the molecule will then immediately lose a certain quanta of vibrational energy within approximately 10^{-12} seconds and decay to the lowest vibrational level of the first excited state. Provided that this particular state is stable against decay on the order of 10^{-9} seconds, a radiative transition to the ground electronic state may result. By definition this transition is termed fluorescence. Obviously, since the fluorescence emitted is strictly dependent upon the physical structure and composition of a molecule and that this is in

turn determined by the molecule-environment interaction, it is seen that the fluorescence emission provides a sensitive direct probe and correlation with the various possible molecular interactions. This is especially true of biological and biochemical processes, due to the fact that the fluorescent molecule-media interaction is a very dynamic phenomena.

Having illustrated the causes and necessary conditions for fluorescence to occur as well as its qualifications as a sensitive "detector", we are led to the stage where an actual physical model must be put forth, examined, verified and re-examined for observable consistency.

2. Experimental Plausibility - A Realistic Approach

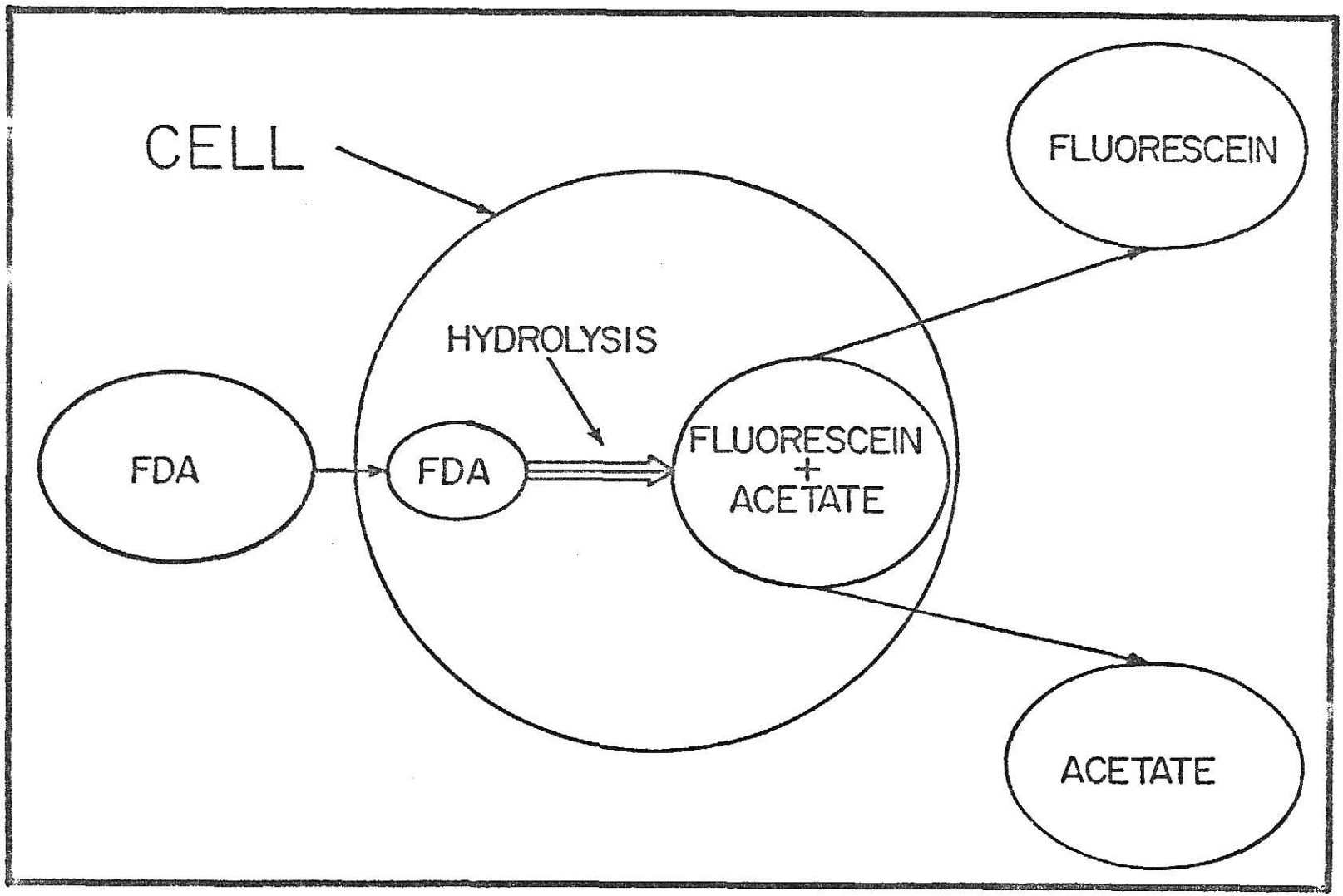
Before proceeding with the construction of a satisfactory model, consider the known experimental results that serve as a building block. Initially, start with two specially prepared sample solutions whose preparation and exact consistency are to be described in full detail later. One solution contains only a known amount of yeast cells and the other solution containing a fluorogenic substrate known as fluorescein diacetate (FDA) of known molarity. Refer to Plate I for a structure comparison between the pure fluorescein molecule and one of its non-fluorescent derivatives. Under given conditions each solution will exhibit no fluorescence characteristic of fluorescein or its compounds which do fluoresce. Assuming that all experimental conditions necessary for a successful reaction have been met, allow the two solutions to mix thoroughly. In the most general terms the results that follow are simply an occurrence of fluorescence emission characteristic of the fluorescein radiation absorption-emission process. This phenomena has been aptly phrased by Rotman and Papermaster[22] as "fluorochromasia". Attention must be paid to the fact that fluorochromasia is not limited to various

species of yeast but can also be found to occur in various types of mammalian cells including human blood lymphocytes. This occurrence has been reported in the literature[13,22] and likewise has been observed in the course of this research in several yeast strains and human blood lymphocytes, both normal and cancerous. The production of this fluorescent compound increases with time until the reaction reaches such a stage in development that the observed fluorescence intensity remains constant for the mixed solution. Qualitatively, this is the essence of the observed results.

So far no mention has been made as to the sources of the fluorescence or its causes, production and reaction kinetics. The point has been reached where some type of plausible biochemical reaction cycle must be formulated. To examine the situation in more detail, the reaction kinetics must be considered on the cellular level. Plate III exhibits possibly the simplest steady state condition of the two mixed solutions that is compatible with sample preparation observations made both by myself and others[14,23]. Allowing the two solutions to mix, we see an individual cell initiate the process by taking up FDA at a given rate specified by k_a. This rate constant need not be constant at all times and indeed it may depend upon such factors as temperature, FDA substrate, cell concentrations, and other effects such as centrifugation[23] that may serve to alter the apparent "structuredness" of the cell. Upon the uptake of FDA the cell begins forming a fluorescent compound assumed to be fluorescein and this process is believed to be some form of enzymatic hydrolysis which liberates the fluorescein from the attached acetate groups at rate k_H. In most instances[14] this rate constant yields an observed linear rate of increase in fluorescence intensity

PLATE III

A basic model for cellular uptake and hydrolysis of FDA, resulting in fluorescein leakage out of the cell. The intention is to represent a temporary steady state concentration of intracellular fluorescein.


CELL
FLUORESCEIN
HYDROLYSIS
FDA
FDA
FLUORESCEIN
+
ACETATE
ACETATE

during the initial part of the cycle. Following the intracellular production, the rate constant decreases until the observed fluorescence intensity remains constant with time. All experiments[12,24] indicate that the cause for this steady-state transition appears to be the leakage of liberated fluorescein through the cell membrane and into the remaining solution contributing to the non-specific background fluorescence. The stage of actual steady state condition is reached when the rate constant of fluorescein leakage is balanced by the rates of uptake and hydrolysis causing the formation of fluorescein.

Although this simple model appears qualitatively compatible with experiment, which is quite sufficient a requirement, it must be emphasized that the steps intermediate between FDA substrate uptake and fluorescein diffusional leakage are entirely open to modification. For example, recombination effects such as the reformation of FDA and the uptake of fluorescein in the free state and their respective rate constants have been tacitly neglected. Likewise, an entirely equivalent model may involve the transformation of the FDA substrate directly into a fluorescent derivative of fluorescein or possibly the weak binding of the free fluorescein molecule to some intracellular substrate. After some period the fluorescein is liberated through some, as yet unknown, process and immediately diffuses through the cell membrane to contribute to non-specific fluorescence.

It is now evident that some type of effort must be made to probe the internal structure of the cell. Previous experimenters have chosen various means by which the probe could be made. Foremost among these means is the measurement of the fluorescence polarization characteristics at various stages of the cell - FDA interaction. For purposes of simplicity,

assume that the cell has previously taken up a sufficient quantity of FDA and has initiated the hydrolysis process and formation of some form of fluorescent fluorescein compound. Now allow linearly polarized radiation, suitable for adequate absorption by the fluorescent compound, to be incident on the cell. In general, the rotational motions of the cell itself are much slower than the assumed individual molecular rotations within the cell and will be neglected for this reason. Should the radiation-absorbing molecule be restricted from all rotational freedom initially, we would observe fluorescence emission that is strongly polarized with emission vector aligned with the absorption transition moment vector for the usual classical description of polarization. Proceeding to the other extreme of complete rotational freedom the observed emission would display very little, if any, polarization. The classical treatment of polarization absorption and emission gives a trivial explanation. This being that in the case of the former, the transition moments of absorption and emission must maintain the same relative orientation. In the latter case, the molecule performs rotations, specified by the interaction with the media such as solvent-solute polar reactions and Brownian motion, subsequent to absorption. Therefore, the emission vector has equal, or near equal, probability of any one of the orientations within 4π steradians. The randomness with which the rotations occur is a direct consequence of the media interactions mentioned earlier and herein lies a technique for observing possible intracellular transformations, reactions and motions.

In more realistic terms the fluorescence emission of a solution will show polarization effects to some degree. This result is attributable to the preferential molecular orientations required for efficient excitation-absorption. Absorption is not the "all-or-nothing" model presented earlier. Rather, elementary theory shows us that the degree of excitation varies as

$\cos^2\theta$, where θ represents the angle between the molecular transition moment vector and the excitation electric vector, assuming linearly polarized excitation. This angular correlation shows that maximum excitation occurs for perfect alignment between the two vectors. Adding to this the fact that no molecule in solution displays perfect rotational freedom, the degree of polarization is seen to be dependent upon the degree with which the excitation vector-transition moment vector orientation is preserved. However, Francis Perrin showed in 1926 that there are only two other parameters which influence the emission polarization and that all three quantities are related by the equation

$$\left\{\frac{1}{P} - \frac{1}{3}\right\} = \left\{\frac{1}{P_o} - \frac{1}{3}\right\}\left\{1 + 6R\tau\right\} \quad , \qquad \text{Eq. 1}$$

where

P_o = the limiting polarization defined as the maximum polarization resulting from no disorientation following excitation,

R = the rate of molecular rotation and

τ = the characteristic lifetime of the molecular excited state.

A great deal of effort has been expended in order to explain the observed values of P in terms of mathematically derived values of R, assuming various molecular shapes[25,26]. Likewise, since this rotational parameter is a function of temperature and viscosity, experimenters have endeavored to correlate polarization directly with these parameters intrinsic to the internal cellular structure, assuming that the excited state lifetime is a non-varying quantity. Generally speaking, nearly all solutions

exhibit disorientation motions within a few nanoseconds. For fluorescent compounds this effect is present on the same time scale as the excited state lifetime and we now see another technique for observing intracellular behavior but on a real time basis rather than by measuring time-averaged quantities.

Since the internal structure and mechanisms of the cell are still very much open to question, rather than theorizing as to this nature and trying to predict any lifetime variations, it is entirely legitimate to leave the intracellular nature unrestricted. Therefore, all experimental results will be assumed to be significant and in direct relation with the cellular biodynamics and hopefully will corroborate previous experimental results and conclusions.

II. EXPERIMENT

A. Experimental Methodology

So as to provide a more clear picture of the basic technique used for the experimental determination of decay lifetimes all pertinent details and descriptions of apparatus and related topics will be discussed in subsequent sections. Therefore, only a general technique description will be presented at this time in order to familiarize the reader.

Fundamentally, the basic technique of lifetime measurements was performed using a routine photon counting electronics system as described in the literature[16,27]. The basic electronic instrumentation is illustrated in Plate IV. However, the particular illumination/detection system used for this investigation employs a means for selective wavelength excitation and for performing measurements on a given cell under microscopical observation. Plate V represents the general experimental system with the laser radiation providing the elimination of generally used broadband flashlamps and the microscope providing for the elimination of the solution cuvette-spectrophotometer generally used for measurements on a macroscopic basis.

Due to the particular optical cavity structure of the pulsed dye laser there is a considerable amount of beam divergence. Thus, a beam control system must be used to provide beam collimation. A simple system is shown in Plate VI representing the optical arrangement. Immediately after collimation the beam could be directed for either transmitted or incident sample illumination, the latter of which proved to be unsuitable as will be explained in section B. As usual, the transmitted laser light and resultant

fluorescence are both collected by the microscope objective and thus must be separated by an appropriate filter system. Interference filters were used to eliminate all exciting laser light for visual observation. A monochromator was used in addition for quantitative measurements. As shown in Plate V the microscope was equipped with a trinocular head providing for convenient visual/electronic mode detection operation.

Plate IV shows that the heart of the technique for direct lifetime measurements is the time-to-pulse height-converter (TAC) whose function is to measure stop pulses timed to corresponding start pulses. Upon receiving a suitable start pulse from the photodiode laser-pulse monitor the TAC is enabled to generate a voltage ramp increasing linearly with time until a suitable stop pulse from the photomultiplier detecting the fluorescence photons is received. Upon completion of this cycle the voltage amplitude generated is strobed out to a pulse height multichannel analyzer (PHMCA). Owing to the linear build-up of the voltage with time we see that a real time emission spectrum is obtained in which the time variable is simply proportional to the individually recorded voltage pulses. However, the most important experimental condition is that the rate of detection of fluorescence photons must be no larger than 50% of the rate of production, i.e., on the average, no more than 1/2 a fluorescence photon be counted for each laser pulse. This calls for extremely low fluorescence and excitation intensities to be used and ensures that pulse "pile-up" distortion will not occur. This phenomena arises from the fact that a given excited molecule will spontaneously emit a photon on a completely random basis. Considering an ensemble of excited molecules the random emissions will now be dependent upon the number of excited molecules remaining.

Ideally this leads to the familiar exponential decay law. As a consequence, more photons are emitted at short times than longer times. The TAC operation is characterized by the disability to detect stop pulses after the first one received and the system remains disabled until reset. It is seen that the TAC will be responsive only to the short-lived photons. Therefore, should the emission intensity be such that the quickly emitted photons are always detected, the TAC will never "see" the longer-lived photons and the data will consequently be distorted in favor of shorter lifetimes. In the event of pulse pile-up distortion, methods have been developed to statistically correct the resulting data[28].

The primary disadvantage of the single-correlated photon counting technique is the long counting times necessary to accumulate sufficient data to minimize statistical fluctuations. This drawback is particularly manifest in the usage of biological samples whose physical state is quite dynamic. Therefore, the highest practical pulse repetition rate should be used in order to minimize data collection time. Many commonly used flash-lamps are capable of several kilohertz repetition rates, a very desirable feature. Unfortunately, the highest stable repetition rate of the pulsed laser used in this experiment was a mere 30 Hertz, implying that data could be collected no faster than 15 counts per second.

In order to improve the instrumentation, timing filter amplifiers (T.F.A.) and level-crossing fast discriminators were used in each of the start-stop channels of the TAC. The purpose of the amplifiers was primarily to ensure good pulse shape and to maximize the signal-to-noise ratio. Good pulse shaping of both the photodiode and photomultiplier pulses provided a region of the initial rise which was relatively free from timing jitter despite variable pulse amplitudes. This feature enables accurate discriminator

triggering, resulting in optimum TAC measurements. Although the photodiode was capable of subnanosecond response and sufficient pulse amplitude, the signal was shaped in order to minimize ringing and to provide a pulse with the fastest rise time. The discriminators were used in order to filter out extraneous pulses which would possibly trigger the TAC falsely and also to provide a suitably fast logic pulse for optimum TAC response. Both discriminators were adjusted to yield approximately the best signal-to-noise ratio. In practice, however, a slightly higher level was used to ensure the elimination of false logic pulses. Variations and improvements on this general technique are described elsewhere in the literature[17,27].

Due to the finite width of the excitation pulse, in addition to the expectation of short lifetimes on the order of the excitation pulse width, it is mandatory to perform a deconvolution to remove any distortions to the assumed decay function. Therefore, a decay spectrum of the total instrument function must be performed under the same experimental conditions as the fluorescence spectra with the changes that the monochromator be reset to the laser line position and a clear glass slide used in place of the sample. Further discussion of this topic will be concluded in Chapter III and Appendix II.

Data aquistion was performed by a pulse height multichannel analyzer and each spectrum was stored in 256 channel segments in order to achieve both modest aquisition time and sufficient timing resolution. Upon completion of a given spectrum the PHA storage was subsequently transferred to both teletype printout and paper tape, the latter serving as computer analysis input.

To perform a suitable time-PH channel calibration, a known amount of delays were inserted into the stop input channel of the TAC after the same pulse had originally been applied to both start and stop inputs. For a

PLATE IV

Electronics Schematic

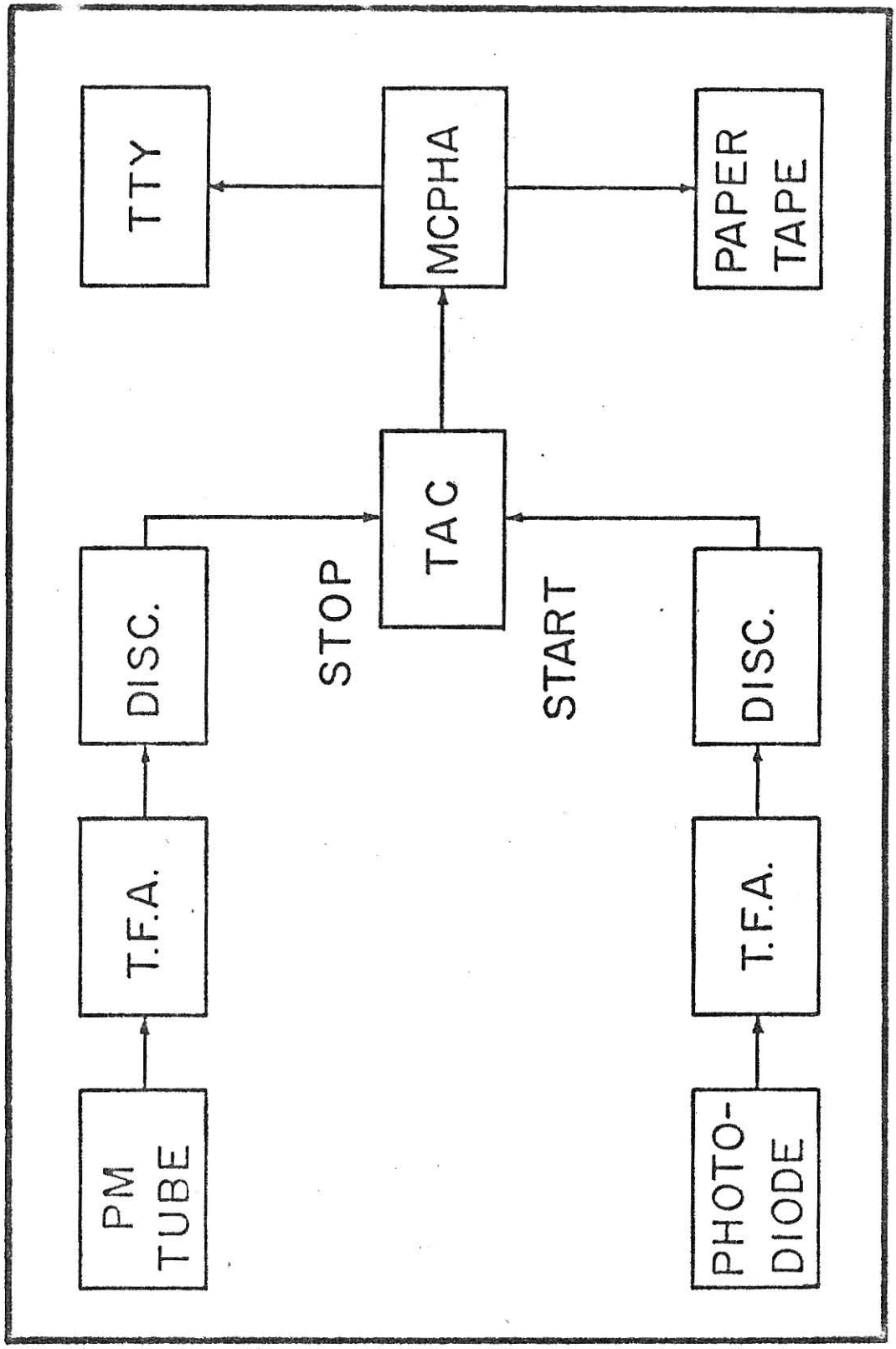

TTY
MCPHA
PAPER TAPE
DISC.
STOP
TAC
START
DISC.
T.F.A.
T.F.A.
PM TUBE
PHOTO-DIODE

PLATE V

General Electro-Optical Schematic

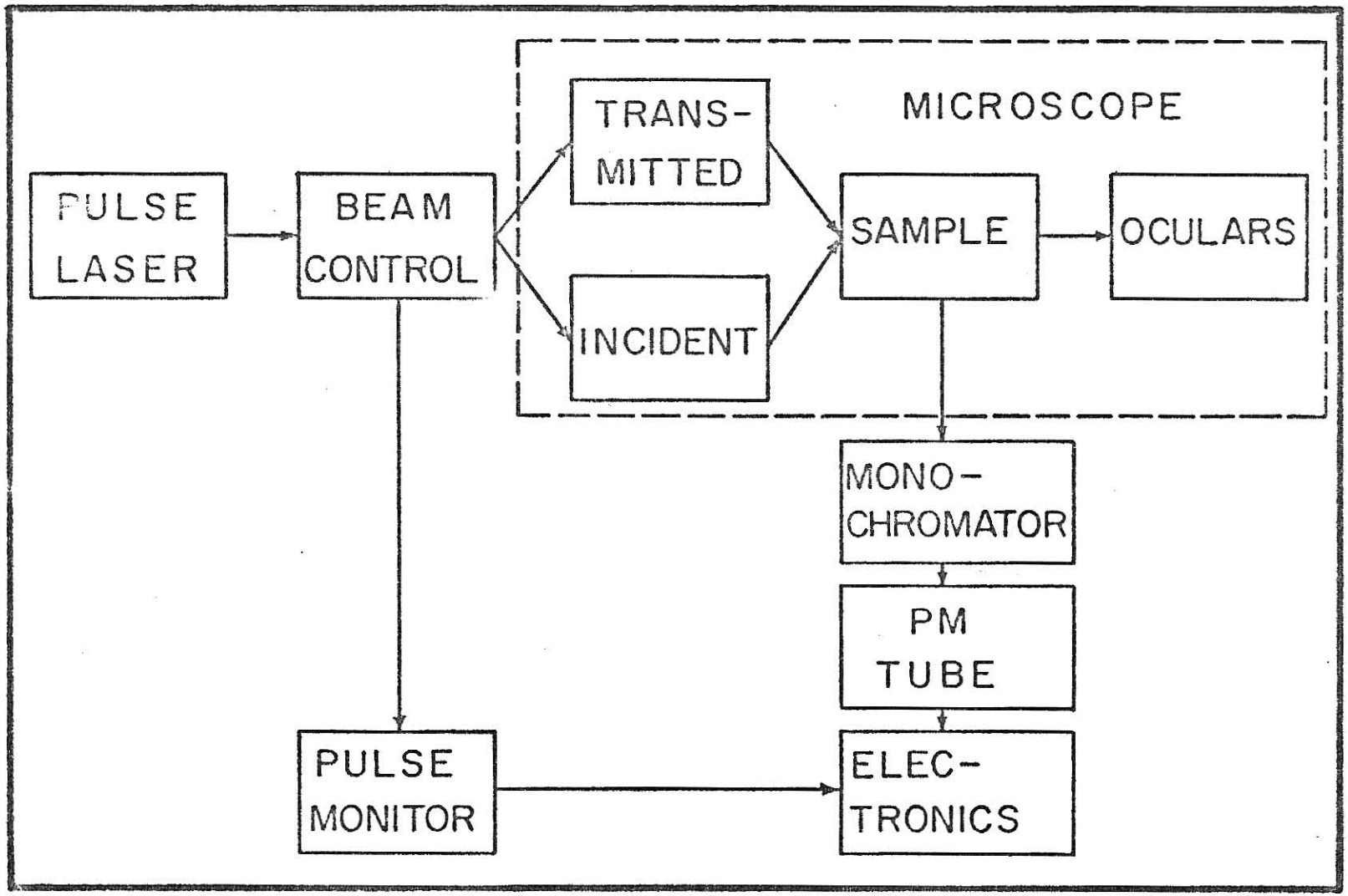

PULSE LASER
BEAM CONTROL
TRANS-MITTED
INCIDENT
MICROSCOPE
SAMPLE
OCULARS
MONO-CHROMATOR
PM TUBE
PULSE MONITOR
ELEC-TRONICS

PLATE VI

Optics Schematic

Alignment Beam (·-·-·-·-·-·-·-·-·-)

Dye Laser Beam (_____)

Alternate Path (- - - - - - - - -)

Reflected Monitor Beam (. . . . . .)

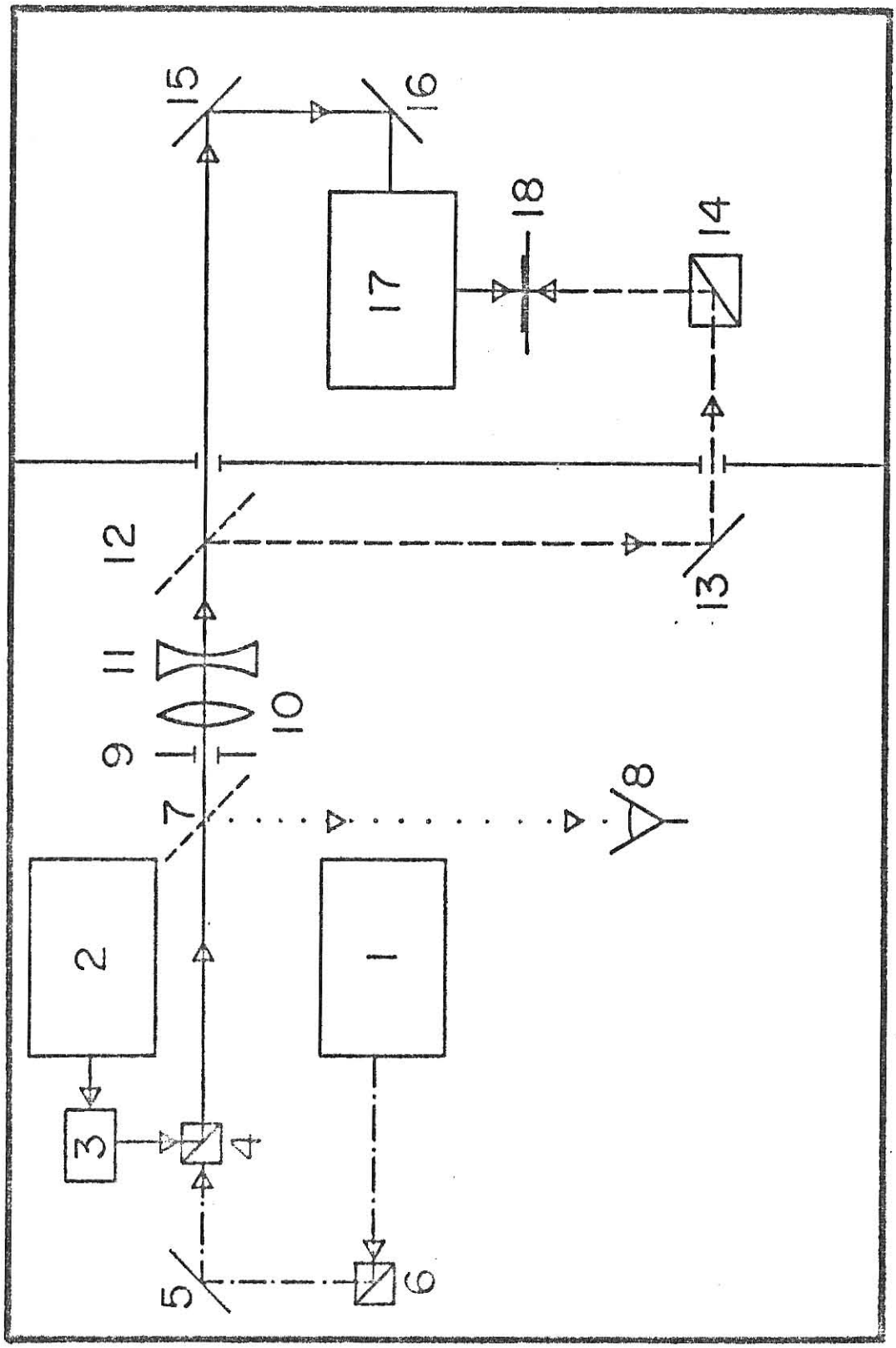

15
16
17
18
14
12
13
11
10
9
7
8
2
1
3
4
5
6

TABLE I

Parts description of Plate VI.

1. Argon laser

2. Pulsed Nitrogen laser

3. Tunable pulsed dye laser

4,6. Pellin-Broca prism

5,12,13,15,16. Moveable-adjustment mirrors

7. Reflecting glass slide

8. Photodiode

9. Aperture-stop

10,11. Beam control lenses

14. Ploem vertical illuminator

17. Microscope

18. Sample

TABLE II

Time - PHA channel calibration values

Known Delay	Channel Number
0.0 reference	10016
2.0 nsec	10019
34.0 nsec	10068

given time delay pulses were recorded in a given channel. By incrementing the delay by a known amount again the data pulses were collected in a different channel, the shift being a direct measure of the time delay introduced and, thus, a direct calibration. Table II provides the known delays and channel shifts obtained for calibration. Note that the channel shifts cover the range of the measured spectra. Upon averaging the three obtained conversion factors, a value of .657 nsec/channel is obtained.

All spectra were obtained with the pulsed dye laser tuned to 490 nm, and emission monochromator set at 490 nm and 520 nm, for instrument functions and fluorescence decay spectra, respectively. The wavelength of 520 nm was chosen for the fluorescence band pass due to the fluorescein fluorescence maximum at that wavelength. Entrance and exit slit widths were chosen corresponding to a band width of 2 nm.

B. Instrumental Considerations

This section is intended to serve as a supplement to the previous section by more fully explaining the primary optical elements and their applications to the experiment. However, no attempt is made to elaborate on design or theory of operation and all necessary equipment specifications and peripheral accessories will be adequately documented in Appendix III.

1. Illumination Sources

Referring to Plate VI it is seen that the primary source of illumination used for fluorescence lifetime measurements is the continuously tunable dye laser. As a source of excitation the dye laser receives its required energy input from a one-megawatt, pulsed nitrogen gas molecular laser emitting in

the ultraviolet at 337 nanometers. In addition to the monochromaticity, the specifications of the pulsed laser system most vital to the experimental technique are its continuously variable repetition rate range of 0-30 pulses per second, with a full width at half maximum of not greater than 10 nanoseconds. As it is not the intent of this thesis to detail a description of lasers as a suitable source of fluorescence excitation[18], it will suffice to mention that the particular dye laser used is continuously tunable over the entire visible spectrum and into the near ultraviolet. However, this large spectral range is obtainable only by using many different dyes in interchangeable dye-flow cells and then by frequency doubling into the ultraviolet.

In order to achieve laser emission at the wavelength of maximum absorption in fluorescein (490 nm), the Coumarin 102 organic dye[29] was used. Although this particular dye does not allow the maximum rated laser power of 250[a] kilowatts per pulse at 475 nm to be achieved, it was the only dye appropriate for operation at 490 nm.

Due to the nature of organic dyes and their use as lasers, the laser action must occur within the fluorescent band of the dye and thus, there is considerable unwanted background in the laser beam. This problem was eliminated by using a Pellin-Broca constant deviation prism to separate the fluorescence from the laser emission. Since the desired laser line is shifted from the fluorescent peak by 15 nm, sufficient splitting was obtained to allow adequate separation by using a suitable aperture following the Pellin-Broca prism.

[a]According to the specifications, the dye laser was rated at 250 kilowatts per pulse at 475 nm in Coumarin 102. However, the maximum obtainable peak power was not more than 200 kilowatts per pulse with 20 milliwatts continuous power at 10 pulses per second. This, however, proved to be more than adequate power for single photon counting.

Supplementing the pulsed laser system is a continuous argon-ion laser source, used primarily for optical alignment and occasionally substage focusing of the sample. The emission of the argon laser is at 488.0 nm, which provided adequate stimulation for absorption due to the 2 nm shift from the fluorescein absorption maximum. As an alignment instrument, the argon laser proved valuable in its ability to produce strong fluorescence in cells which would show little or no fluorescence under conventional illumination. Thus, optical alignment was achieved much more efficiently, even under the most adverse conditions. However, due to the exceptionally large continuous power density found in the argon laser beam, care had to be exercised so that fluorescence fading was made minimal.

For convenience, both continuous and pulsed laser systems were arranged such that as soon as alignment was achieved, insertion of the deflecting prism superimposed the pulsed beam for immediate measurements. Since the argon laser is a fluorescent gas discharge, a Pellin-Broca prism was again used to filter the argon beam although it was not mandatory.

In order that a purely qualitative comparison could be made between illumination sources, the microscope was equipped with a 150-watt xenon standard arc lamp, which is not shown in Plate VI. As compared to the argon laser, the xenon lamp proved far inferior because the power per unit spectral width of exciting light from the argon laser (0.5 watts at 488.0 nm) is much greater than that of a xenon-arc lamp. However, the xenon lamp proved useful in substage sample viewing and more convenient than the argon laser for immediate observation after viewing.

2. Sample Illumination Techniques

In order to illuminate a sample with maximum efficiency and still measure any desired quantities characteristic of the sample emission, two

types of techniques have proven outstanding for direct fluorescence observation. These are

a) transmitted illumination, and

b) incident illumination,

Detailed diagrams of each arrangement are shown in Plates VII and VIII and each will be discussed according to the chronological order of development as listed above.

According to Plate VII, the exciting radiation is collected by a lens which then focuses the beam into a short focal length (4 mm) diverging lens. At first this procedure may seem redundant to focus and subsequently defocus the beam. However, the reason for such a procedure is due to the nature of the condenser used for substage sample illumination, which will be adequately covered later in this chapter. At this point it will be assumed that sufficient exciting light has been collected in the condenser and focussed onto the sample slide. It is from this point of the experiment onward that determines the quality of the image which directly affects the signal-to-noise ratio.

Once illuminated, the sample will fluoresce and the characteristic radiation will be emitted in all random directions. For this reason, objective and condensers with the largest practical numerical aperture were used in order to increase the light-gathering ability of the system. In addition to the fluorescence collected by the objective a substantial amount of the focussed exciting light will also be collected and this light is of prime concern when trying to extract the largest possible signal-to-noise ratio. So that the collected exciting radiation may be efficiently removed from the signal, use is made of the great advances in

PLATE VII

Transmitted Illumination Schematic

Laser Light (_____)

Xenon Lamp (-·-·-·-·-·-·-·-·-·-)

Fluorescence(- - - - - - - - - -)

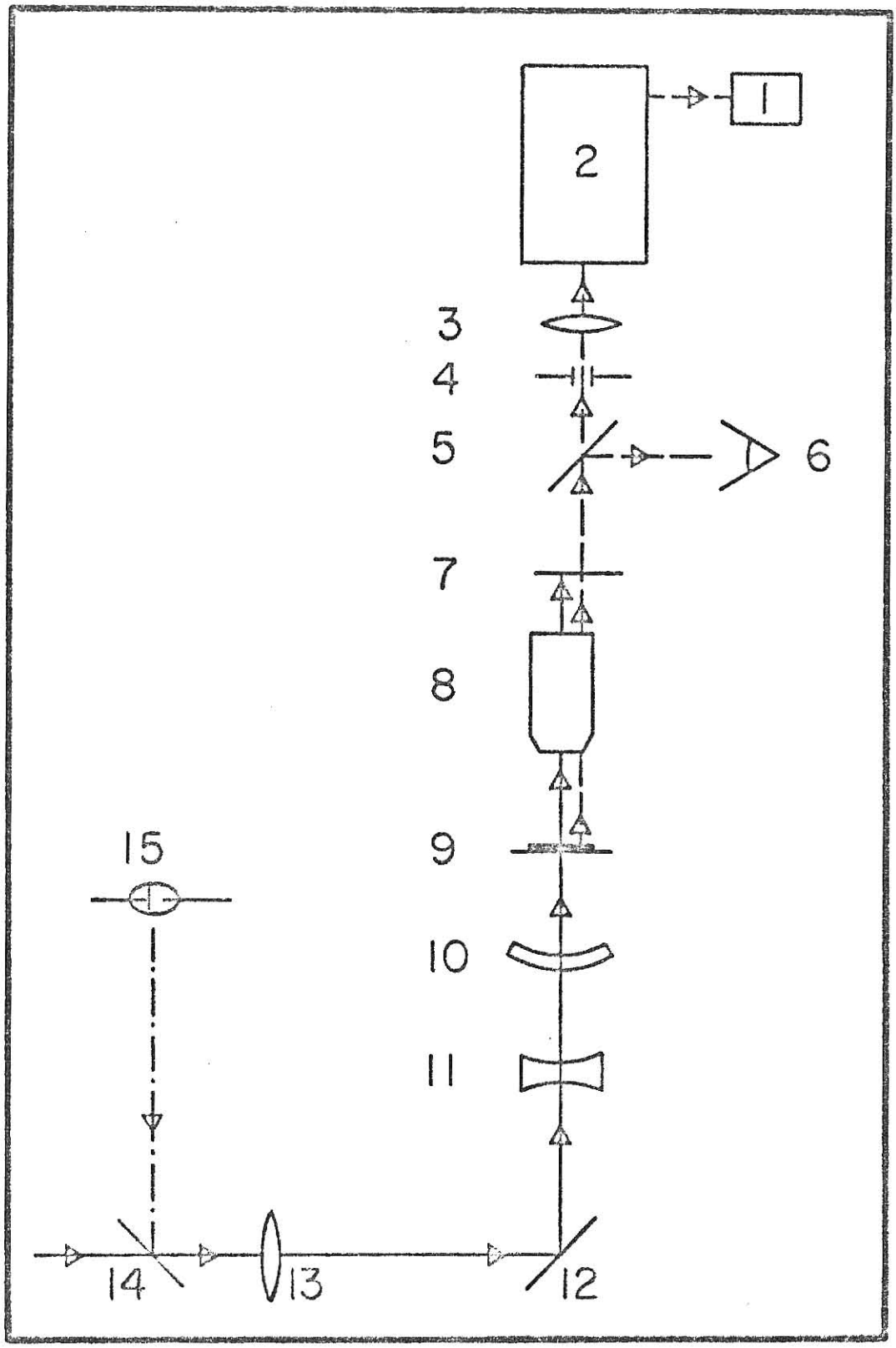

1
2
3
4
5
6
7
8
9
10
11
12
13
14
15

PLATE VIII

Incident Illumination Schematic

Laser Light (_____)

Xenon Lamp (·-·-·-·-·-·-·-·-·)

Fluorescence (- - - - - - - - -)

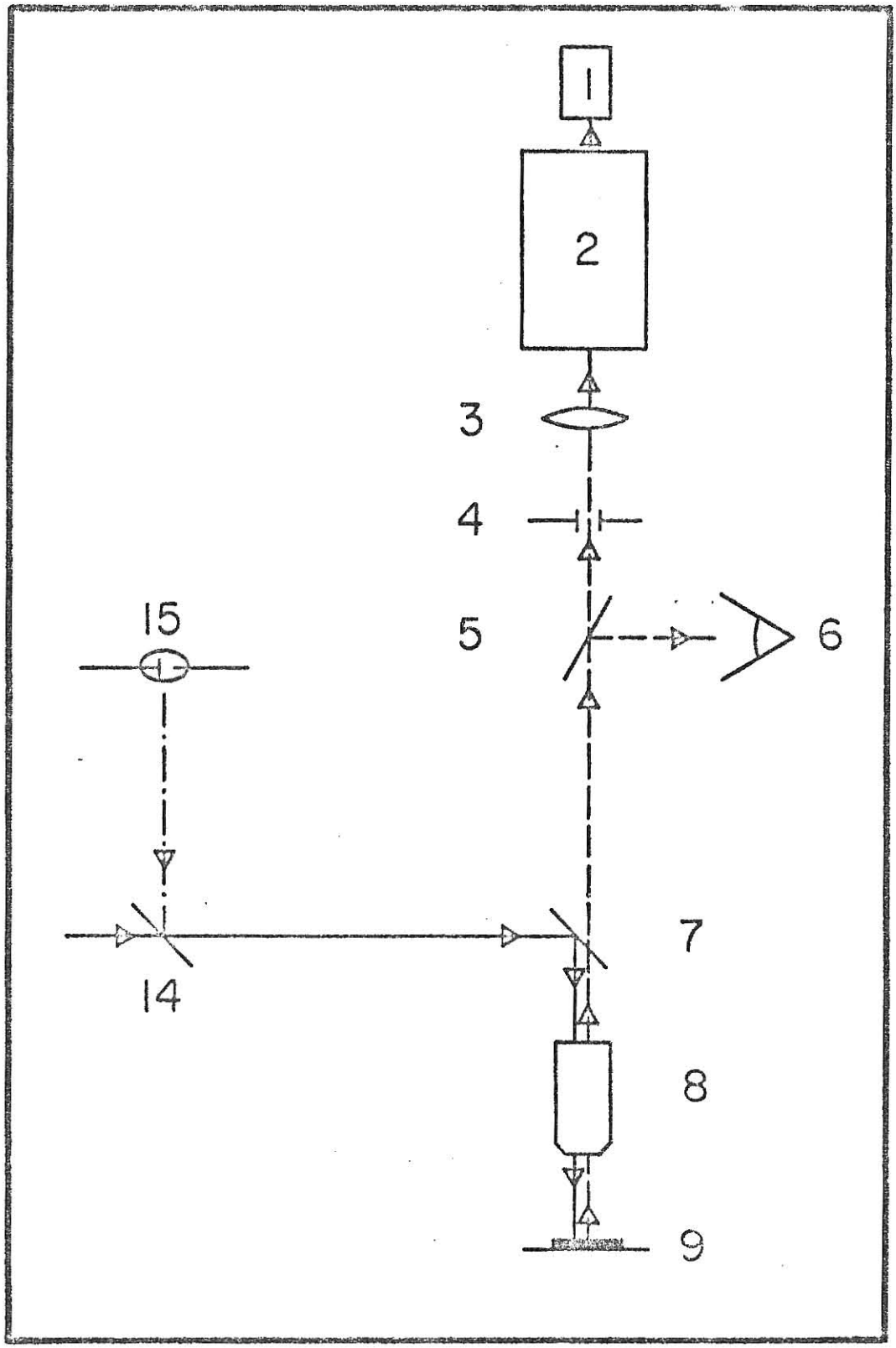

1
2
3
4
5
6
15
14
7
8
9

TABLE III

Parts description of Plates VII and VIII.

1. Photo multiplier
2. Monochromator
3. Collecting lens
4. Field-limiting aperture
5. Prism
12,14. Moveable adjustment mirrors
6. Ocular
7. Barrier filter/dichroic mirror
8. Objective
9. Sample
10. Dry darkfield condenser/Brightfield condenser
11. Diverging lens
13. Focusing lens
14. Xenon Lamp

PLATE IX

Ploem Illuminator barrier filter transmission curves. The particular filter used for the data presented is shown second from the left.

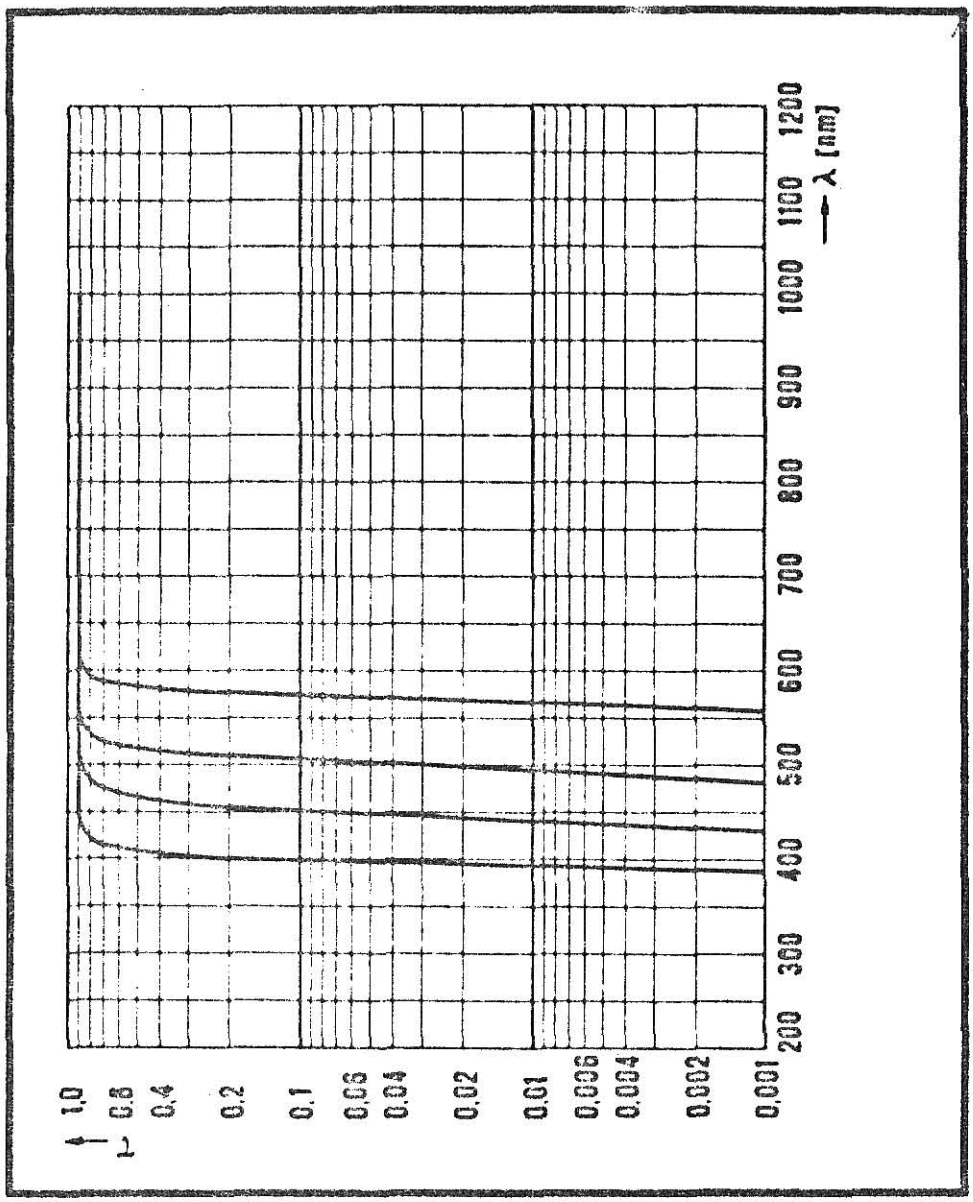

τ
1.0
0.8
0.4
0.2
0.1
0.06
0.04
0.02
0.01
0.006
0.004
0.002
0.001
200
300
400
500
600
700
800
900
1000
1100
1200
λ [nm]

PLATE X

Baird-Atomic barrier filter transmission curve.

ILLEGIBLE DOCUMENT

THE FOLLOWING DOCUMENT(S) IS OF POOR LEGIBILITY IN THE ORIGINAL

THIS IS THE BEST COPY AVAILABLE

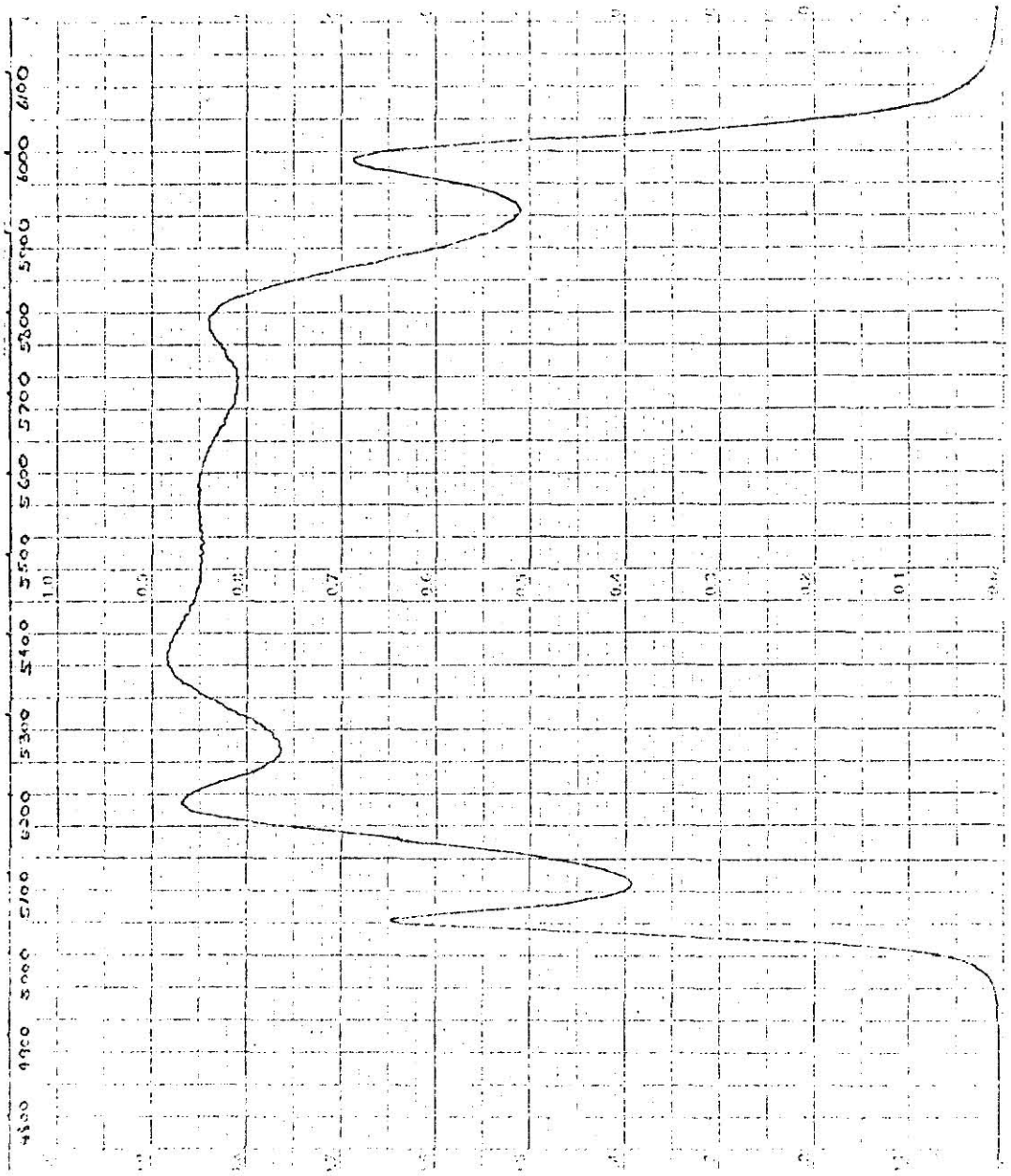

6100
6000
5900
5800
5700
5600
5500
5400
5300
5200
5100
5000
4900
4800

PLATE XI

Typical fluorescein absorption(_____) and emission(- - - - -) spectra.

Intensity units are arbitrary and absorption and emission peaks are not to scale.

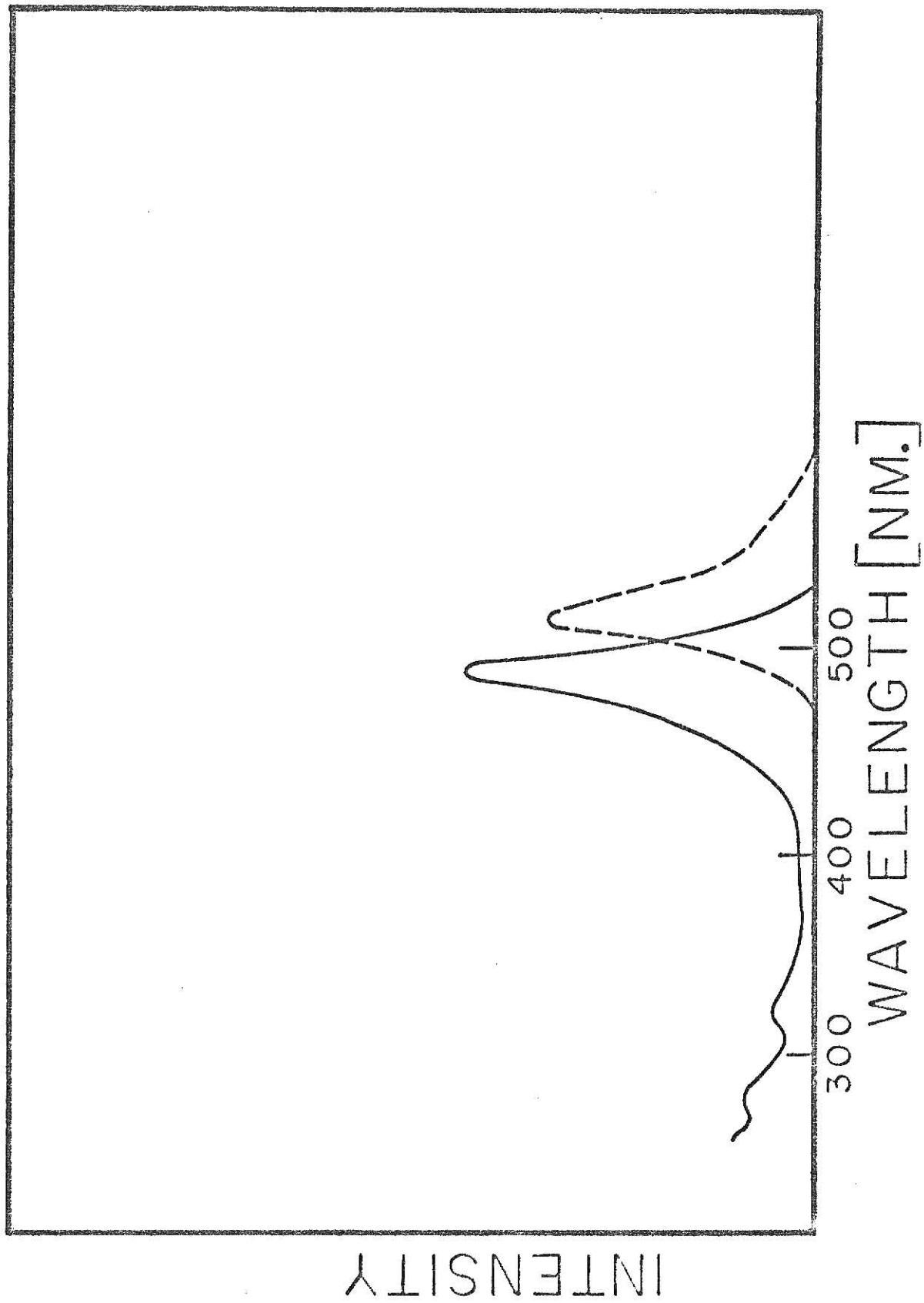
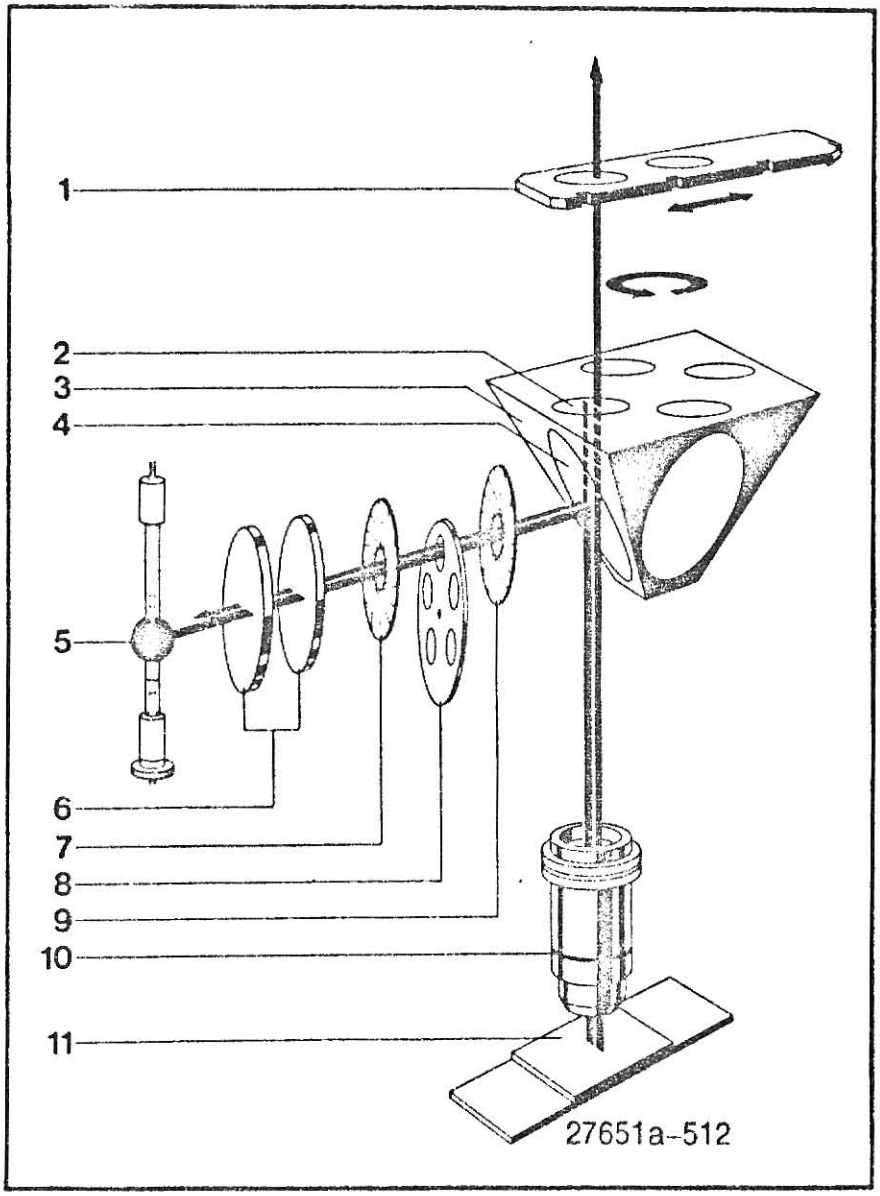

INTENSITY
300
400
500
WAVELENGTH [NM.]

PLATE XII

Ploem Illuminator Construction Schematic.


1
2
3
4
5
6
7
8
9
10
11
27651a-512

the area of interference band-pass filters. The present state-of-the art in interference-thin film filters is in the design of filters with extremely sharp cut-off frequencies, narrow-band-pass and wide-band-pass characteristics over the entire visible spectrum and into the ultraviolet. At this point, it suffices to say that adequate filter designs are available for virtually all fluorescence analysis work. Plates IX and X depict the spectral characteristics of the filters used in this experiment. Owing to the sharp cut-off of the barrier filters used, the laser light is essentially removed from the fluorescence signal, despite the close proximity of the absorption and emission peaks of fluorescein situated at 490 and 520 nm, respectively. Plate XI shows plots of these peaks. The fluorescence can now be detected either visually or electro-optically by sliding the microscope-incorporated prism in and out of the optical path.

A more recent method of illumination employs vertical incident illumination as described by Ploem[30] and pictured diagrammatically in Plate XII. As an entire unit the Ploem illuminator incorporates four complete sets of barrier and exciter filters which allow for either ultraviolet, ultraviolet-blue, blue, or green fluorescence excitation by merely rotating the appropriate filters into place. In view of the fact that only fluorescein fluorochrome is used, the Ploem illuminator reduces to a rather simple piece of apparatus, as shown in Plate VIII. The heart of the vertical illuminator is the use of dichroic mirrors which transmit a given range of wavelengths and reflect others. Making use of this fact, the dichroic mirror reflects the exciting light through the objective, which focusses the light onto the sample. The advantage of this technique lies in the fact that both the image and illumination are brought into simultaneous focus by the

objective, thus eliminating the need for a separate substage condenser. As with the transmitted illumination technique, the fluorescence signal is collected by the objective and filtered by the dichroic mirror and then transmitted to either the ocular or monochromator.

Both illumination techniques were used in preliminary experimentation. The transmitted illumination technique proved far superior to the Ploem Illuminator and therefore was used exclusively for the data to be presented. The difficulties with the Ploem Illuminator are all due to the use of lasers. Kauffman[18] and workers reported that the dichroic mirrors auto-fluoresced strongly under 488.0 nm laser radiation and stated that suitable filters must be substituted. The other main difficulty arises from the beam collimation. Visual observation revealed that only the central portion of the field of view was illuminated - a problem not associated with conventional light sources. A solution to this problem requires some means of reducing beam collimation just prior to entry of the illuminator, possibly by a system of lenses. At this time no endeavor has been designed which will relieve the problem.

3. Condensers

It was pointed out in the previous section that there was a need for maximizing the amount of exciting radiation to be incident onto the sample. The limitation on fluorescence signal is ultimately the power density provided by the condenser since the objective has a fixed field of view. Obviously this is the quantity to be maximized in order to compensate for weakly fluorescent samples or signal losses in the microscope throughput. For transmitted substage illumination this was provided by condensers of

two types:

a) bright field and

b) dark field,

both of which were used for preliminary experimentation. However, the dark field condenser served the purpose quite well and therefore was used exclusively for the actual lifetime measurements. Each has its own advantages and disadvantages when compared to the other and only the given experimental conditions will govern which is more appropriate.

Plate XIII shows the features common to all dark field condensers and the particular type used in this work was a Leitz dry dark field condenser of numerical aperture 0.80-0.95. Obviously, in order to preserve the dark field characteristics, objectives with numerical aperture greater than 0.90 were not used due to the large angle subtended from the focal point to the objective.

The dark field condenser eliminates the central portion of the incident beam and focus the periphery onto the sample by a reflecting system, as shown in the Plate XIII cross-sectional view. It is because of this optical technique that the diverging lens in substage illumination becomes mandatory when employing laser radiation. With standard sources such as mercury or xenon lamps the emission is collected and collimated into a broad beam, of approximately uniform power profile, sufficient to illuminate the total condenser acceptance area. Under normal conditions the aperture stop of the dark field condenser is of sufficient diameter to completely block the nearly collimated laser beam. Therefore a divergent lens must be used to enlarge the beam to illuminate adequately the aperture periphery. Obviously, dark field condensers should not be used when working at exceedingly low illumination levels or with exceedingly low fluorescence yields if at all possible.

Otherwise, a means of controlled beam expansion becomes necessary in order to maximize the laser power deposited in the aperture periphery.

Another difficulty encountered with the use of the dark field condenser arises when the means of focus is considered. Since only the periphery of the beam is focussed, the emerging light is contained within a cone with the vertex at the focal point. However, the cone of light is hollow and should the sample be positioned below or above the focal point, the illuminated area will be a circular cross-section of the cone with only the perimeter illuminated. Thus, any attempt to de-focus, whether unintentional or for the purpose of decreasing the power density, will result in a substantial loss of illumination in the field of view. Focusing of the beam in this manner also leads to serious problems when using coherent radiation sources. Specifically, the dark field condenser blocks the central portion of the beam and then collects the remainder. Since each portion of the apertured beam is correlated, strong and adverse diffraction effects can easily detract from the low intensity image quality. Therefore, proper substage alignment was constantly maintained to reduce the problem to a minimum.

Consideration of these problems associated with the dark field condenser brings us immediately to the use of the bright field condenser shown in Plate XIV. Because all of the exciting radiation is collected and focussed onto the sample, much lower source powers can be effectively used but with the added problem of increased laser light introduced into the objective aperture. As is well known, the added background can be well tolerated provided that proper filtration is used and that the fluorescence easily contrasts the background. In this experiment a monochromator was used in addition to barrier filters and therefore only visual observation of the

PLATE XIII

Typical Cardiod Darkground Condenser

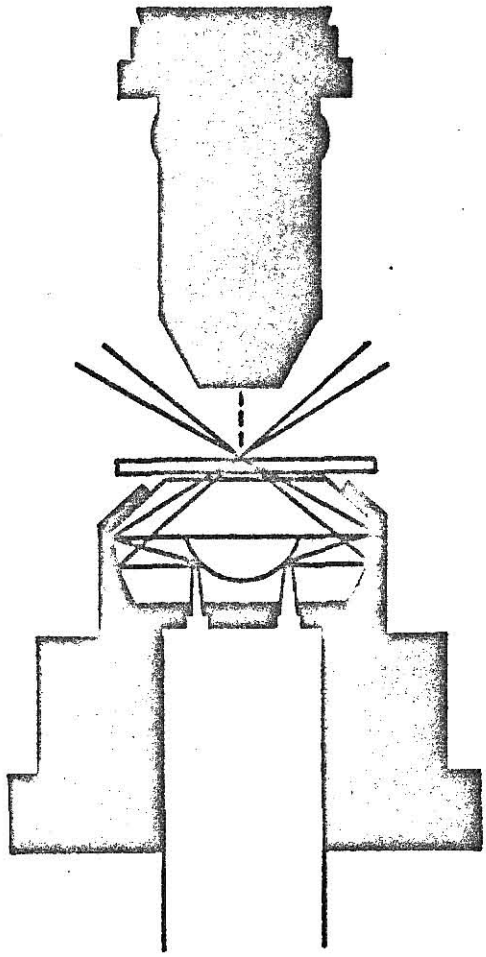
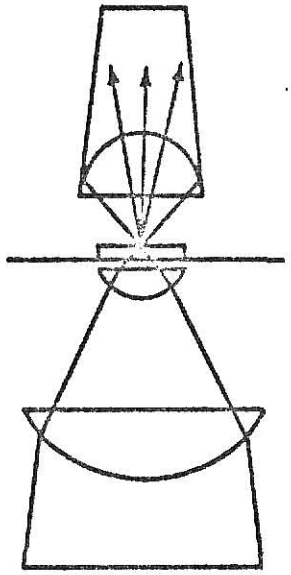


PLATE XIV

Typical Brightfield Condenser.



sample may be hindered by using the bright field condenser.

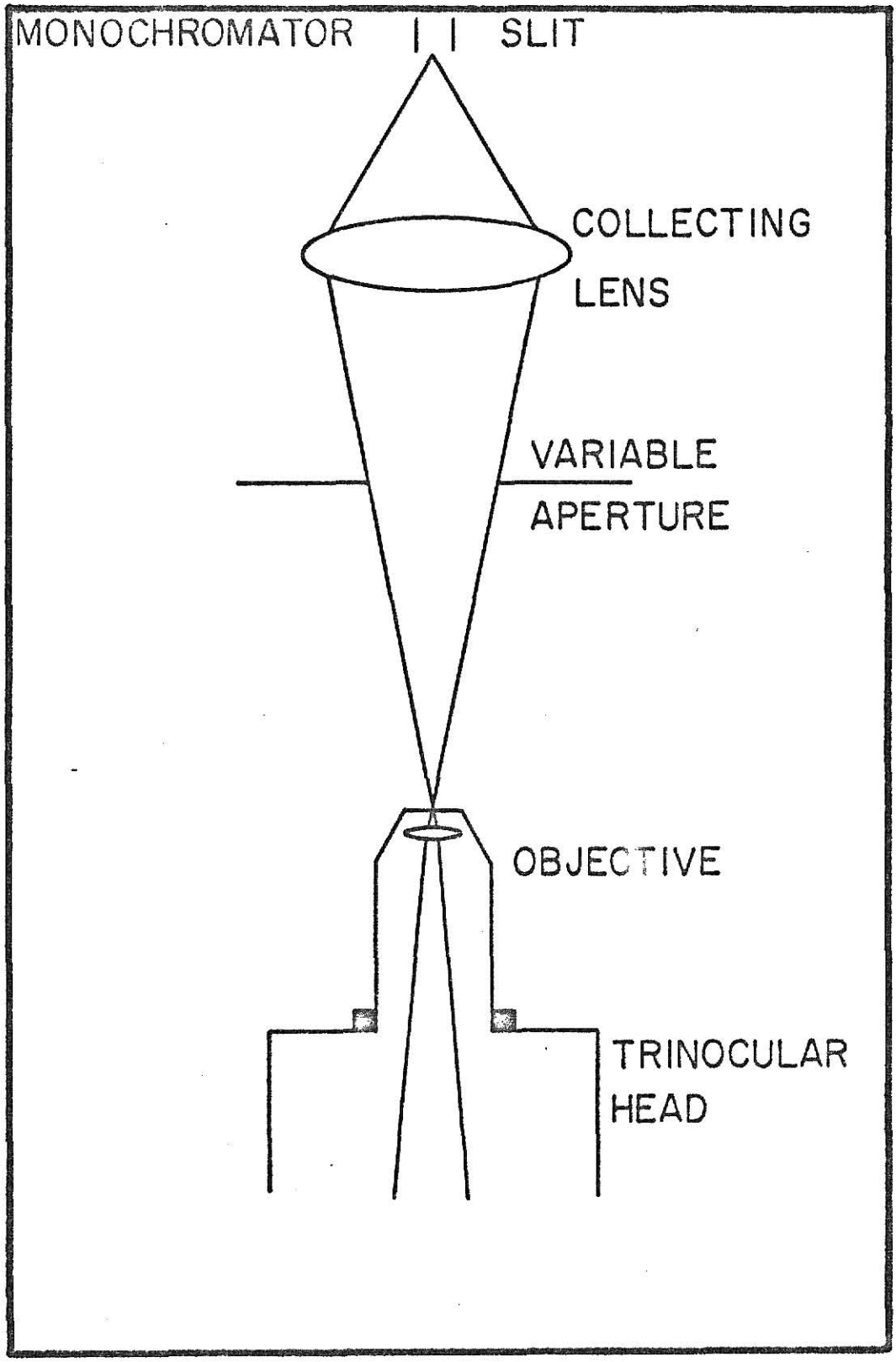
4. Field-Limiting Aperture

Due to the fact that individual cells were to be analyzed, it appeared to be beneficial to have some means by which each cell or part of each cell, would be isolated from the background and remaining field of view. The importance of cell isolation becomes important for two reasons. First, the lifetimes of the excited state within the cell may be different from the lifetime of the non-specific fluorescence present in the media and inclusion of the background will distort the data in a manner which cannot be accurately corrected. Second, single-photon counting techniques require low signal levels and thus the signal-to-noise ratio will be very low unless the background is eliminated. However, the trinocular head does not produce the same magnification for quantitative analysis as for visual observation through the oculars. Rather, the oculars used provided an additional factor of 16 in magnification. This means that additional enlargement must be used in order to produce images substantial in size to allow for adequate masking.

As shown in Plate XV the required enlargement was provided by an inverted 22X objective of numerical aperture 0.65, which gave variable enlargement depending on the distance from the objective. At this point the specific cell to be analyzed has been magnified sufficiently large to ensure that a minimum, if any, of the remaining field of view is passed through the variable aperture. Fortunately, the yeast cells used were quite substantial in diameter (~7 microns), making them quite easy to isolate by masking. Immediately following the aperture is the collecting lens which subsequently demagnifies and focuses the cell image onto the monochromator slit.

PLATE XV

Field-limiting aperture schematic as used to isolate the sample cell from the background.


MONOCHROMATOR
SLIT
COLLECTING
LENS
VARIABLE
APERTURE
OBJECTIVE
TRINOCULAR
HEAD

To remove ambiguity, Plate XV requires further explanation. The particular inverted objective, in conjunction with the microscope optics, resulted in a projected image whose size depended on the distance from the inverted objective to the aperture. Strictly speaking, the aperture must lie in an image plane to provide for good, masked, image quality. However, due to the particular optical arrangement, good focal image quality was maintained throughout a large range of magnifications. Compensating for any flaws in the masking ability of the aperture was the above mentioned cell size allowing for spectroscopical observation of only the central portion of the cell.

C. Sample Preparation Methodology

In order that the data obtained should be meaningful, the samples were necessarily prepared in a fashion suitable for lifetime spectra comparison. It must be stated that, since the motivation for this thesis is based on investigating the validity of a previous assumption and previous experimentation, sample preparation was carried out in a manner identical with that described in earlier reports[14]. However, all attempts to duplicate the results of earlier investigators resulted in either complete failure or unreproducible samples. Whether the problem lies in an incomplete description by these investigators or with our technique of sample preparation has not been determined and only after following a special procedure of preparation were suitably fluorescent samples obtained. The procedure followed for sample preparation is discussed below, supplemented with tables providing cell culture growth information and the cells and solutions used for experiments. Appendix I will provide the exact time table and observations

recorded leading to the procurement of suitably fluorescent cell samples.

For the fastest rate of enzymatic hydrolysis and large quantum yields of fluorescence the optimum molarity of FDA solution appeared to be 100 μM. Substantial fluorescence has been earlier reported[14] with the enzymatic hydrolysis of 2.5 μM FDA in yeast, but we were completely unable to obtain results at this concentration and, furthermore, only occasional fluorescence was observed with 10 μM, 25 μM, and 50 μM solutions of FDA. Corresponding to each of these concentrations the cells and FDA solutions were allowed to stand for up to 60 minutes with only an occasional cell exhibiting fluorescence after this time. Using concentrations much above 100 μM resulted in unwanted precipitate in the solution. Table IV provides a list of the FDA dilutions used prepared from a fresh base solution of 10^4 μM FDA in acetone.

Observation showed that the dilutions and base solution given in Table IV must be kept at temperature substantially below room temperature at all times. A temperature of 0°C or cooler proved to be quite sufficient for efficient cell/FDA interaction to occur. Using FDA solutions that had been standing at room temperature for any period of time greater than 10 minutes showed a serious loss of activity in the hydrolysis/absorption process with a decline of nearly 100% in activity after 1 hour at room temperature. No explanation for this peculiar behavior is offered at this time although it was found that this is the most critical factor in the hydrolysis/fluorescence process. However, dilutions must be brought to room temperature by such means as stirring the sample vile in water just prior to addition of cells in order to avoid the risk of chilling the cells to the point at which cell performance, such as hydrolysis rate, is altered.

From the point of view of simply obtaining cell fluorescence it is not critical to any extent whether or not cells are left standing at room temperature in water after removal from the culture. However, it was observed that significant background fluorescence was present the longer that the cells remained in sterile water at room temperature before addition to FDA and also the longer that the cell/FDA mixture was allowed to stand at room temperature. In either case, the background, although noticeable spectroscopically, caused no problems in observance of cell fluorescence. The reason for fluorescence not interfering with cell observation has been previously stated. That is, cellular size permitted viewing of the central portion of the cell only.

Using a fresh 100 μM FDA dilution a satisfactory amount of cell fluorescence could be observed approximately 30 minutes after the cell/FDA mixture was initiated and the fluorescence per cell appeared to be quite stable for periods of up to several hours. Noticeable and significant background fluorescence did not occur until 2 to 3 hours after initial mixing. Even at this point the change in cell fluorescence was negligible (approximately constant), indicating that the cell/FDA absorption-diffusion process had possibly equilibrated.

In so far as the above effects were noted in relation to the rate of hydrolysis and quantum efficiency in a qualitative way, no attempt was made to determine any kinetic factors such as rate constants for the hydrolysis process or to determine the effect of cell culture growth stage on these processes. However, throughout all microscopical observations there did not appear to be any preferential stage of the cell cycle. While not all cells were involved in the absorption/hydrolysis process an equal percentage of budded and unbudded cells produced fluorescence. Since the

only phenomena of particular interest to this thesis are lifetime-media effects, cell culture growth rates were recorded as in Tables V and VI for possible correlation with the times at which data were taken on the samples. It is seen that, according to Appendix I, the cells, when properly mixed with FDA, retain their ability to hydrolyze and hold a substantial volume-concentration of fluorescein after at least 11 hours in the culture and upto 15 hours time in the culture plus upto at least an additional 12 hours after removal from the culture.

In addition to data taken on internal and external cell fluorescence, experiments were performed on different concentrations of fluorescein solutions. The purpose of these experiments was not to provide any detailed information other than to simply obtain a possible estimate of instrumental variations and/or concentration effects on the fluorescence lifetime. The solutions of diluted fluorescein are stated in Table V.

TABLE IV

FDA dilutions from stock solution of 10^4 μM FDA in acetone.

Solution	Dilution
100 µM FDA	2 × .025 mℓ FDA: 4.95 mℓ sterile H_2O
25 µM FDA	1 mℓ 100 µM FDA: 3 mℓ sterile H_2O
10 µM FDA	.5 mℓ 100 µM FDA: 4.5 mℓ sterile H_2O

TABLE V

A listing of samples prepared in order.that lifetime spectra could be made and compared.

Saccharomyces cerevisiae

	Strain	Type	
1)	XL67B - 3a	4n Mating Type a (Tetraploid)	
2)	X2180 - 1B	1n Mating Type a	
3)	XP300 - 26C		(Grown but not used)

Pure Fluorescein Solutions

	Molarity	Solution	Dilution
1)	10^{-4} Molar	#1	
2)	$.33\times10^{-4}$ Molar	#2	1 mℓ 10^{-4}M: 1.0 mℓ H_2O
3)	$.909\times10^{-5}$ Molar	#3	.1 mℓ 10^{-4}M: 1.0 mℓ H_2O
4)	$.476\times10^{-5}$ Molar	#4	.1 mℓ 10^{-4}M: 2.0 mℓ H_2O

TABLE VI

Cell count for samples used in Spectra J-Series, K-Series, and L-Series.

Time 0:00 hours started cultures @10^6 cells/mℓ in SC.

TIME	STRAIN	CELL/mℓ IN CULTURE	DILUTION
4:15 hours	XP300-26C	3.75×10^6	1/10×1/100
	X2180-1B	4.20×10^6	1/10×1/100
	XL67B-3a	3.89×10^6	1/10×1/100
6:00 hours	XP300-26C	5.42×10^6	1/10×1/100
	X2180-1B	7.83×10^6	1/10×1/100
	XL67B-3a	7.36×10^6	1/10×1/100
10:45 hours	XP300-26C	4.84×10^7	1/50×1/100
12:50 hours	X2180-1B	7.7×10^7	1/50×1/100
	XL67B-3a	2.94×10^7	1/10×1/100
15:20 hours	X2180-1B	6.15×10^8	1/50×1/100
	XL67B-3a	8.06×10^7	1/50×1/100
	XP300-26C	1.46×10^8	1/50×1/100

III. DATA ANALYSIS

A. Formulation and Theory

Generally, the measurement of excited-state decay lifetimes involves the measurement of transients that occur on the nanosecond time scale. In view of this short decay lifetime, the limiting factor in such an experiment is commonly the finite decay lifetime, or rather the full width at half maximum (FWHM), of the excitation source which are generally of the order of nanoseconds in duration. Indeed, in this thesis the laser excitation pulse width has been measured to be approximately 7 nanoseconds and since fluorescence decay times on the order of nanoseconds were initially anticipated, it became necessary to extract the desired information from the data by means of deconvolution. The necessity for this procedure arises because any decay time that is similar in duration to the excitation pulse will produce only a slight broadening or distortion in the tail of the excitation decay spectrum. Should the decay time to be measured be many times greater than the excitation pulse, direct determination of this decay time may be affected, assuming the proper decay law is known.

Consider again the fluorescence decay time which is nearly the same as the excitation decay time. As mentioned, measurement of this transient will involve distortion due to the excitation decay and the problem arises as to which means for analytically and numerically obtaining the desired data is appropriate. Several methods have been proposed and used effectively in the literature. Among these are

(1) the method of moments[31],

(2) Fourier transform[20],

(3) Laplace transform[20], and

(4) the Multiple-series method[32].

A complete treatise on these techniques is given in the provided references and it will suffice to say that all four methods work well under certain different circumstances. However, all methods are based upon the theoretical foundation that the undistorted decay function, G(t), and the excitation pulse distorted by the detection system, I(t), strictly obey the convolution theorem. In a precise formulation this theorem is stated as

$$F(t) = \int_0^{t_N} I(t)\, G(t_N - t)\, d(t) = \int_0^{t_N} I(t_N - t')\, G(t')\, dt' \qquad \text{Eq. 1}$$

where

F(t) = observed, or calculated, decay spectrum,

I(t) = instrument function including any distortion of the detection system, and

G(t) = decay function response to undistorted delta-pulse excitation.

The justification for assuming the validity of this formulation is well founded on mathematical grounds by the principle of superposition in transform space[32]. However, this is not a very physically enlightening approach nor is it a justification on a physical basis. Therefore, I wish to approach the problem from a strictly experimental view and show that indeed the convolution theorem is obeyed for specified functions.

Assume for convenience that the desired decay function is purely exponential,

i.e.,

$$G(t) = Ae^{-t'/\alpha} \qquad \text{Eq. 2}$$

where

A = normalization constant

α = decay lifetime

t'= dummy variable to describe the decay relative to the excitation.

Experimentally, what we observe is a spectrum of intensity (counts) vs. time (channels). Due to the nature of data acquisition, time is no longer a continuous variable. Rather, it is discretely broken down into channels, each of width $\Delta t'$ predetermined by experimental considerations. For a delta-pulse excitation, what is observed is the resultant decay spectrum

$$F(t_N) = G(t_N) = A_N e^{-t'_N/\alpha} \quad , \qquad \text{Eq. 3}$$

where the subscript (N) is to denote the discrete nature of the time base measurement. However, reality forbids such a function and the finite time width of the excitation must now be considered. This situation is shown in Plate XVI. Fundamentally, we see that each channel representing a time interval $\Delta t'$ can be considered to give rise to excitation and that the decay does not arise strictly from an instantaneous pulse at the beginning of each channel as shown in Plate XVI. This has been drawn primarily for clarity of understanding the underlying principle. Now consider N channels labeled 1 to N as in Plate XVII, where (I_N) represents the number of counts in the N^{th} channel and $\Delta t'$ is denoted as before as the time parameter to measure the decay after excitation at t'_N. Therefore, we can express

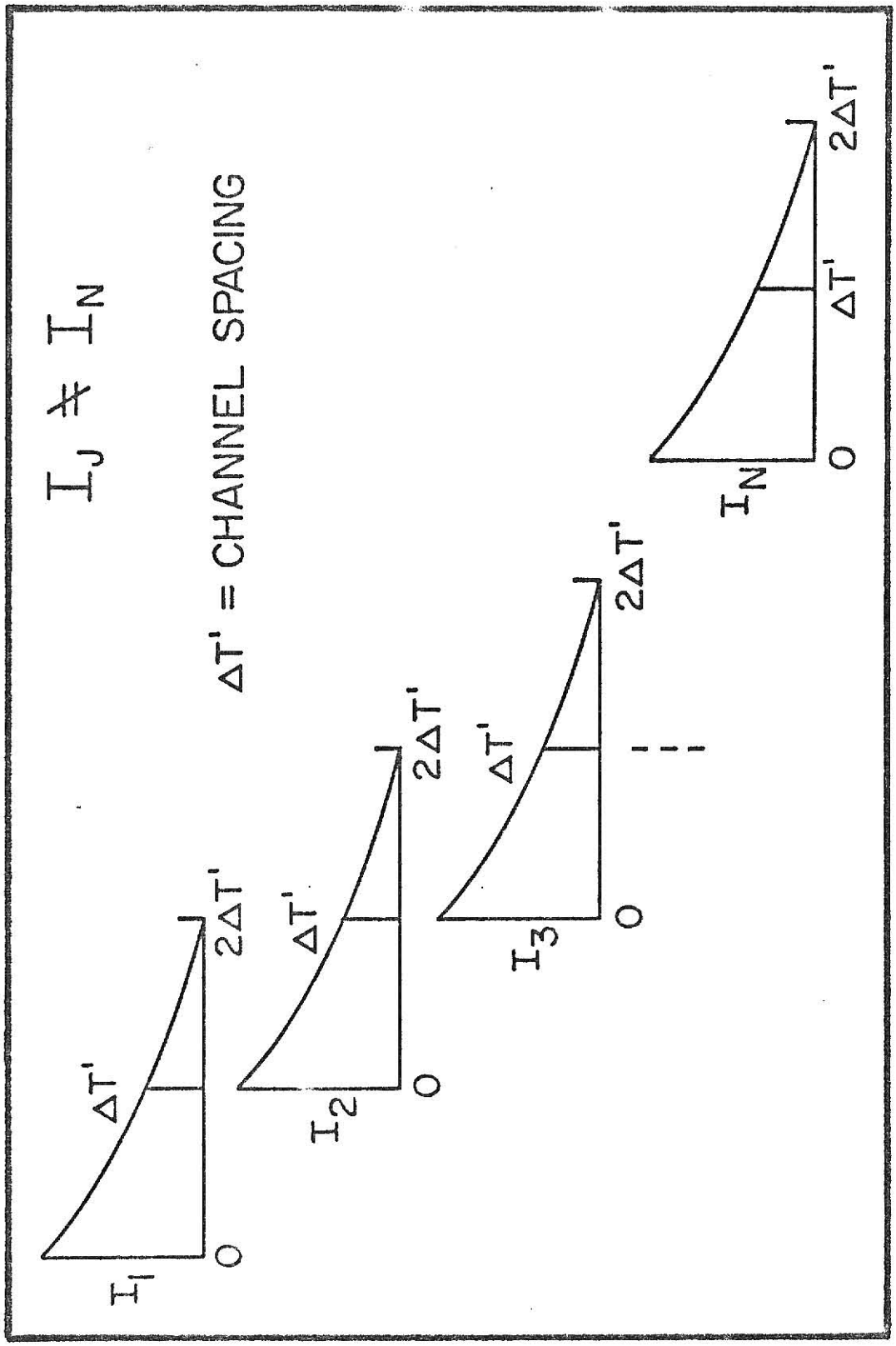
PLATE XVI

An idealized model of convolution showing an excitation pulse and several resultant decays which add superpositionally per channel.

COUNTS
CHANNELS [T']
ΔT'

PLATE XVII

A model describing the channel-decay superposition in a general N^{th} channel fashion.


$I_J \neq I_N$
$\Delta T'$ = CHANNEL SPACING
I_1
I_2
I_3
I_N
$\Delta T'$
$2\Delta T'$
0

$$G(t_N') = I_N e^{-t_N'/\alpha} . \qquad \text{Eq. 4}$$

We wish to find the total contribution in the N^{th} channel due to all other previous channels of excitation.

In order to preserve the number of counts, it must be required that

$$\int_0^\infty A_N e^{-t'/\alpha}\, dt' = I_N = A_N \int_0^\infty e^{-t'/\alpha}\, dt' \quad . \qquad \text{Eq. 5}$$

Upon evaluation we find that

$$A = I_N/\alpha \quad . \qquad \text{Eq. 6}$$

Proceeding channel by channel and using conservation of counts, we ascertain the following:

Channel 1 contributions:

$$I_1 \int_0^\infty e^{-t'/\alpha}\, d\left(\frac{t'}{\alpha}\right) = I_1 = I_1 \left\{ \int_0^{\Delta t'} e^{-t'/\alpha}\, d\left(\frac{t'}{\alpha}\right) + \int_{\Delta t'}^\infty e^{-t'/\alpha}\, d\left(\frac{t'}{\alpha}\right) \right\} \qquad \text{Eq. 7}$$

$$I_1 \int_0^{\Delta t'} e^{-t'/\alpha}\, d\left(\frac{t'}{\alpha}\right) = I_1 \left\{ 1 - \int_{\Delta t'}^\infty e^{-t'/\alpha}\, d\left(\frac{t'}{\alpha}\right) \right\} = I_1 \left\{ 1 - e^{-\Delta t'/\alpha} . \right\} \qquad \text{Eq. 8}$$

Therefore, the contribution in channel 1 is

$$I_1 \left[1 - e^{-\Delta t'/\alpha} \right] \quad . \qquad \text{Eq. 9}$$

Channel 2 contributions:

$$I_1 \int_0^{\infty} e^{-t'/\alpha} d\left(\frac{t'}{\alpha}\right) = I_1 = I_1 \left\{ \int_0^{\Delta t'} e^{-t'/\alpha} d\left(\frac{t'}{\alpha}\right) + \int_{\Delta t'}^{2\Delta t'} e^{-t'/\alpha} d\left(\frac{t'}{\alpha}\right) + \int_{2\Delta t'}^{\infty} e^{-t'/\alpha} d\left(\frac{t'}{\alpha}\right) \right\} \qquad \text{Eq. 10}$$

The contribution in channel 2, due to channel 1 is

$$I_1 \int_{\Delta t'}^{2\Delta t'} e^{-t'/\alpha} d\left(\frac{t'}{\alpha}\right) = I_1 \left\{ 1 - \int_0^{\Delta t'} e^{-t'/\alpha} d\left(\frac{t'}{\alpha}\right) - \int_{2\Delta t'}^{\infty} e^{-t'/\alpha} d\left(\frac{t'}{\alpha}\right) \right\} \qquad \text{Eq. 11a}$$

$$= I_1 \left\{ e^{-\Delta t'/\alpha} - e^{-2\Delta t'/\alpha} \right\} \quad . \qquad \text{Eq. 11b}$$

However, there is a contribution in channel 2 due to channel 2 excitation, given by

$$I_2 \left[1 - e^{-\Delta t'/\alpha} \right] \quad . \qquad \text{Eq. 12}$$

Summing these two contributions, we obtain the total contribution in channel 2 to be

$$\left\{ I_1 e^{-\Delta t'/\alpha} + I_2 \right\} \left\{ 1 - e^{-\Delta t'/\alpha} \right\} \quad . \qquad \text{Eq. 13}$$

Channel 3 contributions:

In order to avoid the tedium of algebra I will state only the result, which is obtained in the same manner as for channels 1 and 2:

$$\left[I_1 e^{-2\Delta t'/\alpha} + I_2 e^{-\Delta t'/\alpha} + I_3 \right] \left[1 - e^{-\Delta t'/\alpha} \right] . \qquad \text{Eq. 14}$$

The pattern of development is now apparent and the expressions may therefore be generalized to the total N^{th} channel contributions.

$$I_N^C = \sum_{j=1}^{N} I_j e^{-(N-j)\Delta t'/\alpha} \left\{ 1 - e^{-\Delta t'/\alpha} \right\} \qquad \text{Eq. 15a}$$

$$= \left\{ 1 - e^{-\Delta t'/\alpha} \right\} \sum_{j=1}^{N} I_j e^{-(N-j)\Delta t'/\alpha} . \qquad \text{Eq. 15b}$$

In order to verify that this is the convolution theorem in discrete form, equation (15) must possess certain analytical properties.

A. In the limit as α approaches zero, we no longer have multiple contributions in a given channel. Therefore, the sum collapses to a single term for which N = j.

$$\lim_{\alpha \to 0} I_j^C = I_N = \lim_{\alpha \to 0} \left\{ 1 - e^{-\Delta t'/\alpha} \right\} I_N = I_N . \qquad \text{Eq. 16}$$

B. In the limit as α tends to infinity we find

$$\lim_{\alpha\to\infty} \quad I_N^C \longrightarrow \sum_{j=1}^{N} I_j \left[1-1\right] \times 1 = 0 \ , \qquad \text{Eq. 17}$$

which implies there is no emission which is in agreement with one might expect for an ∞-lifetime.

C. In the limit that $\Delta t'$ tends to zero, we note N tends to infinity. Since the sum must remain finite, it follows that

(1) $\quad \frac{N\Delta t'}{\alpha} \longrightarrow \frac{t_n}{\alpha}$,

(2) $\quad \frac{j\Delta t'}{\alpha} \longrightarrow \frac{t}{\alpha}$,

(3) $\quad \frac{\Delta t'}{\alpha} \longrightarrow d\left(\frac{t}{\alpha}\right)$, and

$$\lim_{\Delta t'\to 0} \left\{1 - e^{-\Delta t'/\alpha}\right\} \sum_{j=1}^{N} I_j e^{-(N-j)\Delta t'/\alpha} = \int_0^{t_n} I(t)\, e^{(t_n-t)/\alpha} d\left(\frac{t}{\alpha}\right) \qquad \text{Eq. 18}$$

where $e^{-\Delta t'/\alpha}$ has been expanded in a power series. Equation (18) is simply the convolution integral as stated in Equation (1) for the case of a purely exponential decay law, we see that indeed there is a physical basis for requiring the specified function I(t) and G(t) to obey the convolution theorem.

Equation (15) is particularly useful for computer analysis for three reasons:

(1) The summation is carried out over distinct, equidistant channels specified by integers.

(2) The function G(t) need not be necessarily purely exponential. Rather,

any desired decay may be used to provide a closed form discrete function, provided that the initial integrations are capable of analytical evaluation. Being that decay laws are generally of simple form, this is no problem.

(3) The function I(t) is by nature empirically discrete.

Appendix II provides a suitable program for data analysis employing Equation (15) and a documentary of the program functions. Reasons for employing the specified form for G(t) will soon become apparent, primarily for statistical rather than necessarily physical considerations.

B. Statistics and Errors

Rather than dwell heavily on a qualitative discussion of the decay lifetime data at this stage, clarity and conciseness require that data presentation and interpretation be deferred until the next chapter. Therefore, so that the results obtained can be viewed in the proper perspective with respect to statistical and instrumental uncertainties, I now wish to qualify the discussion which follows with appropriate reasoning the presented estimates.

Initially, it is important to establish the instrumental variability since this will turn out to be the largest uncertainty in determining the decay lifetimes. Such factors that must be included in this estimate are (1) the timing jitter associated with triggering, (2) the discriminator timing jitter and walk as well as (3) the transit time variations within the photomultiplier tube. Each source of error need not be specified since an estimate can be determined experimentally. Unfortunately, a large sample of such data necessary for a highly accurate estimate is not

available and the estimate to be calculated is made from a small sample of the data presented in Table VII. Using the obtained lifetimes for experiments run consecutively on a given concentration of pure fluorescein solution, in particular, spectra G-2A, G-2B, G-2C and the equations for calculating sample means and sample variances, the estimate obtained is

$$\sigma \simeq S = .374 \text{ channels.}$$

The particular equations[33] used in this estimate are

$$\mu \simeq \bar{y} = \frac{1}{N} \sum y_i \quad \text{and} \qquad \text{Eq. 19}$$

$$\sigma \simeq S = \frac{1}{N-1} \sum (y_i - \bar{y})^2 \quad , \qquad \text{Eq. 20}$$

where

$\bar{y}$ = the sample mean, an estimate of the true parent distribution value, μ,

S = the sample standard deviation, an estimate of the true parent distribution standard deviation, and

y_i = the individual lifetime values used in the estimate.

However, being that the number of data values used in this calculation is only three, it is clear that the obtained estimate is actually larger than what would be obtained had many more values been measured. Therefore, the quoted value of .374 channels for the instrumental uncertainty is an upper bound. As a further check on the instrumental stability, all data presented and analyzed is in a format using two instrument functions for the initial data deconvolution. The purpose of this is quite simply to present numerically and graphically the explicit effect which the instrumental

TABLE VII

Computer-calculated output of a representative sample of collected data.

Instrument function: H-2A

File	Data Spectrum	χ^2	Total Error	Lifetime (channels)	Lifetime Uncertainty
AA FITBIN	L-2B	1.41	.099	3.69	.083
BB	L-1B	1.66	.111	4.00	.086
CC	L-3A	.945	.081	4.25	.084
DD	L-1A	1.30	.107	5.58	.094
EE	K-3B	.600	.068	5.04	.088
FF	K-2B	.967	.080	4.64	.081
GG	K-1B	.663	.074	5.53	.091
HH	K-3A	.734	.076	5.04	.088
II	K-2A	.843	.082	5.10	.090
JJ	K-1A	.900	.087	5.74	.092
KK	J-3B	.841	.087	5.95	.095
LL	J-2B	.768	.081	6.17	.092
MM	J-1B	.788	.083	6.00	.093
NN	J-3A	1.16	.096	4.89	.089
OO	J-2A	.959	.086	5.14	.088
PP	J-1A	.646	.075	5.89	.093
QQ	E-1	1.23	.104	5.30	.094
RR	G-4C	2.39	.142	4.85	.092
SS	G-4B	.964	.093	5.58	.094

File	Data Spectrum	χ^2	Total Error	Lifetime (channels)	Lifetime Uncertainty
TT	G-3B	1.50	.114	5.19	.093
UU	G-3A	1.03	.095	5.52	.094
VV	G-2C	.808	.083	5.94	.092
WW	G-2B	.819	.087	6.53	.096
XX	G-2A	.786	.084	5.85	.095
YY	G-1B	.636	.076	5.95	.096
ZZ	G-1A	2.51	.149	5.29	.094
ØØ	F-1A	.616	.076	6.25	.097

TABLE VIII

Statistics of a representative sample of collected data.

Spectrum	Counts (peak)	σ_{peak} (Poisson)	Counts (Total)	Duration (sec)	Average rate of Data Collection
F-1A	632	25.14	12816	1268	10.11
G-1A	605	24.60	12809	1533	8.36
G-1B	642	25.34	12812	1291	9.92
G-2A	633	25.16	12808	1264	10.13
G-2B	636	25.22	12795	1296	9.87
G-2C	621	24.92	12824	1560	8.22
G-3A	655	25.60	12812	1539	8.32
G-3B	667	25.83	12808	1468	8.72
G-4B	632	25.14	13003	1458	8.92
G-4C	641	25.32	12816	1339	9.57
E-1	627	25.04	12796	1470	8.70
J-1A	733	27.07	14841	1586	9.36
J-2A	751	27.40	14848	1440	10.31
J-3A	708	26.61	14022	1796	7.80
J-1B	688	26.23	14270	1556	9.17
J-2B	689	26.25	14313	1565	9.14
J-3B	696	26.38	14682	1485	9.88
K-1A	732	27.06	14914	1648	9.05
K-2A	704	26.53	14401	1257	11.46
K-3A	763	27.62	14577	1473	9.90
K-1B	738	27.17	15236	1432	10.64

Spectrum	Counts (peak)	σ_{peak} (Poisson)	Counts (Total)	Duration (sec)	Average rate of Data Collection
K-2B	761	27.59	14011	1652	8.48
K-3B	782	27.96	14014	1858	7.54
L-1A	736	27.13	15275	1416	10.79
L-3A	713	26.70	14467	1920	7.53
L-1B	748	27.35	14029	1689	8.31
L-2B	824	28.70	14033	1727	8.12
M-1	747	27.33	10310	1145	9.00
H-2A	674	25.96	9619	806	11.94

variabilities have on the data. It should be pointed out that all results obtained using the two different instrument functions are the same to within the estimated instrumental uncertainty of 6.1%.

In the most general analysis, the decay law, G(t), would necessarily be of a general form which would include a number of variable parameters. Such a form may be[32]

$$G(t) = \sum_{j=1}^{N} A_j e^{-t/\tau_j} \quad , \qquad \text{Eq. 21}$$

where τ_j represents a given set of fixed lifetimes bearing no physical significance necessarily. This expression presupposes no explicit decay law and provides for the extraction of more than one possible decay mode in the samples. However, using such a technique is beneficial only in the event of very good counting statistics, usually on the order of five decades of counts in the spectrum peak and even under these conditions the significance of more than one extracted lifetime must be carefully scrutinized. Table VIII provides the counting statistics associated with the spectra and inspection shows that the Poisson variance allows for the physically and statistically meaningful existence of only one lifetime. Therefore, the earlier establishments of the form of G(t) to one exponential is thoroughly justified by statistical analysis and the associated deconvolution results.

Statistical treatment of the data in calculating associated fitting errors has been presented in two formats:

(1) The non-linear least squares analysis required for deconvolution is adequately documented in Appendix II specifying the equations used in determining fitting errors and parameter errors,

(2) The linear least squares analysis of the deconvoluted lifetimes presented in the following chapter is based upon the minimization of chi-squared:

$$\chi^2 = \sum \frac{(y_i - a - bx_i)^2}{\sigma_i^2} \quad , \qquad \text{Eq. 22}$$

thus determining the best fit to the straight line given by

$$y = a + bx \quad .$$

In the usual sense[34],

$$a = \frac{1}{\Delta}\left[\sum x_i^2 \sum y_i - \sum x_i \sum x_i y_i \right] \qquad \text{Eq. 23a}$$

$$b = \frac{1}{\Delta} \cdot \left[N \sum x_i y_i - \sum x_i \sum y_i \right], \qquad \text{Eq. 23b}$$

$$\Delta = N \sum x_i^2 - \left[\sum x_i \right]^2 \qquad \text{Eq. 23c}$$

$$\sigma_a^2 = \frac{\sigma^2}{\Delta} \sum x_i^2 \qquad \sigma_b^2 = \frac{N\sigma^2}{\Delta} \quad , \qquad \text{Eq. 23d}$$

$$\sigma^2 \approx S^2 = \frac{1}{N-2} \sum (y_i - a - bx_i)^2, \qquad \text{Eq. 23e}$$

where the notation from this point on in the discussion associates y with the dependent variable decay lifetime and x with the appropriate independent variable.

IV. DATA PRESENTATION

In Chapter III (Section B) it was pointed out that data analysis was carried through by using two instrument functions for variability comparisons. Therefore, seemingly duplicate sets of plots and data tables actually represent the use of these two functions. Inspection of the corresponding legends will clearly indicate which instrument function has been used in order that all plots and data tables may be properly correlated. For both the deconvolution and the linear least squares analysis Tables IX and X provide the specification of the samples used as well as the lifetimes obtained for each instrument function. For all linear fits, the vertical error bars represent the instrumental uncertainty and the horizontal bars merely mark the data points.

A. Deconvolution

Plates XVIII through XXV are a representative selection of the data that have given the best non-linear fits with the model presented in Chapter III (Section A), and were chosen from Tables VII and XI. These tables provide the information calculated by the computer which describe the goodness of fit, fitting error, parameters and parameter uncertainty for all data that was analyzed. These particular plates indicate both the instrument function profile and a given fluorescence decay spectrum which have been normalized to the total number of counts in the instrument function profile.

For reasons specified in Appendix II, the superimposed peaks have been channel-shifted in order to place them in both correct vertical and

horizontal perspective to each other. The criteria for determining the correct channel shift was solely on the basis of which relative peak position yielded the best fit between the observed data and the calculated decay spectrum. The particular decay spectra shown correspond to three different samples: (1) Plates XVIII, XIX, XX and XXI show the decay spectrum of 10^{-4} M solution of fluorescein, (2) Plates XXII and XXIII show the decay spectrum of intracellular fluorescein, and (3) Plates XXIV and XXV show the decay spectrum of background fluorescence in a cell/FDA solution. Using these same spectra Plates XXVI through XXXIII show these spectra with the corresponding computer fits using the two mentioned instrument functions. Examination of these fits and Tables VII and XI indicate that the prescribed use of the described model of convolution and channel shifting appears to be quite legitimate.

Although the fits are generally quite satisfactory, the fluorescence decay spectra indicate that the fit could be improved upon considerably. The initial rise of the peaks appears rather uniform and smooth. However, the peak and entire decay tail exhibit some rather pronounced bumps which can be attributed to a very real instrumental phenomenon, or phenomena. Close inspection reveals that these bumps seem to be quite periodic in nature and therefore may be termed more appropriately as oscillations. Previous reports[16] have indicated that the possible causes for such oscillations or secondary peaks are either varying transit times of photo electrons in the photo multiplier tube caused by maladjustment of the dynode voltages or pickup of r-f noise generated by the excitation source. At the time of this work no attempt has been made to remove these instrumental effects although the means to accomplish this correction are routine.[16]

By comparing Tables VII and XI it is seen that the results of using two instrument functions for the same convolution and fit yield lifetime values that certainly lie within the estimated instrumental uncertainty of .374 channels. Therefore, although the instrument functions appear to be noticeably different, the corresponding decay fits are only slightly different. The differences are within the instrumental error.

B. Concentration-Decay Lifetime Relationship in Pure Fluorescence Solution

Throughout the course of the decay measurements, each lasting on the order of half an hour, the cell without a doubt experiences many changes in environment, both external and internal. Among these changes is the production of fluorescein within the cell structure. This fluorescent dye progresses through a range of intercellular concentrations, which are not known values. As previously discussed, providing that there is sufficient FDA uptake into the cell to balance the rate of fluorescein leakage out of the cell, a temporary steady-state situation is reached where the intracellular fluorescein concentration remains essentially constant. As a consequence it is natural to ask the question, "Is there any significant concentration effect on the decay lifetime in the event that the concentration increases during the experiment"? No attempt has been made to rigorously determine the concentration dependence but only to obtain an estimate. Since this preliminary estimate indicated no significant effect, a rigorous determination was considered unnecessary at this time.

Plates XXXIV and XXXV and their corresponding data Tables XII and XIII show the results of the preliminary investigation, again using the deconvoluted data obtained from two instrument functions. The linear least

squares analysis in Table XII shows the best fit line to have a slope of .445 channels/10^{-4} M, thus initially indicating a possible concentration dependence. However, the uncertainty in the determination of this slope is .399 channels/10^{-4} M. The only conclusion to be reached from the analysis is that there is no concentration dependence of the decay lifetime. This conclusion is not by any means the final word but rather it implies that should there actually be a dependence it is very possibly of minor significance over the range of concentrations used in this study. Obviously, instrumental precision improvement and many more observations are necessary in order to totally confirm this statement. By comparison, the data obtained from the two instrument functions again shows no variability bearing any significance and at this point no further reference will be made to this fact. Data is presented in both fashions and the reader will be left to compare for himself.

C. Cell Culture Age-Decay Lifetime Relationship

Prior to presenting the results concerning cell ages, it must be pointed out that the variable T_1 representing culture age does not necessarily correspond to the time of cell growth within the culture. Specifically, the cells, in some cases, had been removed from the culture several hours before using them. Therefore T_1 actually represents the time of cell growth in the culture plus the time in solution out of the culture until use, based on culture age for convenience. For the J and K-Series spectra, the cell samples were taken from the culture after 12.83 hours and mixed with FDA .42 hours later. The L-Series spectra cell samples were removed from

the culture after 15.33 hours and mixed with FDA 6.17 hours later.

Due to the fact that all but one of the cell samples were removed from the culture at a time when they were progressing from the exponential growth to stationary growth, it has tacitly been assumed that cell variations were minimal with respect to changes due to culture growth. As a consequence the independent variable T_1 may appropriately be described as a measure of the time that the cells were removed from the culture and subsequently left standing in sterile water.

Let us first consider the intracellular fluorescence data presented graphically in Plates XXXVI and XXXVII, and the respective Tables XIV and XV. Once again the results are distinctly conclusive with the uncertainty in the slope, σ_b, on the order of the slope itself. Since the optimal value of the slope is only of magnitude .032 the cell age can be assumed to have no observable effect upon the decay lifetime of intracellular fluorescein. However, if the same analysis is applied to the background fluorescence of the cell/FDA solution the results are quite different, as shown in Plates XXXVIII and XXXIX and Tables XVI and XVII. Inspection reveals that the resultant slope of the linear fit has increased by a factor of nearly ten in magnitude over that of the intracellular fluorescence analysis. Also, the slope is negative and on the order of ten times greater than the uncertainty in the slope. Comparison of these two cases yields possibly profound consequences. If the linear fits are extrapolated to time $T_1 = 0$, the fitting analysis reveals that the associated lifetime differences between the two cases is on the order of 4.1 channels, well outside the limits of instrumental uncertainty. Although measurements were not made on the samples until they had nearly finished exponential growth, such extrapolation may possibly be meaningless. However, such a large change in the fitted slope

throughout the region where measurements had been made indicate strongly that the decay lifetime inside the cell may not be assumed to be identical with that as measured outside of the cell, contrary to assumption by previous investigators[12]. In particular, the comparison shows the decay lifetime out of the cell to be longer than that in the cell initially and for a period of approximately 19 hours. After a 19 hour period the relative magnitudes reverse in size due to the negative slope.

This result is seemingly in agreement with what one might expect to happen. The lifetime inside the cell remains constant due to a possibly higher state of interaction within the cell, thus quenching out the longer excitations and accounting for the initial relative magnitudes of the two values. As time progresses, the cellular leakage of fluorescein produces an increasing concentration of fluorescein in solution and thus enabling concentration quenching to occur, accounting for the decreasing lifetime of the background fluorescence. This is completely compatible with the earlier discussion of concentration effects on the decay lifetime since it is entirely possible that the range of concentrations over which the measurements were made was such as not to display the phenomena of concentration quenching. As a matter of interest, comparison of Tables XII and XIV indicate that the lifetime axis intercepts are equivalent to within the instrumental uncertainty, thus showing that concentration quenching phenomena is possibly dominant in intracellular fluorescence as well as over the range of concentrations used for pure fluorescein. Obviously, an intensive and complete investigation of the possibility of this occurrence is in order for verification.

In relation to the work performed by others regarding polarization effects of intracellular fluorescein, the significance of the results obtained in this thesis strongly indicates that changes in polarization may not be attributable solely to changes in the "structuredness" of the cell at all but rather to concentration effects on the lifetime. Further support of this reasoning lies in the fact that the small changes in polarization observed by others could very likely be due to the result of measurements made on macroscopic samples, from which it is essentially impossible to remove all of the background fluorescence by spinning the cells out of the solution or by filtration as is generally done. This remaining background fluorescence could very likely be contributing to, if not accounting for, the observed polarization characteristics. However, at this time the proposed model has no firm quantitative foundation to rest upon and further investigation is mandatory.

At this stage it is informative to make a quantitative estimate of the degree of polarization that could be expected from the lifetime changes anticipated from the preceeding analysis. Rearrangement of Equation 1 of Chapter I (Section B) yields

$$P = \frac{3}{1+A+6AR\tau} \quad , \qquad \text{Eq. 1a}$$

where

$$A = \frac{1}{P_o} - \frac{1}{3} \quad .$$

Expressing Equation 1a in terms of percentage changes, it can be shown quite simply that

$$\frac{\Delta P}{P} = - \frac{6AR\Delta\tau}{1+A+6AR\tau} \quad . \qquad \text{Eq. 1b}$$

It is seen from this equation that a percentage increase in the lifetime produces a corresponding percentage decrease in the polarization. If the assumptions that the factor 6AR can be neglected with negligible consequences and that $P_o = \frac{1}{7}^{35}$, Equation 1B reduces to

$$\frac{\Delta P}{P} \simeq \Delta\tau/\tau \quad . \quad . \qquad \text{Eq. 1c}$$

From the least squares analysis of Table XVI the best fit linear equation of background fluorescence is

$$\tau_B = 10.05 \text{ channels} - .231\ (T_1) \text{ channels.} \qquad \text{Eq. } 2$$

Evaluating this equation for $T_1 = 23$ hours, the calculated lifetime is

$$\tau_B = 4.74 \text{ channels} \ .$$

Using the data of Table XIV, the intracellular lifetime can be considered to be

$$\tau_I = 5.95 \text{ channels} \ ,$$

indicating a lifetime difference of

$$|\Delta\tau| = 1.21 \text{ channels} \quad .$$

Utilizing Equation 1c,

$$\frac{\Delta P}{P} \simeq \frac{1.21}{5.95} = .203 \quad ,$$

indicating a 20.3% change in polarization from the initial value of P, due to the observed decay lifetime variation. Obviously this effect cannot be considered negligible and, in fact, becomes more significant for smaller values of T_1 according to this analysis.

D. Cell/FDA Mixture Duration - Lifetime Relationship

Plates XL and XLI and Tables XVIII and XIX show the data and analysis parameters associated with assuming a linear relationship between decay lifetime and the time that the cells and FDA were allowed to mix together, specified as T_2. Unfortunately, the results of this analysis do not corroborate the results of the previous section. Rather, it can only be stated that there is no dependence to be seen of the lifetime on T_2 due to the uncertainties in the slopes, σ_b, being on the order of the slope themselves. Although Plates XLII and XLIII and Table XX and XXI, which refer to background fluorescence lifetime as a function of T_2, show an increase in slope of three over that for intracellular fluorescein, it must be noticed that the corresponding increase in slope uncertainty prevents meaningful conclusions to be reached concerning any dependencies.

TABLE IX

Specifications of samples used for data deconvolution, calculated lifetimes included.

Instrument function: M-1

T_1 = culture age

T_2 = time duration of cell/FDA mixture until corresponding spectrum was begun.

Spectrum	Specimen	Concentration (M)	Strain	T_1 (hours)	T_2 (hours)	Lifetime (channels)	Lifetime (nsec)
F-1A	Fluorescein	10^{-4}				6.45	4.24
G-1A	Fluorescein	10^{-4}				5.50	3.61
G-1B	Fluorescein	10^{-4}				6.16	4.05
G-2A	Fluorescein	$.33\times10^{-4}$				6.05	3.98
G-2B	Fluorescein	$.33\times10^{-4}$				6.73	4.42
G-2C	Fluorescein	$.33\times10^{-4}$				6.12	4.02
G-3A	Fluorescein	$.909\times10^{-5}$				5.73	3.76
G-3B	Fluorescein	$.909\times10^{-5}$				5.40	3.55
G-4B	Fluorescein	$.476\times10^{-5}$				5.79	3.80
G-4C	Fluorescein	$.476\times10^{-5}$				5.08	3.34
E-1	Yeast/FDA		XL67B-3a	7.0	1.0	5.50	3.61
J-1A	Yeast/FDA		XL67B-3a	14.0	.75	6.07	3.99
J-2A	Yeast/FDA		XL67B-3a	14.5	1.25	5.32	3.50
J-3A	Yeast/FDA		XL67B-3a	15.0	1.75	5.08	3.34
J-1B	Background		XL67B-3a	16.25	3.0	6.18	4.06
J-2B	Background		XL67B-3a	16.75	3.5	6.34	4.16
J-3B	Background		XL67B-3a	17.25	4.0	6.14	4.03
K-1A	Yeast/FDA		X2180-1B	18.08	4.83	5.93	3.90
K-2A	Yeast/FDA		X2180-1B	18.66	5.42	5.29	3.48
K-3A	Yeast/FDA		X2180-1B	19.08	5.83	5.23	3.44
K-1B	Background		X2180-1B	20.0	6.75	5.71	3.75
K-2B	Background		X2180-1B	20.5	7.25	4.83	3.17
K-3B	Background		X2180-1B	21.0	7.75	5.25	3.45
L-1A	Yeast/FDA		X2180-1B	23.33	1.83	5.77	3.79
L-3A	Yeast/FDA		X2180-1B	24.75	3.25	4.44	2.92
L-1B	Background		X2180-1B	25.83	4.33	4.23	2.78
L-2B	Background		X2180-1B	26.33	4.83	3.91	2.57

TABLE X

Specifications of samples used for data deconvolution, calculated lifetimes included.

Instrument function: H-2A

T_1 = culture age

T_2 = time duration of cell/FDA mixture until corresponding spectrum was begun.

Spectrum	Specimen	Concentration (M)	Strain	T_1 (hours)	T_2 (hours)	Lifetime (channels)	Lifetime (nsec)
F-1A	Fluorescein	10^{-4}				6.25	4.11
G-1A	Fluorescein	10^{-4}				5.29	3.48
G-1B	Fluorescein	10^{-4}				5.95	3.91
G-2A	Fluorescein	$.33\times10^{-4}$				5.85	3.84
G-2B	Fluorescein	$.33\times10^{-4}$				6.53	4.29
G-2C	Fluorescein	$.33\times10^{-4}$				5.94	3.90
G-3A	Fluorescein	$.909\times10^{-5}$				5.52	3.63
G-3B	Fluorescein	$.909\times10^{-5}$				5.19	3.41
G-4B	Fluorescein	$.476\times10^{-5}$				5.58	3.67
G-4C	Fluorescein	$.476\times10^{-5}$				4.85	3.19
E-1	Yeast/FDA		XL67B-3a	7.0	1.0	5.30	3.48
J-1A	Yeast/FDA		XL67B-3a	14.0	.75	5.89	3.87
J-2A	Yeast/FDA		XL67B-3a	14.5	1.25	5.14	3.38
J-3A	Yeast/FDA		XL67B-3a	15.	1.75	4.89	3.21
J-1B	Background		XL67B-3a	16.25	3.0	6.00	3.94
J-2B	Background		XL67B-3a	16.75	3.5	6.17	4.05
J-3B	Background		XL67B-3a	17.25	4.0	5.95	3.91
K-1A	Yeast/FDA		X2180-1B	18.08	4.83	5.74	3.77
K-2A	Yeast/FDA		X2180-1B	18.66	5.42	5.10	3.35
K-3A	Yeast/FDA		X2180-1B	19.09	5.83	5.04	3.31
K-1B	Background		X2180-1B	20.0	6.75	5.53	3.63
K-2B	Background		X2180-1B	20.5	7.25	4.64	3.05
K-3B	Background		X2180-1B	21.0	7.75	5.04	3.31
L-1A	Yeast/FDA		X2180-1B	23.33	1.83	5.58	3.67
L-3A	Yeast/FDA		X2180-1B	24.75	3.25	4.25	2.79
L-1B	Background		X2180-1B	25.83	4.33	4.00	2.63
L-2B	Background		X2180-1B	26.33	4.833	3.69	2.42

TABLE XI

Computer-calculated output of a representative sample of collected data.

Instrument function: M-1

File	Spectrum	χ^2	Total Error	Lifetime (channels)	Lifetime Uncertai
AAA FITBIN	F-1A	.681	.077	6.45	.093
BBB	G-1A	2.33	.139	5.50	.091
CCC	G-1B	.639	.074	6.16	.093
DDD	G-2A	.697	.077	6.05	.092
EEE	G-2B	1.02	.093	6.73	.089
FFF	G-2C	.861	.083	6.12	.092
GGG	G-3A	.934	.088	5.73	.091
HHH	G-3B	1.24	.101	5.40	.090
III	G-4B	.845	.084	5.79	.091
JJJ	G-4C	2.16	.131	5.08	.089
KKK	E-1	1.08	.094	5.50	.090
LLL	J-1A	.558	.067	6.07	.090
MMM	J-2A	.635	.068	5.32	.085
NNN	J-3A	.842	.079	5.08	.086
OOO	J-1B	.659	.073	6.18	.090
PPP	J-2B	.792	.079	6.34	.089
QQQ	J-3B	.738	.079	6.14	.092
RRR	K-1A	.699	.074	5.93	.089
SSS	K-2A	.647	.070	5.29	.087
TTT	K-3A	.528	.062	5.23	.086
UUU	K-1B	.507	.063	5.71	.088
VVV	K-2B	1.11	.082	4.83	.078
WWW	K-3B	.500	.060	5.25	.085
XXX	L-1A	1.08	.095	5.77	.091
YYY	L-3A	.684	.067	4.44	.081
ZZZ	L-1B	1.21	.092	4.23	.084
[illegible]	L-2B	.877	.075	3.91	.081

PLATE XVIII

Channel-shift corrected plots of an instrument function and an observed 10^{-4} M fluorescein solution decay spectrum, normalized to total number of counts.

• instrument function, spectrum M-1

■ fluorescein, spectrum F-1A

lifetime = 6.45 channels, 4.24 nsec

.657 nsec/channel

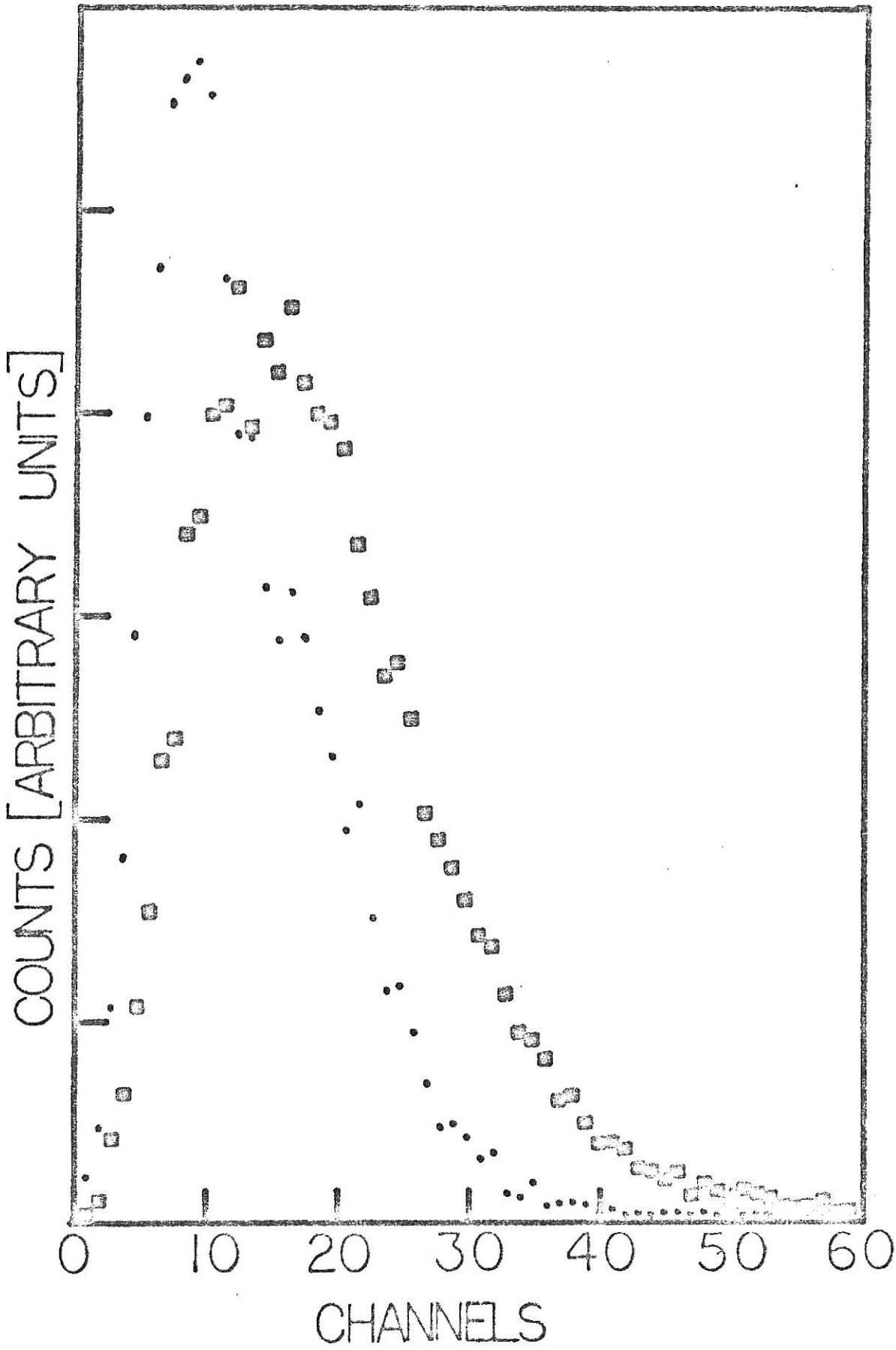

COUNTS [ARBITRARY UNITS]
0
10
20
30
40
50
60
CHANNELS

PLATE XIX

Channel-shift corrected plots of an instrument function and an observed 10^{-4} M fluorescein solution decay spectrum, normalized to total number of counts.

• instrument function, spectrum H-2A

■ fluorescein, spectrum F-1A

lifetime = 6.25 channels, 4.11 nsec

.657 nsec/channel

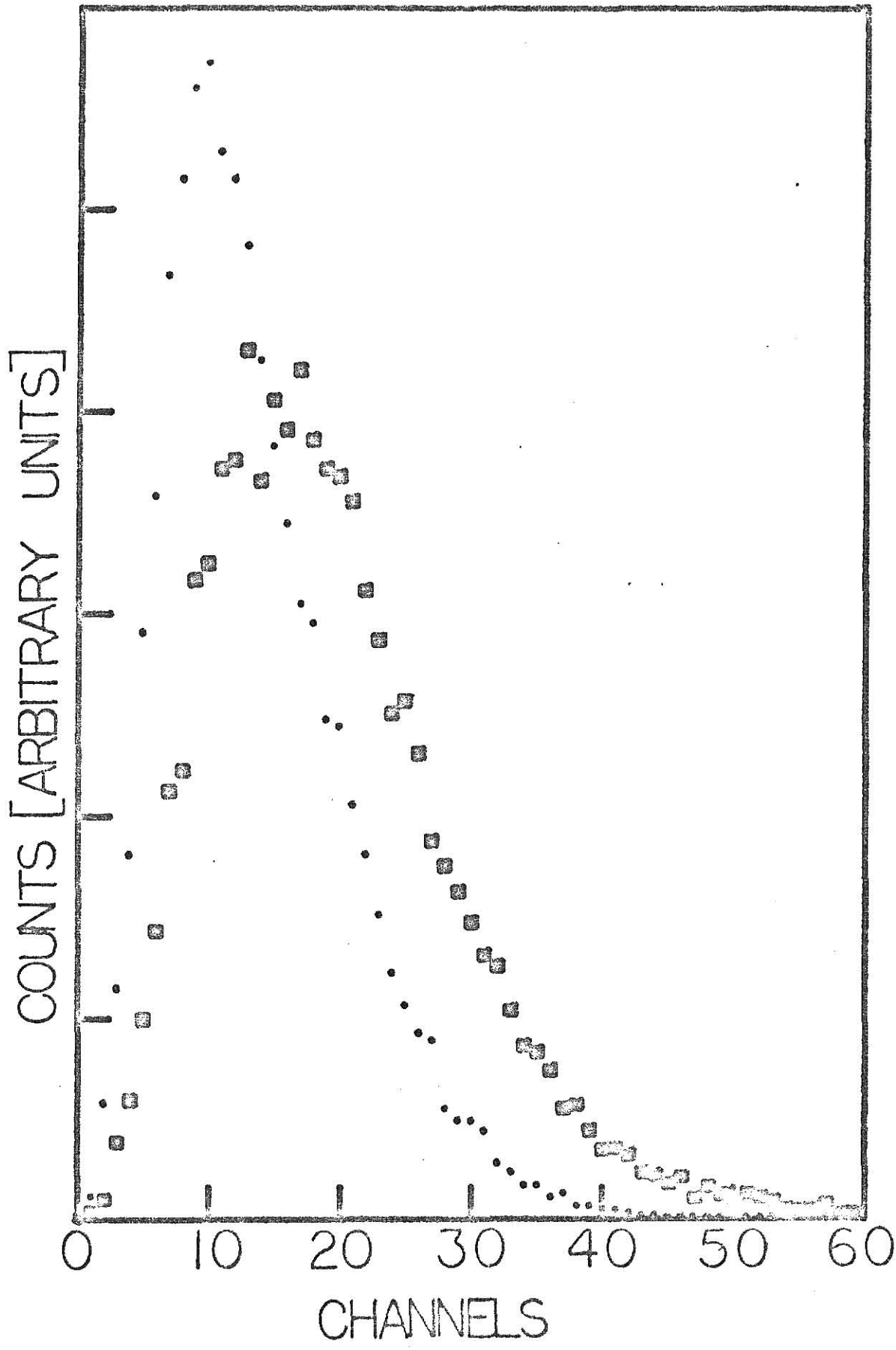

COUNTS [ARBITRARY UNITS]
0
10
20
30
40
50
60
CHANNELS

PLATE XX

Channel-shift corrected plots of an instrument function and an observed 10^{-4} M fluorescein solution decay spectrum, normalized to total number of counts.

• instrument function, spectrum M-1

■ fluorescein, spectrum G-1B

lifetime = 6.16 channels, 4.05 nsec

.657 nsec/channel

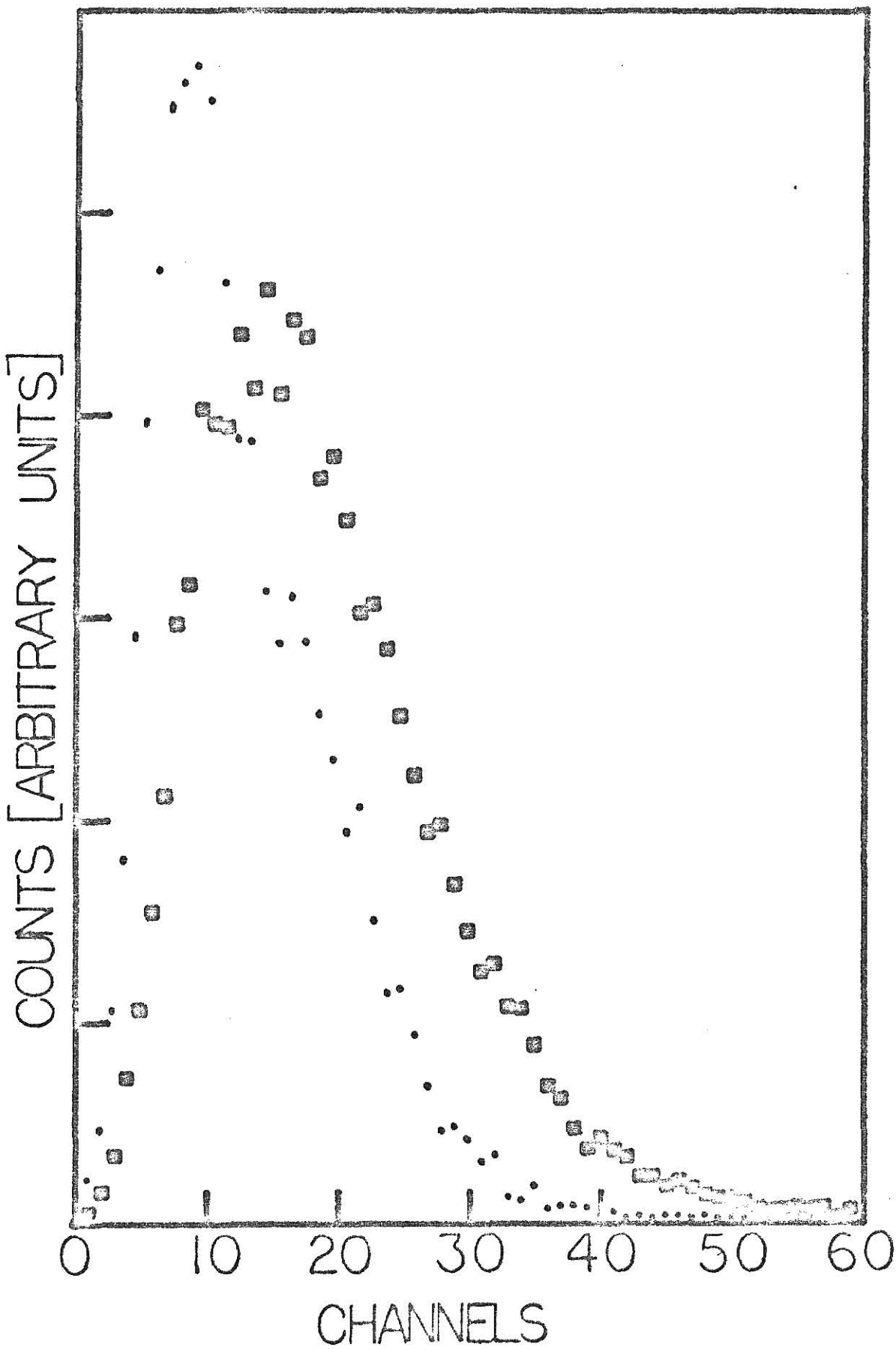

COUNTS [ARBITRARY UNITS]
0
10
20
30
40
50
60
CHANNELS

PLATE XXI

Channel-shift corrected plots of an instrument function and an observed 10^{-4} M fluorescein solution decay spectrum, normalized to total number of counts.

• instrument function, spectrum H-2A

■ fluorescein, spectrum G-1B

lifetime = 5.95 channels, 3.91 nsec

.657 nsec/channel

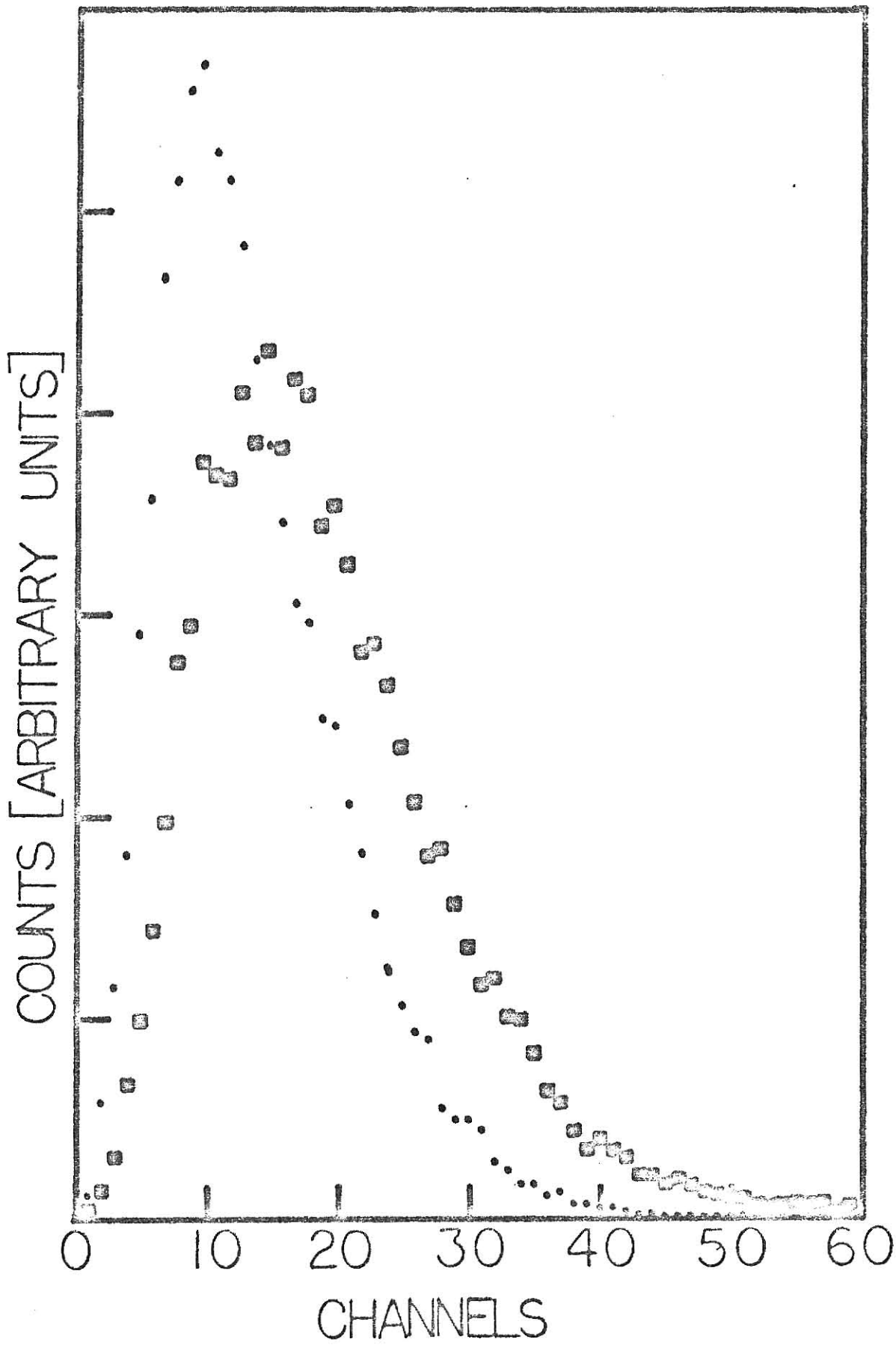

COUNTS [ARBITRARY UNITS]
0
10
20
30
40
50
60
CHANNELS

PLATE XXII

Channel-shift corrected plots of an instrument function and an observed intracellular fluorescein decay spectrum, normalized to total number of counts.

• instrument function, spectrum M-1

■ intracellular fluorescein, spectrum J-1A

lifetime = 6.07 channels, 3.99 nsec

.657 nsec/channel

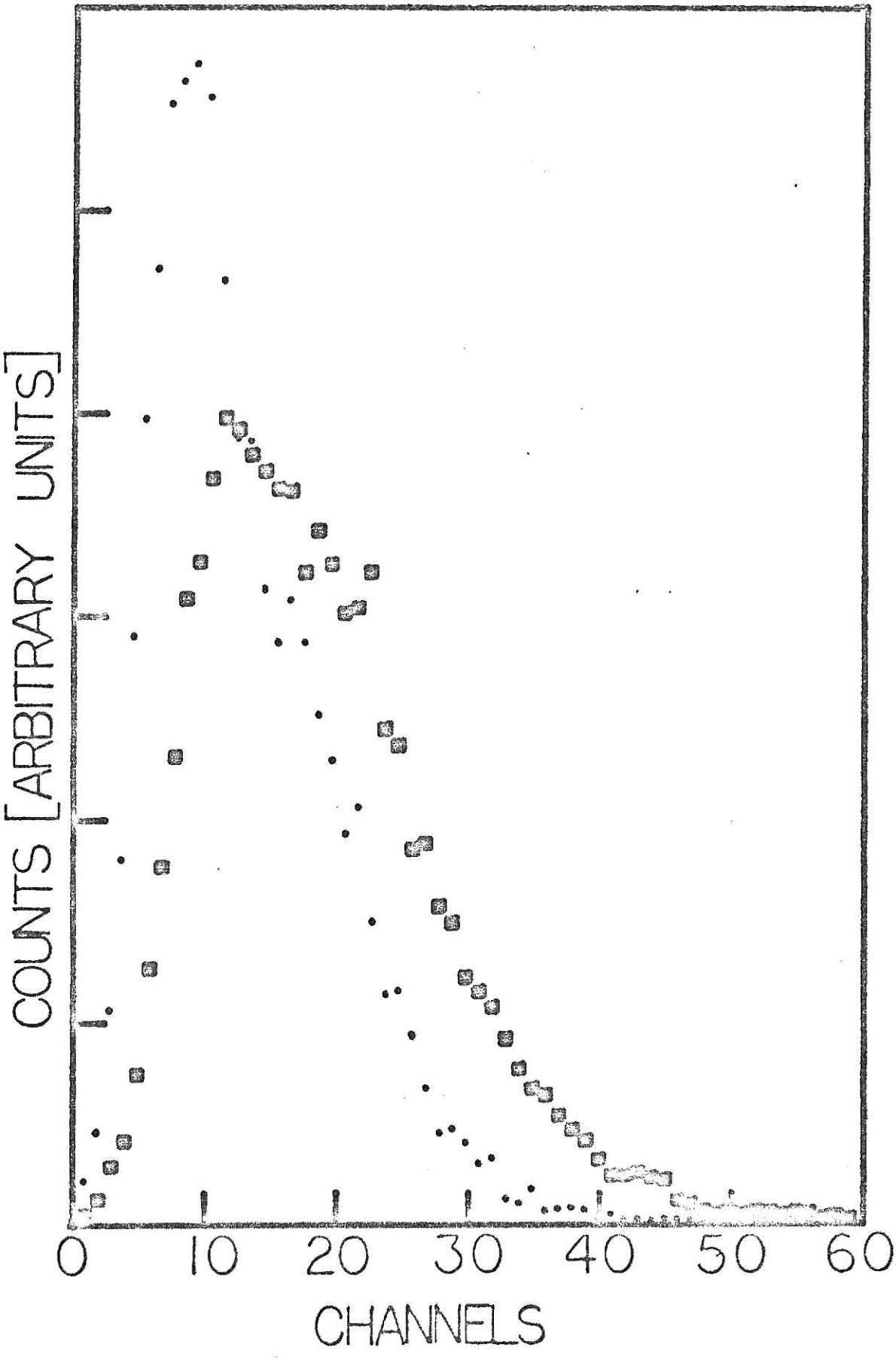

COUNTS [ARBITRARY UNITS]
0
10
20
30
40
50
60
CHANNELS

PLATE XXIII

Channel-shift corrected plots of an instrument function and an observed intracellular fluorescein decay spectrum, normalized to total number of counts.

• instrument function, spectrum H-2A

■ intracellular fluorescein, spectrum J-1A

lifetime = 5.89 channels, 3.87 nsec

.657 nsec/channel

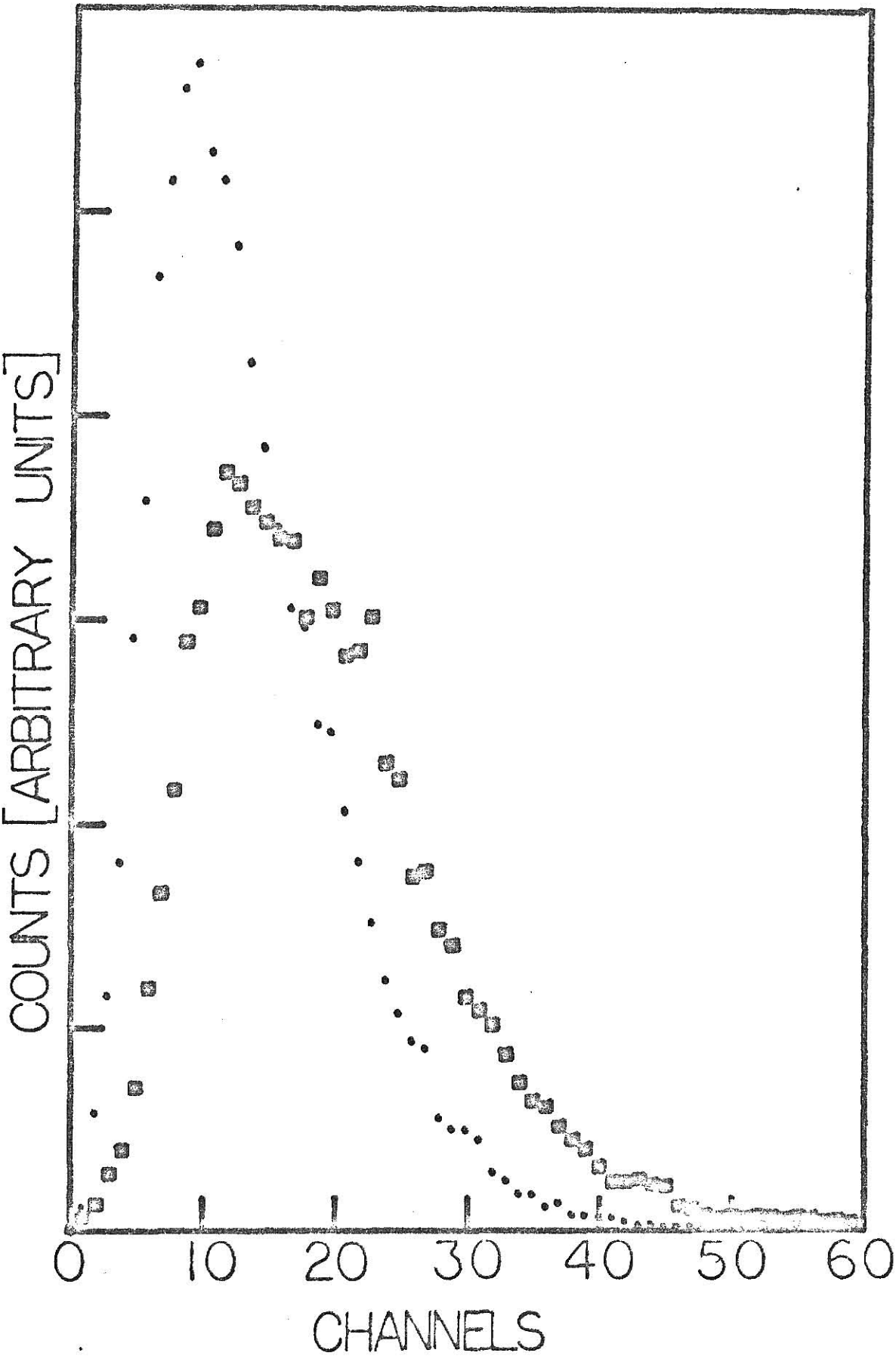

COUNTS [ARBITRARY UNITS]
0
10
20
30
40
50
60
CHANNELS

PLATE XXIV

Channel-shift corrected plots of an instrument function and an observed cell/FDA solution background fluorescence decay spectrum, normalized to total number of counts.

• instrument function, spectrum H-2A

■ background fluorescence, spectrum K-3B

lifetime = 5.04 channels, 3.31 nsec

.657 nsec/channel

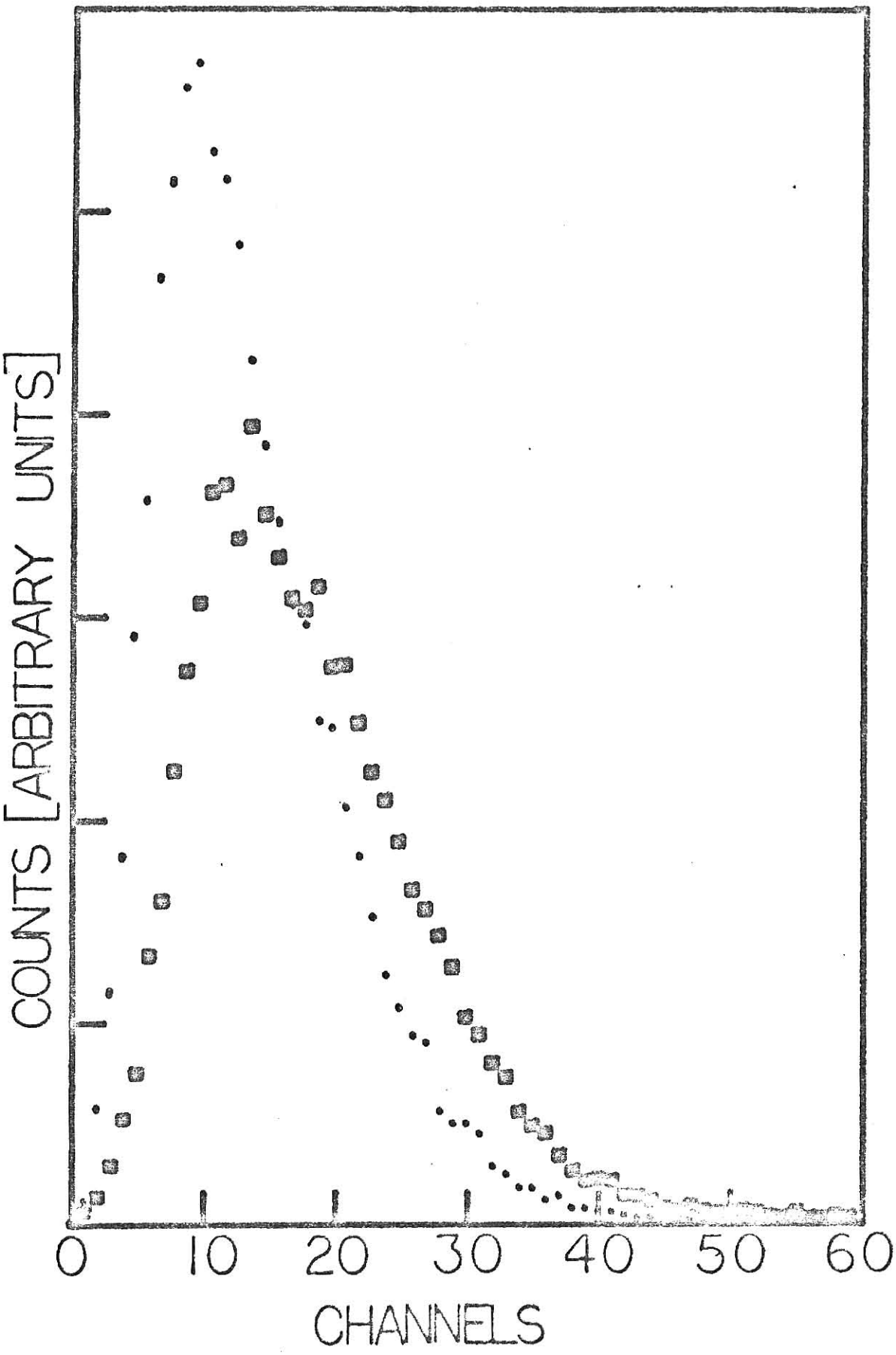

COUNTS [ARBITRARY UNITS]
0
10
20
30
40
50
60
CHANNELS

PLATE XXV

Channel-shift corrected plots of an instrument function and an observed cell/FDA solution background fluorescence decay spectrum, normalized to total number of counts.

• instrument function, spectrum M-1

■ background fluorescence, spectrum K-3B

lifetime = 5.25 channels, 3.45 nsec

.657 nsec/channel

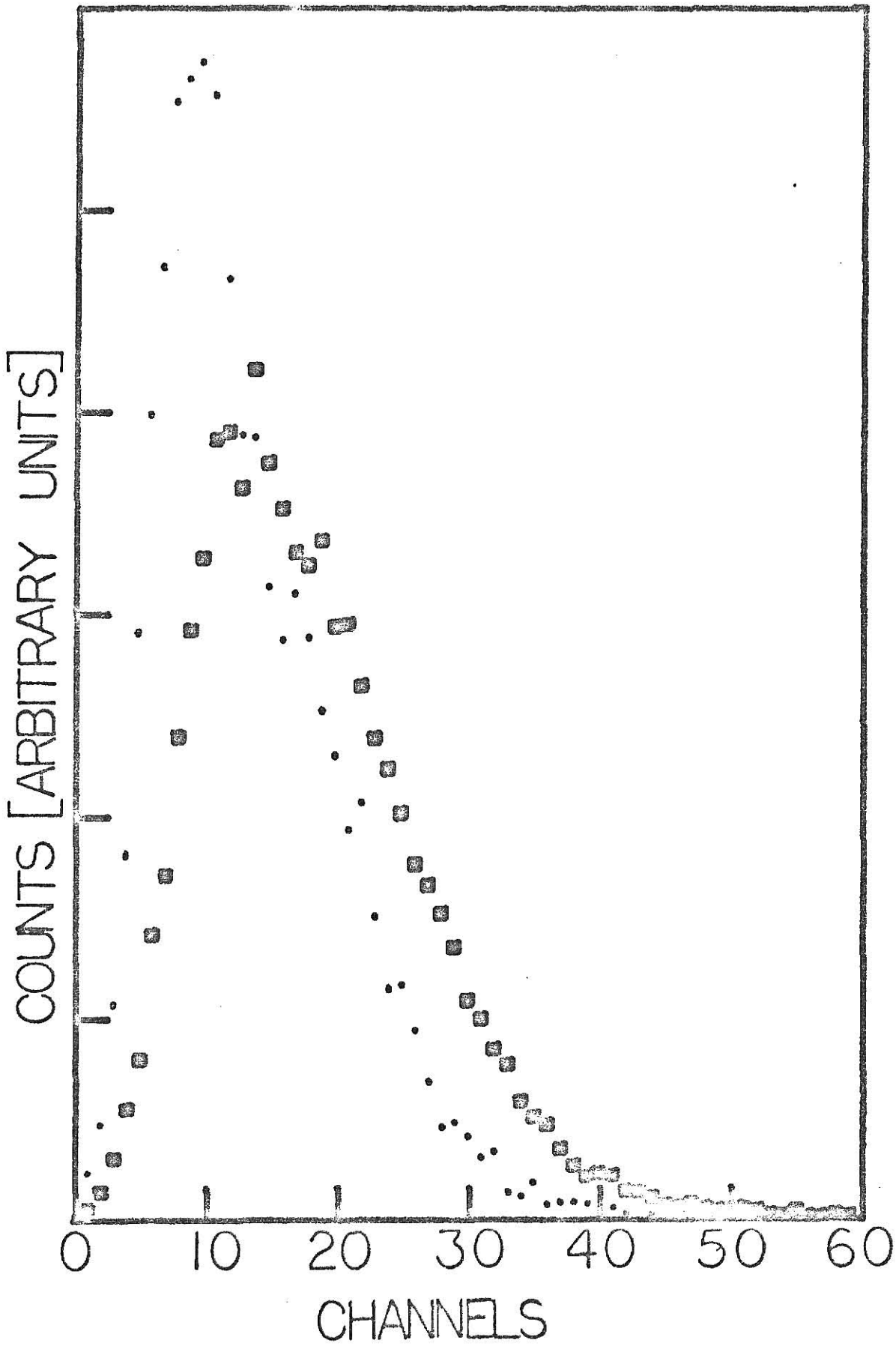

COUNTS [ARBITRARY UNITS]
0
10
20
30
40
50
60
CHANNELS

PLATE XXVI

Least squares fit of an instrument function-exponential decay convolution to a 10^{-4} M fluorescein solution decay spectrum.

■ fluorescein, spectrum F-1A

⊙ convolution, spectrum H-2A

$\chi^2 = .616$

lifetime = 6.25 channels, 4.11 nsec

.657 nsec/channel

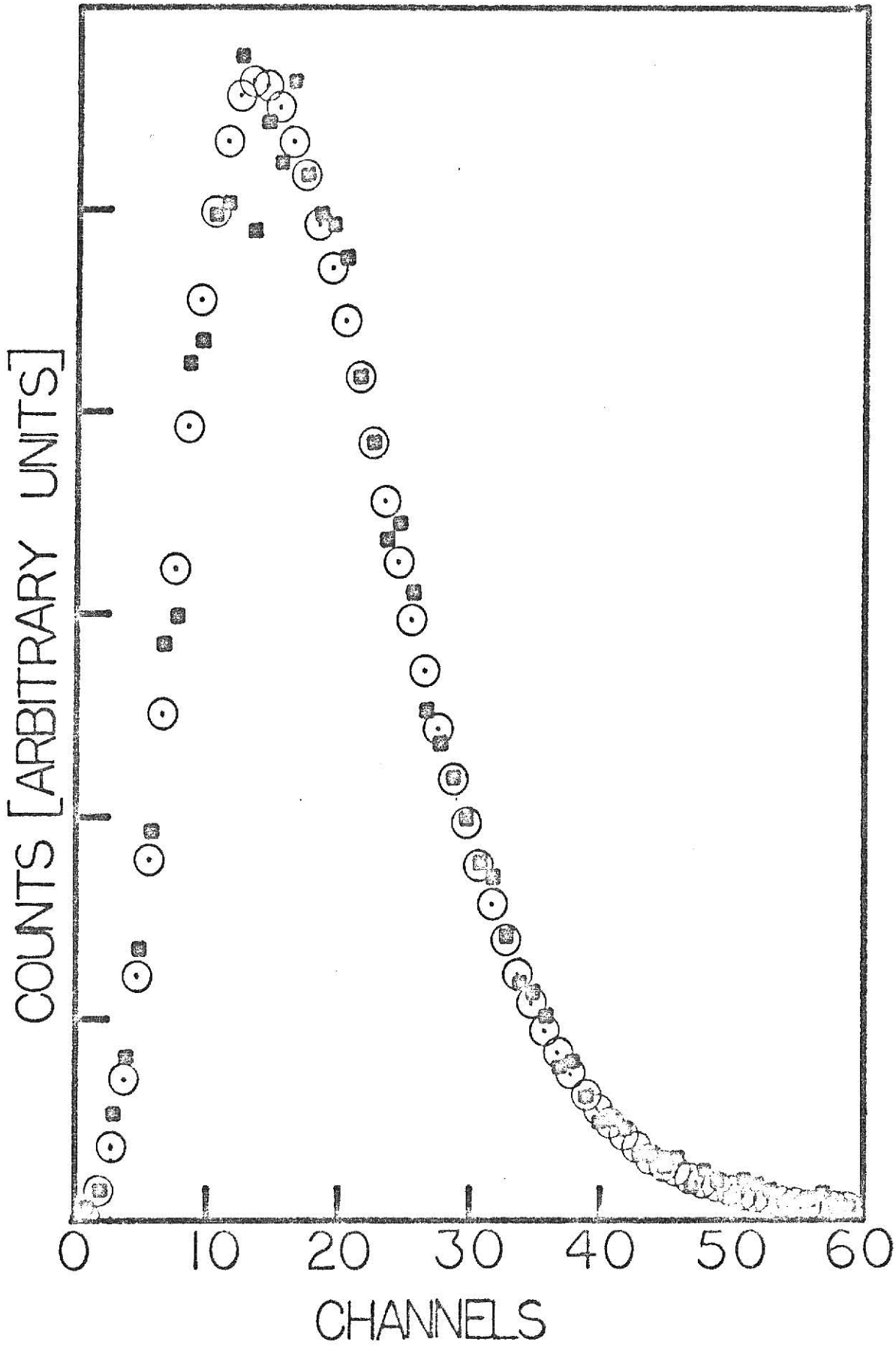

COUNTS [ARBITRARY UNITS]
0
10
20
30
40
50
60
CHANNELS

PLATE XXVII

Least squares fit of an instrument function-exponential decay convolution to a 10^{-4} M fluorescein solution decay spectrum.

■ fluorescein, spectrum F-1A

⊙ convolution, spectrum M-1

$\chi^2 = .681$

lifetime = 6.45 channels, 4.24 nsec

.657 nsec/channel

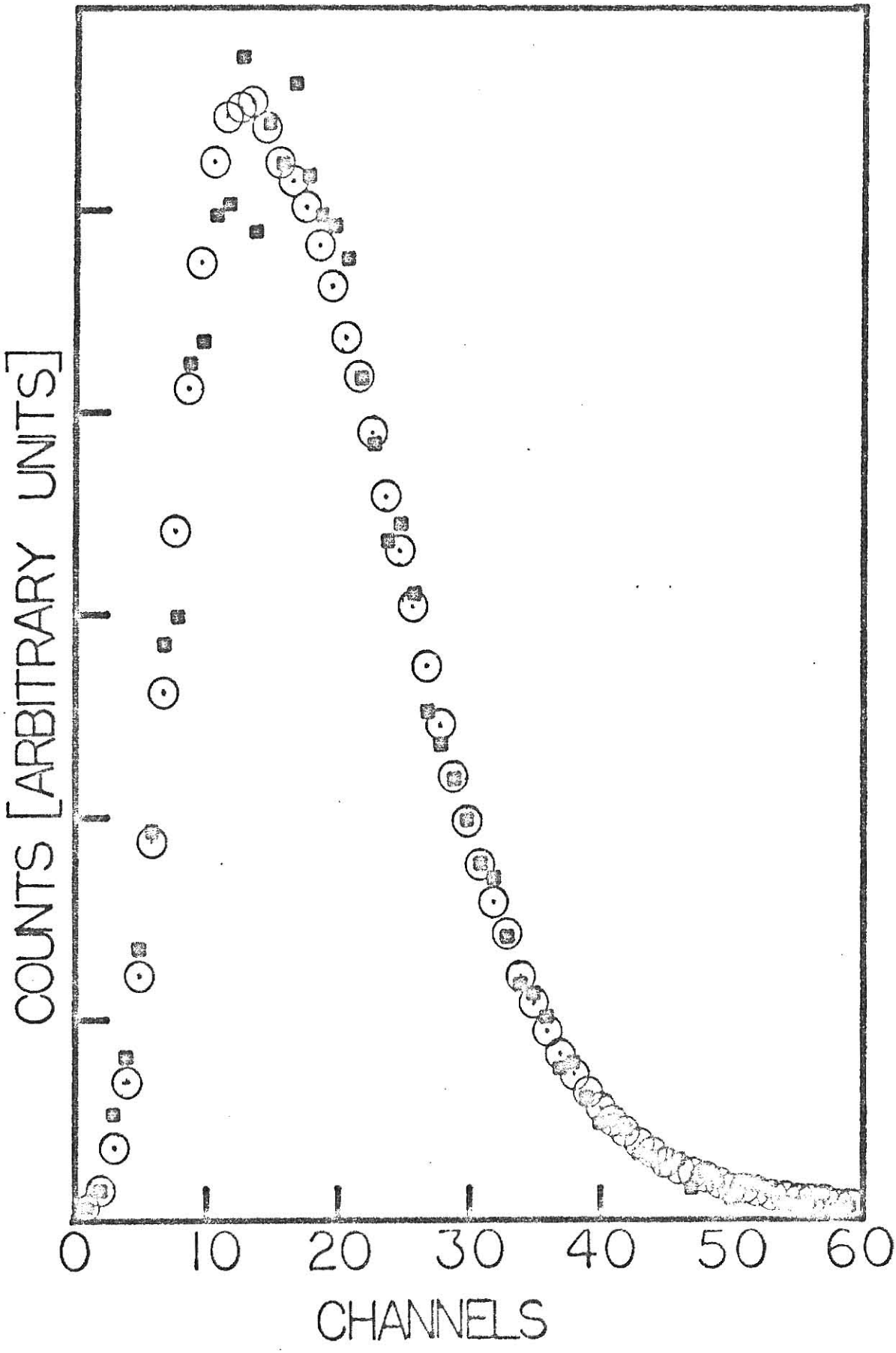

COUNTS [ARBITRARY UNITS]
0
10
20
30
40
50
60
CHANNELS

PLATE XXVIII

Least squares fit of an instrument function-exponential decay convolution to a 10^{-4} M fluorescein solution decay spectrum.

■ fluorescein, spectrum G-1B

⊙ convolution, spectrum M-1

$\chi^2 = .639$

lifetime = 6.16 channels, 4.05 nsec

.657 nsec/channel

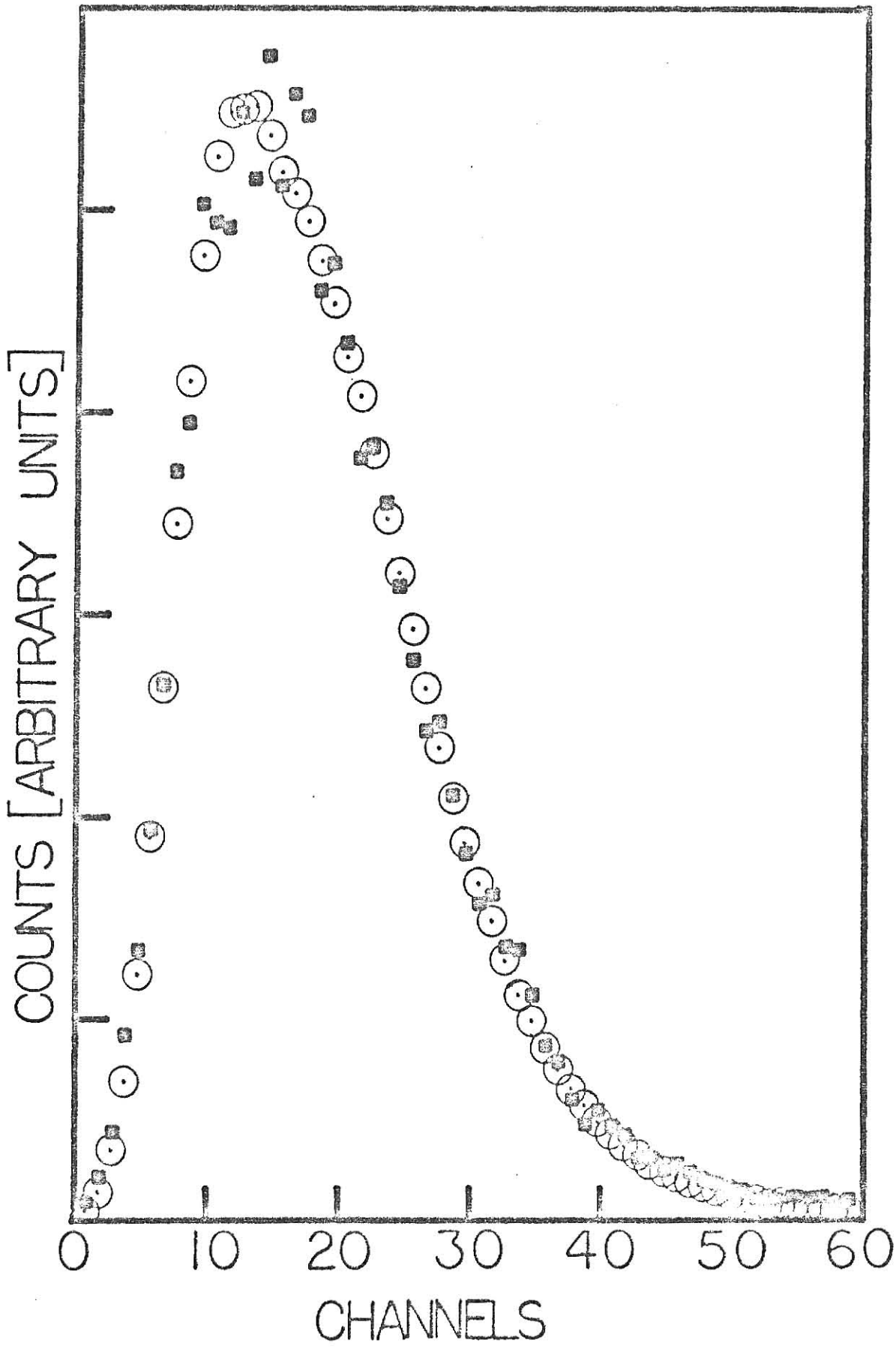

COUNTS [ARBITRARY UNITS]
0
10
20
30
40
50
60
CHANNELS

PLATE XXIX

Least squares fit of an instrument function-exponential decay convolution to a 10^{-4} M fluorescein solution decay spectrum.

■ fluorescein, spectrum G-1B

⊙ convolution, spectrum H-2A

$\chi^2 = .636$

lifetime = 5.95 channels, 3.91 nsec

.657 nsec/channel

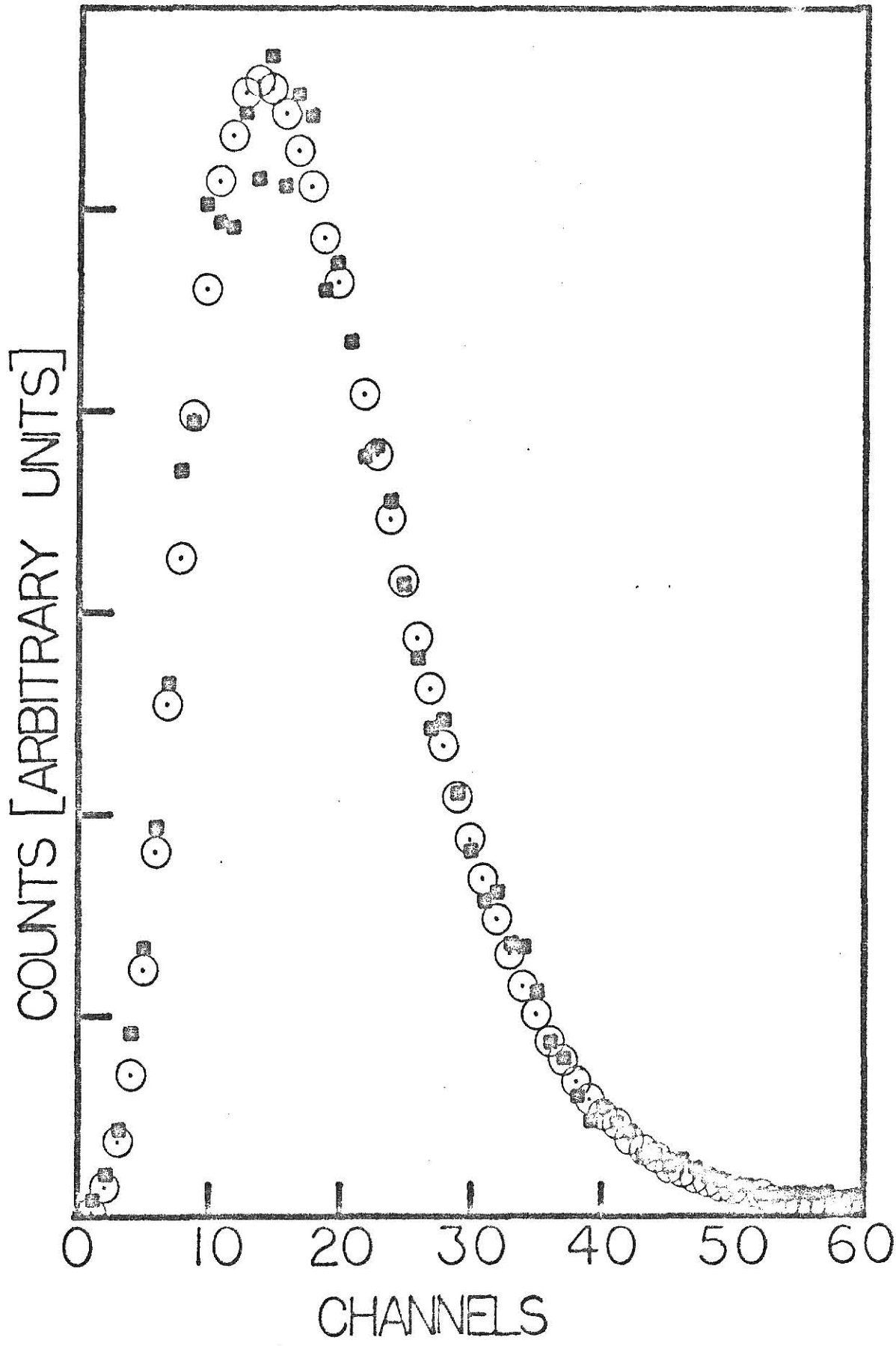

COUNTS [ARBITRARY UNITS]
0
10
20
30
40
50
60
CHANNELS

PLATE XXX

Least squares fit of an instrument function-exponential decay convolution to an intracellular fluorescein decay spectrum.

■ intracellular fluorescein, spectrum J-1A

⊙ convolution, spectrum M-1

$\chi^2 = .558$

lifetime = 6.07 channels, 3.99 nsec

.657 nsec/channel

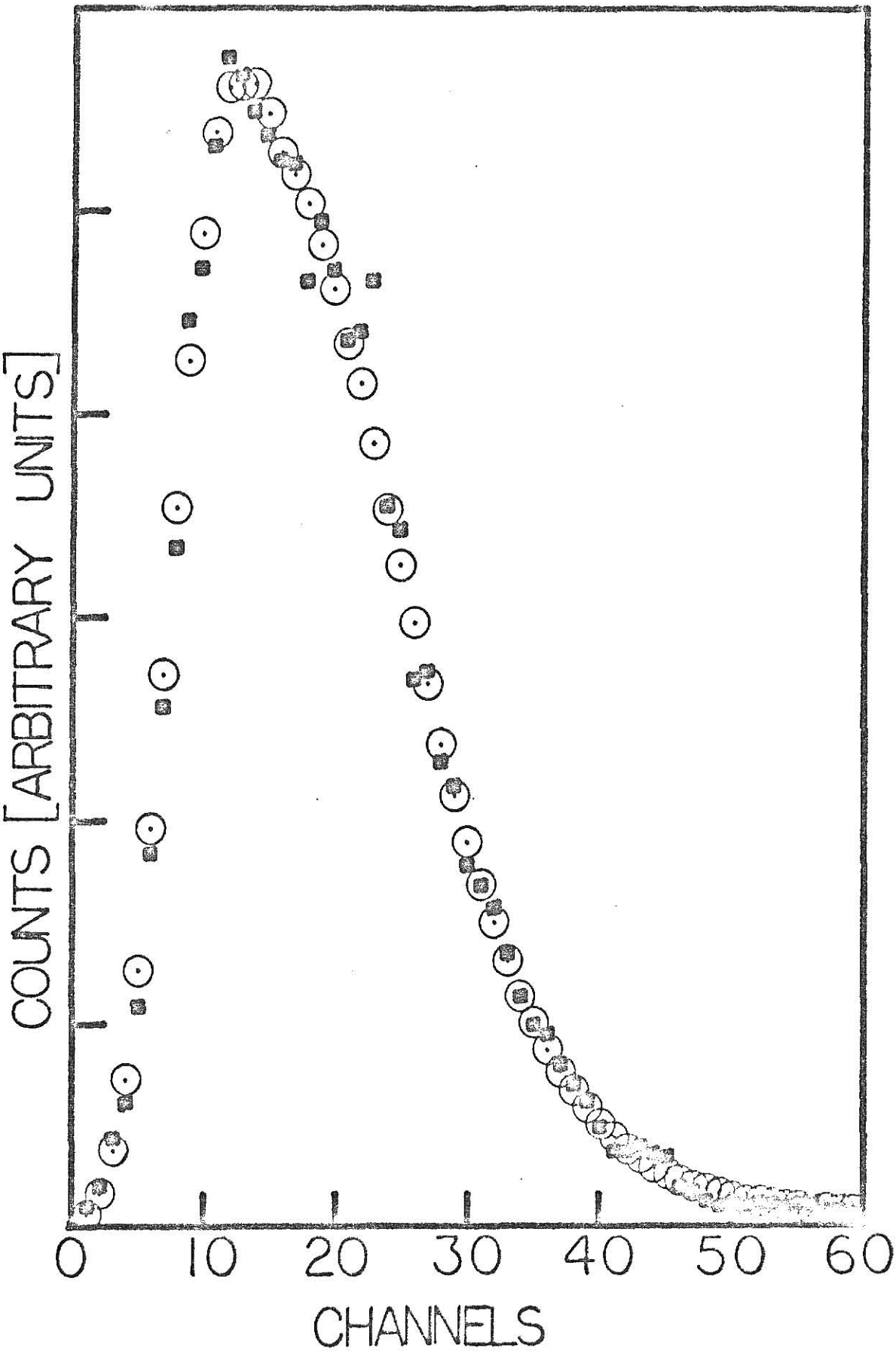

COUNTS [ARBITRARY UNITS]
0
10
20
30
40
50
60
CHANNELS

PLATE XXXI

Least squares fit of an instrument function-exponential decay convolution to an intracellular fluorescein decay spectrum.

■ intracellular fluorescein, spectrum J-1A

⊙ convolution, spectrum H-2A

$\chi^2 = .646$

lifetime = 5.89 channels, 3.87 nsec

.657 nsec/channel

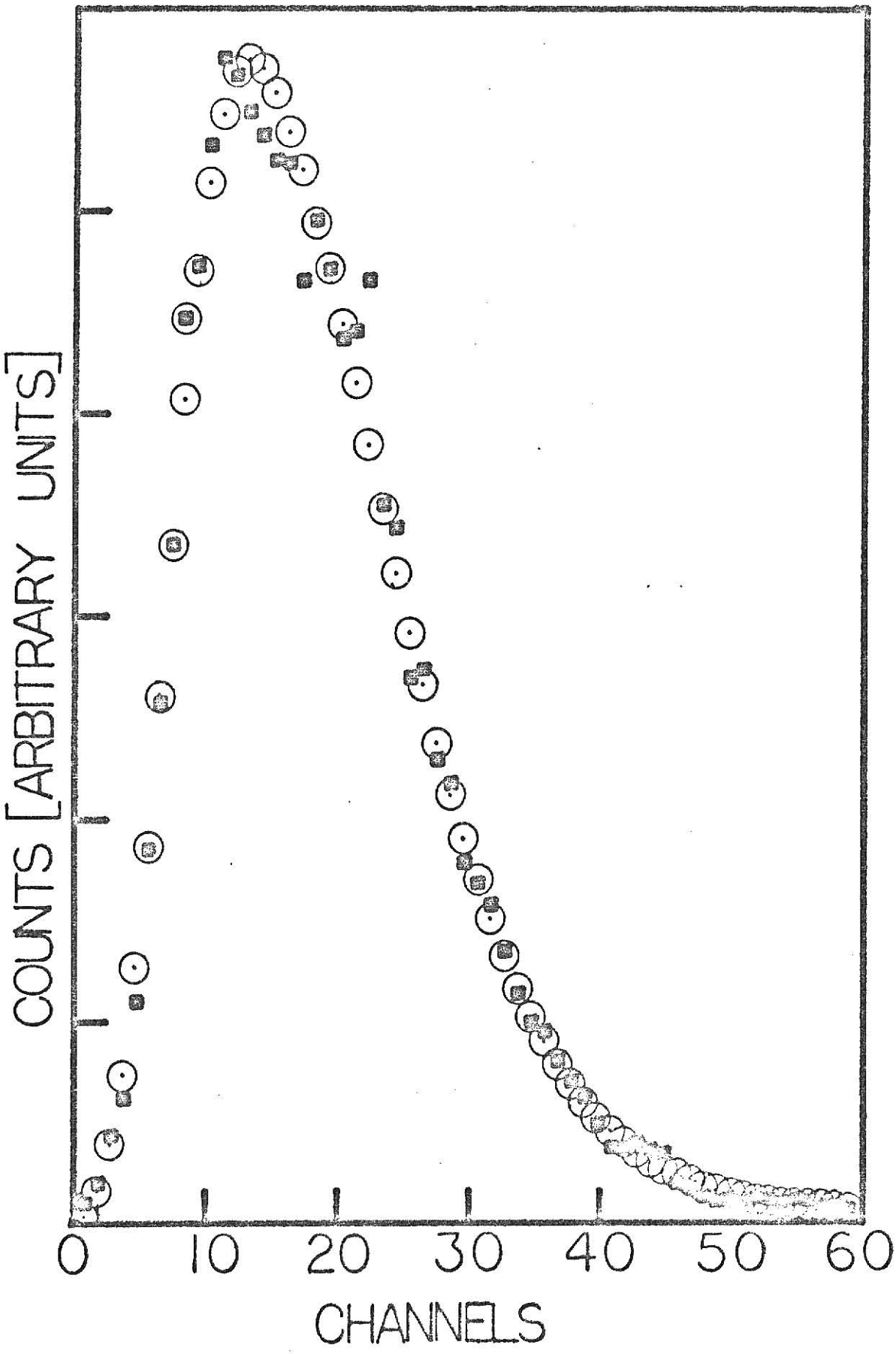

COUNTS [ARBITRARY UNITS]
0
10
20
30
40
50
60
CHANNELS

PLATE XXXII

Least squares fit of an instrument function-exponential decay convolution to a cell/FDA solution background fluorescence decay spectrum.

■ background fluorescence, spectrum K-3B

⊙ convolution, spectrum M-1

$\chi^2 = .500$

lifetime = 5.25 channels, 3.45 nsec

.657 nsec/channel

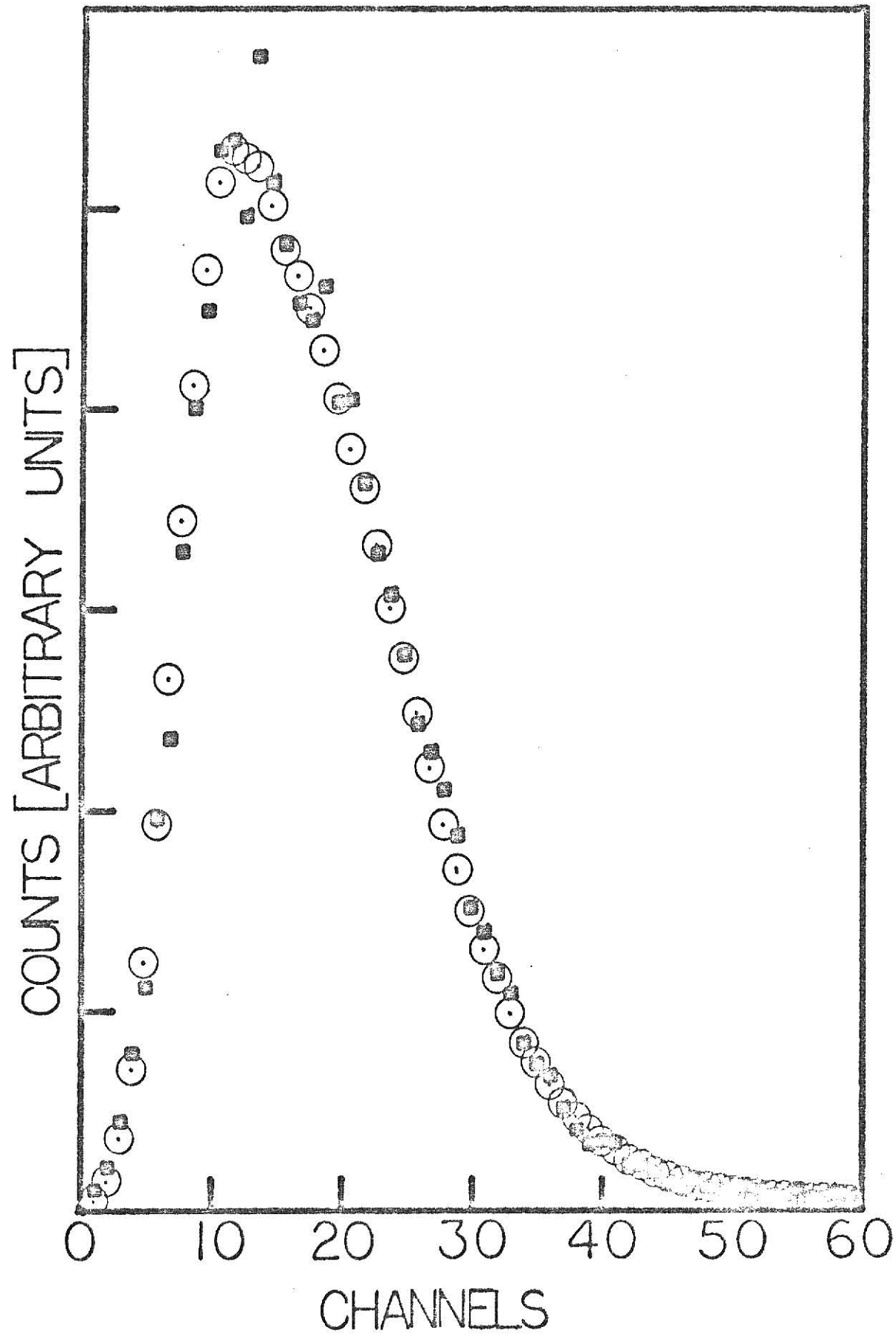

COUNTS [ARBITRARY UNITS]
0
10
20
30
40
50
60
CHANNELS

PLATE XXXIII

Least squares fit of an instrument function-exponential decay convolution to a cell/FDA solution background fluorescence decay spectrum.

■ background fluorescence, spectrum K-3B

⊙ convolution, spectrum H-2A

$\chi^2 = .600$

lifetime = 5.04 channels, 3.31 nsec

.657 nsec/channel

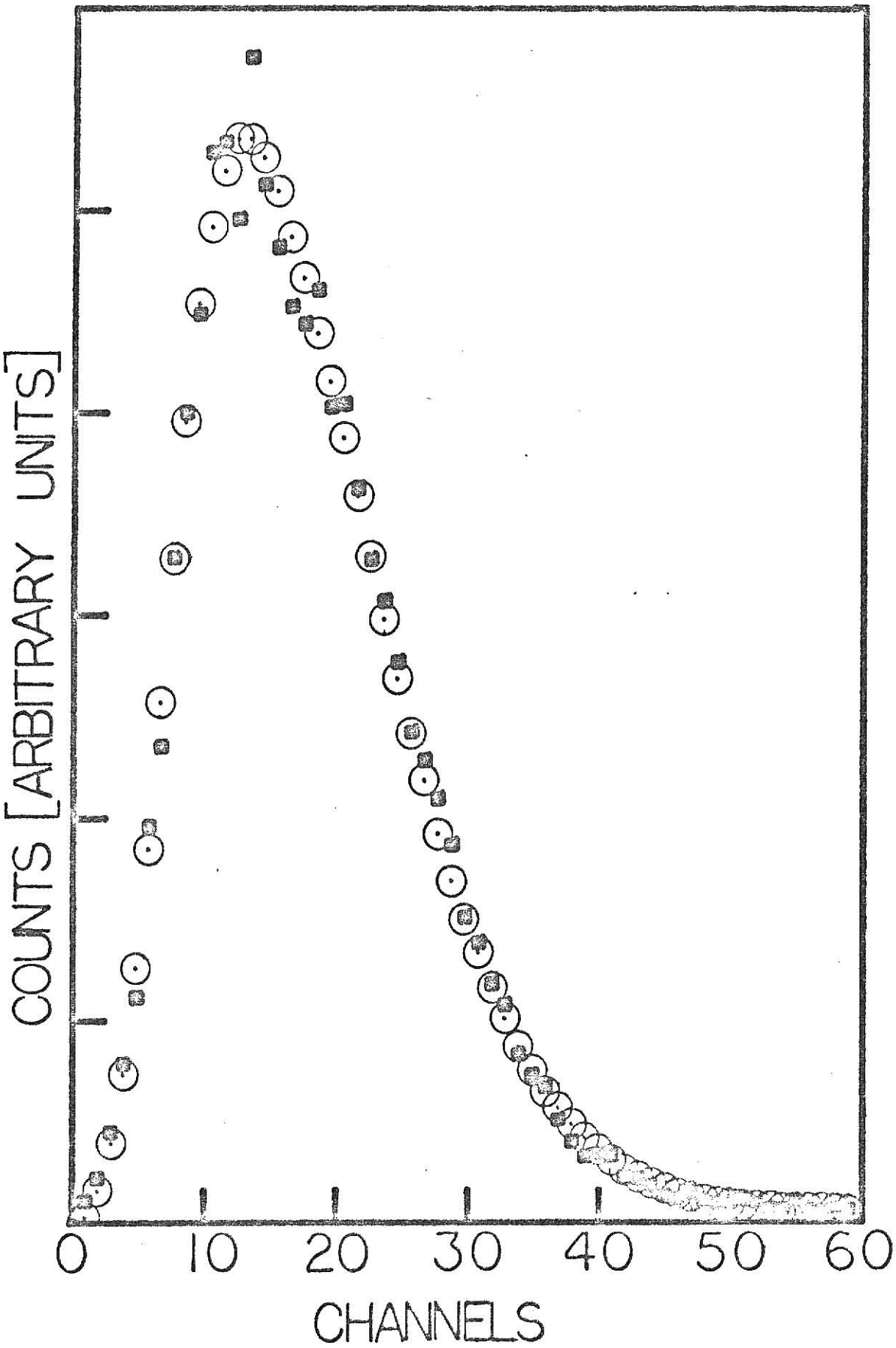

COUNTS [ARBITRARY UNITS]
0
10
20
30
40
50
60
CHANNELS

TABLE XII

Statistics of the linear least squares fit of lifetime vs. concentration for pure fluorescein, as shown in Plate XXXIV.

Lifetimes (channels)	Concentration ($\times 10^{-4}$ M)
5.08	.0476
5.79	.0476
5.40	.0909
5.73	.0909
6.12	.333
6.73	.333
6.05	.333
6.16	1.00
5.50	1.00
6.45	1.00

b = .445 channels/10^{-4} M a = 5.70 channels σ = 1.32

σ_b = .399 channels/10^{-4} M σ_a = .231 channels σ_{INST} = .374 channels

Instrument Function: Spectrum M-1

.657 nsec/channel

PLATE XXXIV

Linear least squares fit of lifetime vs. concentration for pure fluorescein solution. Refer to Table XII.

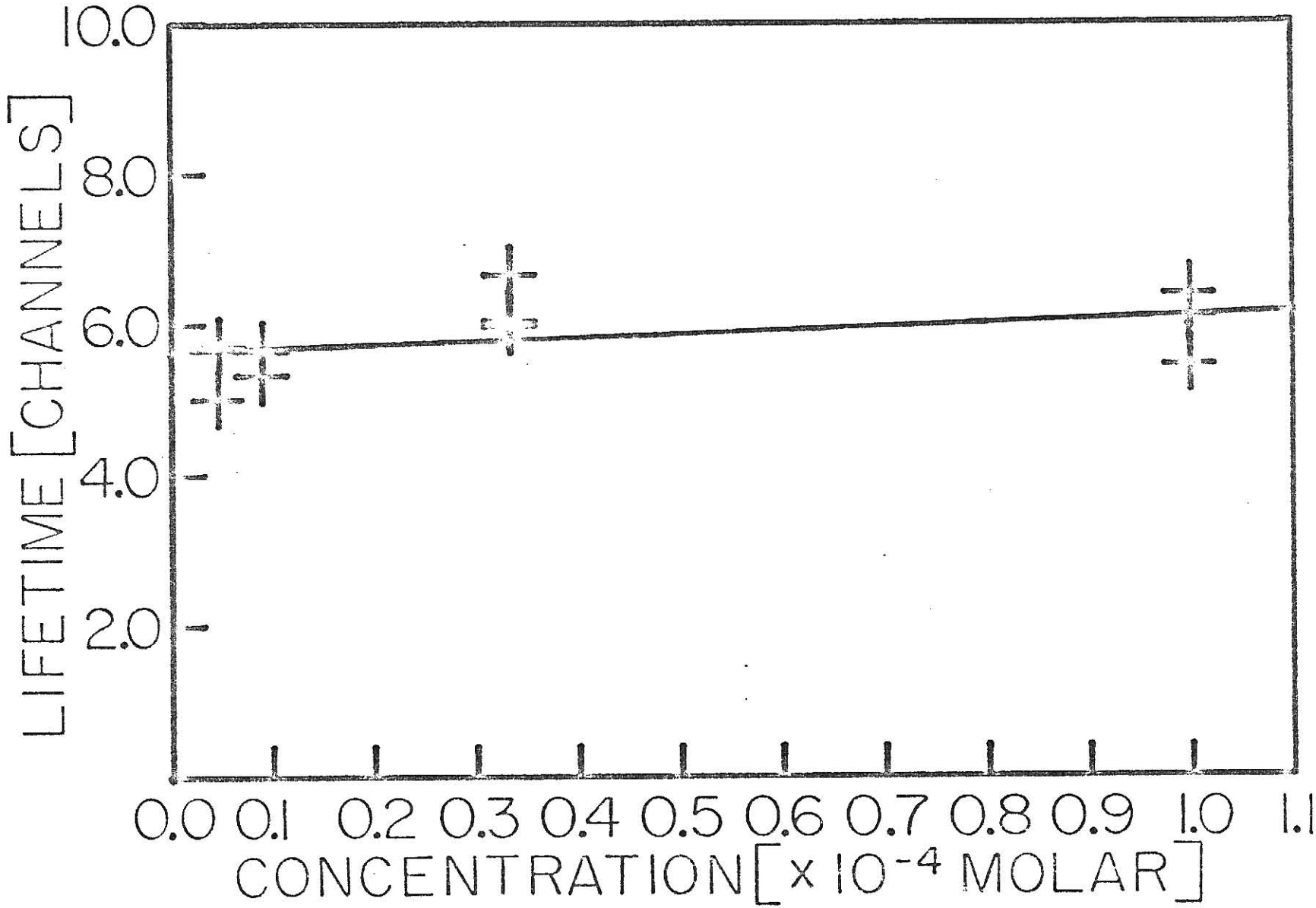

LIFETIME [CHANNELS]
10.0
8.0
6.0
4.0
2.0
0.0 0.1 0.2 0.3 0.4 0.5 0.6 0.7 0.8 0.9 1.0 1.1
CONCENTRATION [x 10⁻⁴ MOLAR]

TABLE XIII

Statistics of the linear least squares fit of lifetime vs. concentration for pure fluorescein, as shown in Plate XXXV.

Lifetime (channels)	Concentration ($\times 10^{-4}$ M)
4.85	.0476
5.58	.0476
5.19	.0909
5.52	.0909
5.94	.333
6.53	.333
5.85	.333
5.95	1.00
5.29	1.00
6.23	1.00

b = .462 channels/10^{-4} M a = 5.49 channels σ = 1.34

σ_b = .405 channels/10^{-4} M σ_a = .234 channels σ_{INST} = .374 channels

Instrument Function: Spectrum H-2A

.657 nsec/channel

PLATE XXXV

Linear least squares fit of lifetime vs. concentration for pure fluorescein solution. Refer to Table XIII.

LIFETIME [CHANNELS]
10.0
8.0
6.0
4.0
2.0
0.0 0.1 0.2 0.3 0.4 0.5 0.6 0.7 0.8 0.9 1.0 1.1
CONCENTRATION [x 10⁻⁴ MOLAR]

TABLE XIV

Statistics of the linear least squares fit of lifetime vs. T_1 for intracellular fluorescein, as shown in Plate XXXVI.

Lifetime (channels)	T_1 (hours)
5.50	7.0
6.07	14.0
5.32	14.5
5.08	15.0
5.93	18.08
5.29	18.66
5.23	19.08
5.77	23.33
4.44	24.75

$b = -.032$ channels/hour $a = 5.95$ channels $\sigma = 1.33$

$\sigma_b = .033$ channels/hour $\sigma_a = .587$ channels $\sigma_{INST} = .374$ channels

Instrument Function: Spectrum M-1

.657 nsec/channel

PLATE XXXVI

Linear least squares fit of lifetime vs. T_1 for intracellular fluorescein. Refer to Table XIV.

T_1 = cell culture age.

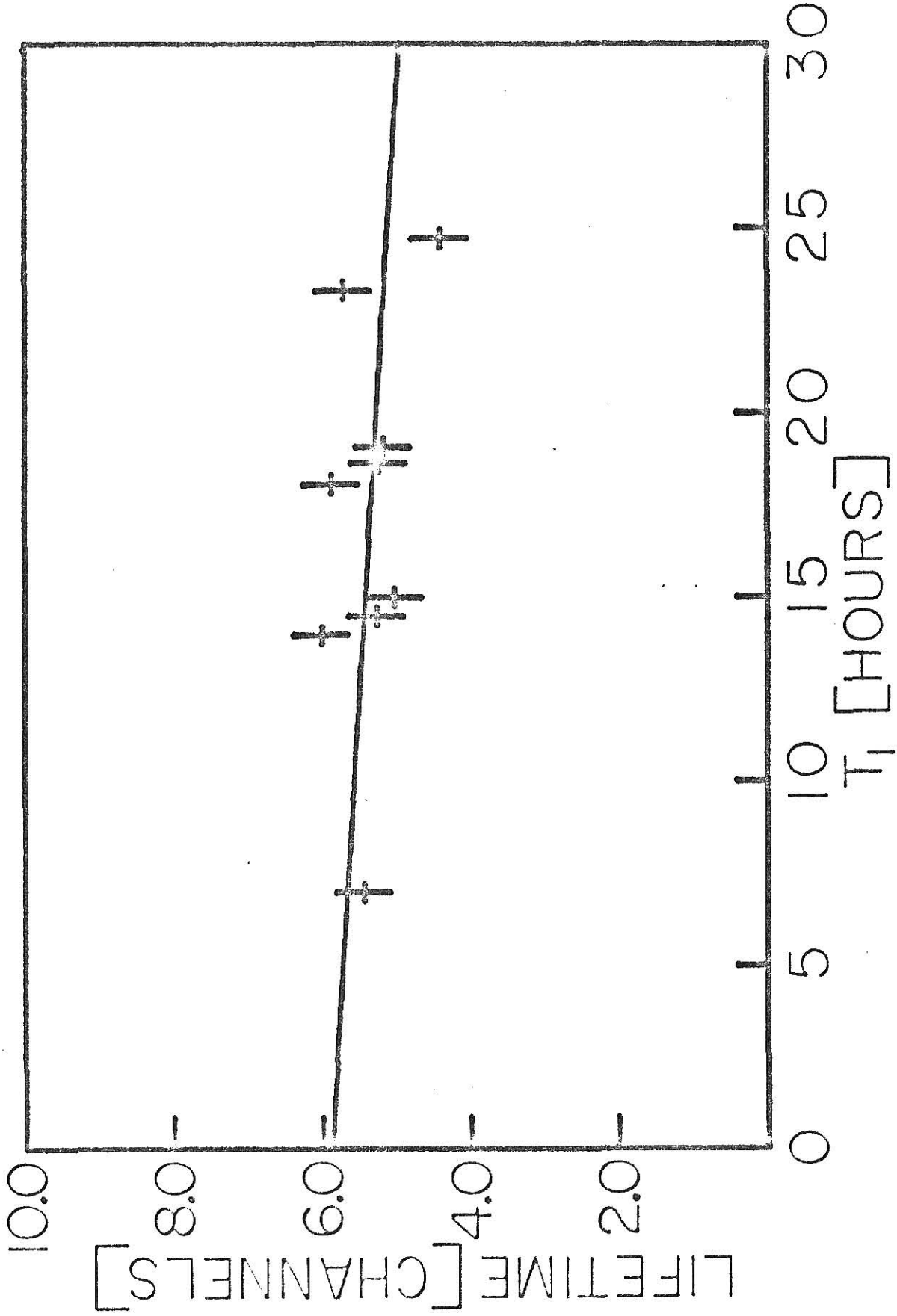

LIFETIME [CHANNELS]
10.0
8.0
6.0
4.0
2.0
0
5
10
15
20
25
30
T_1 [HOURS]

TABLE XV

Statistics of the linear least squares fit of lifetime vs. T_1 for intracellular fluorescein, as shown in Plate XXXVII.

Lifetime (channels)	T_1 (hours)
5.30	7.0
5.89	14.0
5.14	14.5
4.89	15.0
5.74	18.08
5.10	18.66
5.04	19.08
5.58	23.33
4.25	24.75

$b = -.031$ channels/hour $a = 5.75$ channels $\sigma = 1.33$

$\sigma_b = .033$ channels/hour $\sigma_a = .591$ channels $\sigma_{INST} = .374$ channels

Instrument Function: Spectrum H-2A

.657 nsec/channel

PLATE XXXVII

Linear least squares fit of lifetime vs. T_1 for intracellular fluorescein. Refer to Table XV.

T_1 = cell culture age.

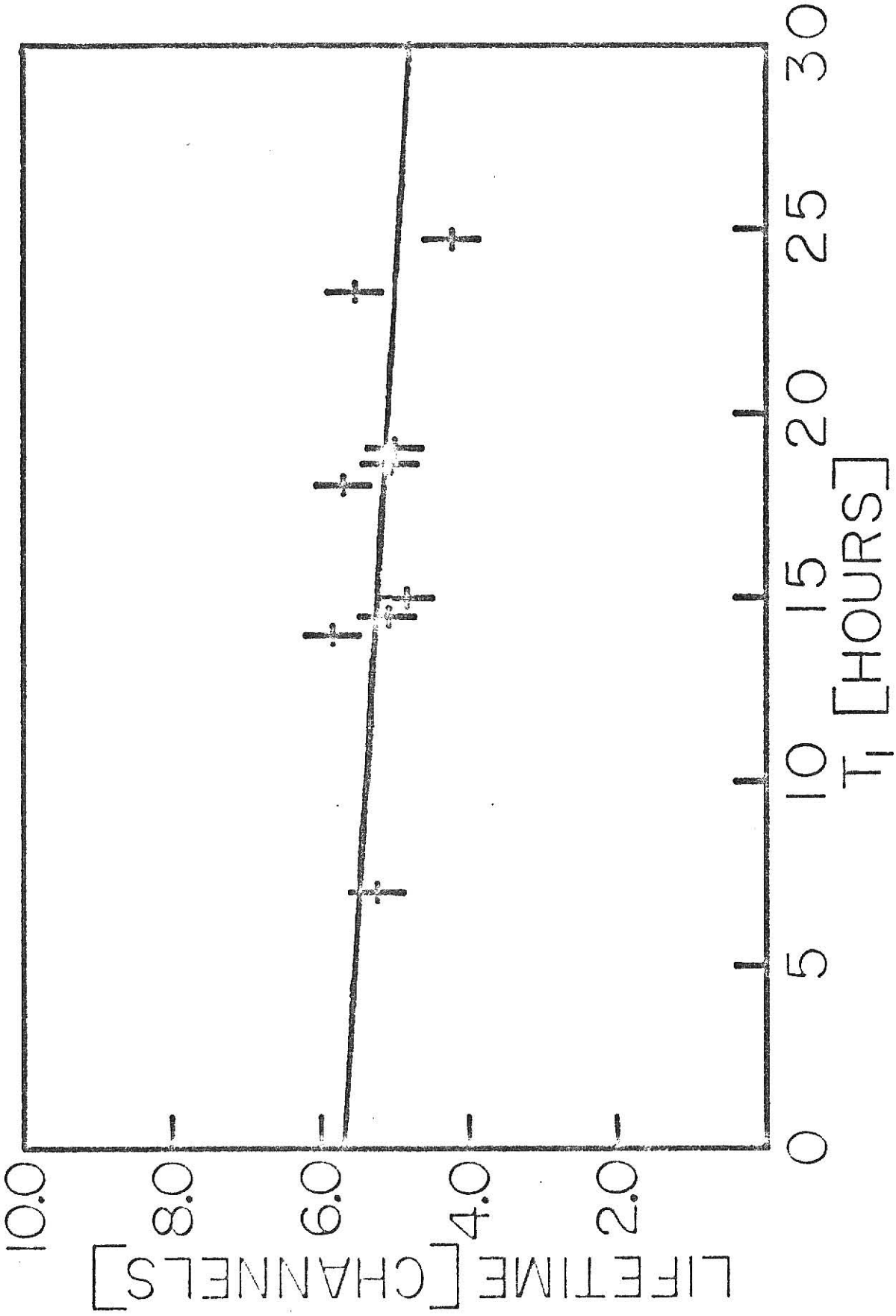

LIFETIME [CHANNELS]
10.0
8.0
6.0
4.0
2.0
0
5
10
15
20
25
30
T_1 [HOURS]

TABLE XVI

Statistics of the linear least squares fit of lifetime vs. T_1 for cell/FDA background fluorescence, as shown in Plate XXXVIII.

Lifetime (channels)	T_1 (hours)
6.18	16.25
6.34	16.75
6.14	17.25
5.71	20.0
4.83	20.5
5.25	21.0
4.23	25.83
3.91	26.33

$b = -.231$ channels/hour $a = 10.05$ channels $\sigma = .678$

$\sigma_b = .024$ channels/hour $\sigma_a = .514$ channels $\sigma_{INST} = .374$ channels

Instrument Function: Spectrum M-1

.657 nsec/channel

PLATE XXXVIII

Linear least squares fit of lifetime vs. T_1 for cell/FDA background fluorescence. Refer to Table XVI.

T_1 = cell culture age.

LIFETIME [CHANNELS]
10.0
8.0
6.0
4.0
2.0
0
5
10
15
20
25
30
T_I [HOURS]

TABLE XVII

Statistics of the linear least squares fit of lifetime vs. T_1 for cell/FDA background fluorescence, as shown in Plate XXXIX.

Lifetime (channels)	T_1 (hours)
6.00	16.25
6.17	16.75
5.95	17.25
5.53	20.0
4.64	20.5
5.04	21.0
4.00	25.83
3.69	26.33

$b = -.236$ channels/hour $a = 9.95$ channels $\sigma = .683$

$\sigma_b = .025$ channels/hour $\sigma_a = .517$ channels $\sigma_{INST} = .374$ channels

Instrument Function: H-2A

.657 nsec/channel

PLATE XXXIX

Linear least squares fit of lifetime vs. T_1 for cell/FDA background fluorescence. Refer to Table XVII.

T_1 = cell culture age.

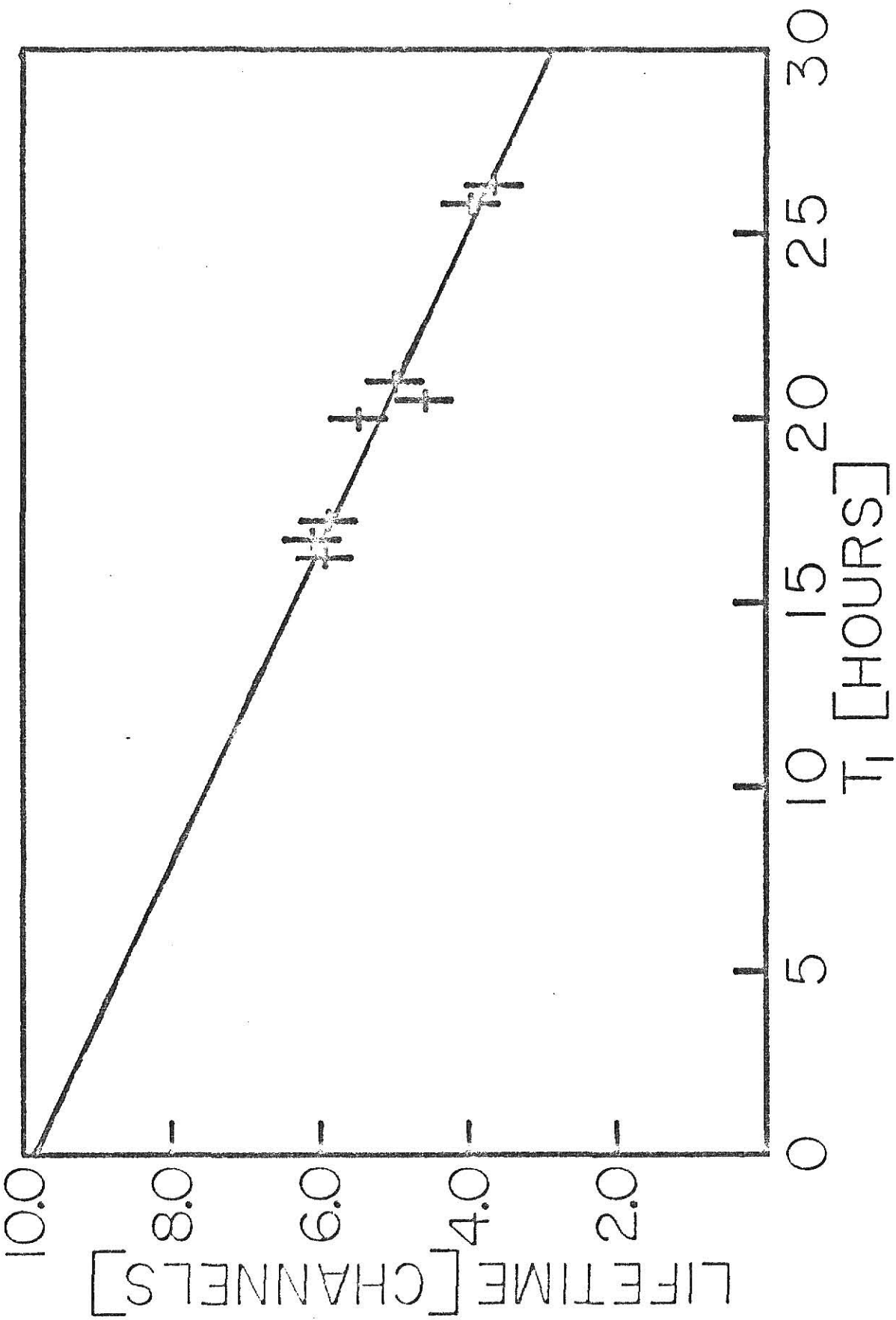

LIFETIME [CHANNELS]
10.0
8.0
6.0
4.0
2.0
0
5
10
15
20
25
30
T_I [HOURS]

TABLE XVIII

Statistics of the linear least squares fit of lifetime vs. T_2 for intracellular fluorescein, as shown in Plate XL.

Lifetime (channels)	T_2 (hours)
6.07	.75
5.50	1.00
5.32	1.25
5.08	1.75
5.77	1.83
4.44	3.25
5.93	4.83
5.29	5.42
5.23	5.83

b = -.050 channels/hour a = 5.54 channels σ = 1.38

σ_b = .091 channels/hour σ_a = .314 channels σ_{INST} = .374 channels

Instrument Function: Spectrum M-1

.657 nsec/channel

PLATE XL

Linear least squares fit of lifetime vs. T_2 for intracellular fluorescein. Refer to Table XVIII.

T_2 = mixing time of cells and FDA.

LIFETIME [CHANNELS]
10.0
8.0
6.0
4.0
2.0
0
2
4
6
8
10
T2 [HOURS]

TABLE XIX

Statistics of the linear least squares fit of lifetime vs. T_2 for intracellular fluorescein, as shown in Plate XLI.

Lifetime (channels)	T_2 (hours)
5.89	.75
5.30	1.00
5.14	1.25
4.89	1.75
5.58	1.83
4.25	3.25
5.74	4.83
5.10	5.42
5.04	5.83

$b = -.050$ channels/hour $a = 5.36$ channels $\sigma = 1.39$

$\sigma_b = .091$ channels/hour $\sigma_a = .315$ channels $\sigma_{INST} = .374$ channels

Instrument Function: Spectrum H-2A

.657 nsec/channel

PLATE XLI

Linear least squares fit of lifetime vs. T_2 for intracellular fluorescein. Refer to Table XIX.

T_2 = mixing time of cells and FDA.

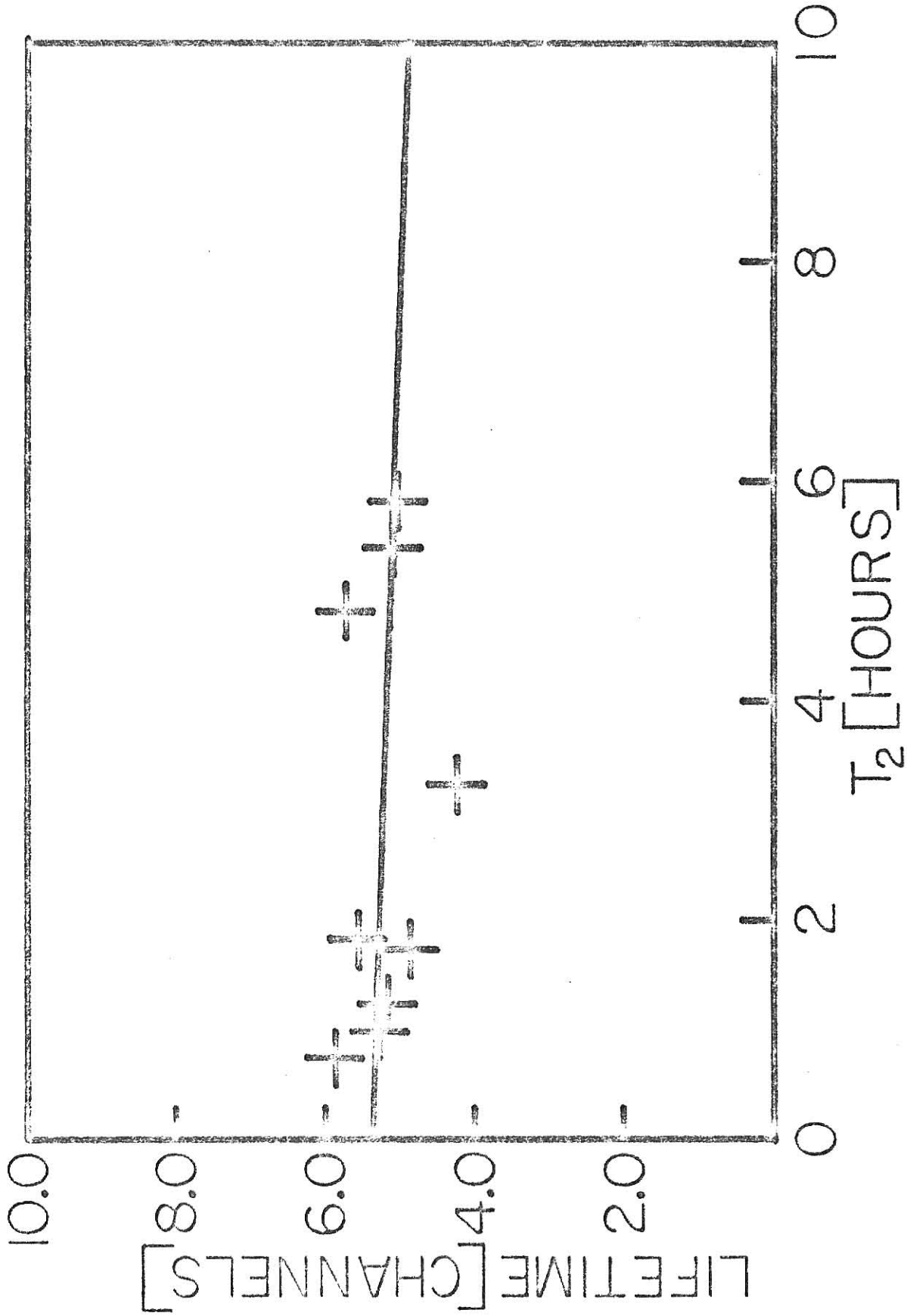

LIFETIME [CHANNELS]
10.0
8.0
6.0
4.0
2.0
0
2
4
6
8
10
T2 [HOURS]

TABLE XX

Statistics of the linear least squares fit of lifetime vs. T_2 for cell/FDA background fluorescence, as shown in Plate XLII.

Lifetime (channels)	T_2 (hours)
6.18	3.0
6.34	3.5
6.14	4.0
4.23	4.33
3.91	4.83
5.71	6.75
4.83	7.25
5.25	7.75

$b = -.159$ channels/hour $a = 6.15$ channels $\sigma = 2.54$

$\sigma_b = .198$ channels/hour $\sigma_a = 1.08$ channels $\sigma_{INST} = .374$ channels

Instrument Function: Spectrum M-1

.657 nsec/channel

PLATE XLII

Linear least squares fit of lifetime vs. T_2 for cell/FDA background fluorescence. Refer to Table XX.

T_2 = mixing time of cells and FDA.

LIFETIME [CHANNELS]
10.0
8.0
6.0
4.0
2.0
0
2
4
6
8
10
T2 [HOURS]

TABLE XXI

Statistics of the linear least squares fit of lifetime vs. T_2 for cell/FDA background fluorescence, as shown in Plate XLIII.

Lifetime (channels)	T_2 (hours)
6.00	3.0
6.17	3.5
5.95	4.0
4.00	4.33
3.69	4.83
5.53	6.75
4.64	7.25
5.04	7.75

$b = -.162$ channels/hour $a = 5.96$ channels $\sigma = 2.59$

$\sigma_b = .202$ channels/hour $\sigma_a = 1.09$ channels $\sigma_{INST} = .374$ channels

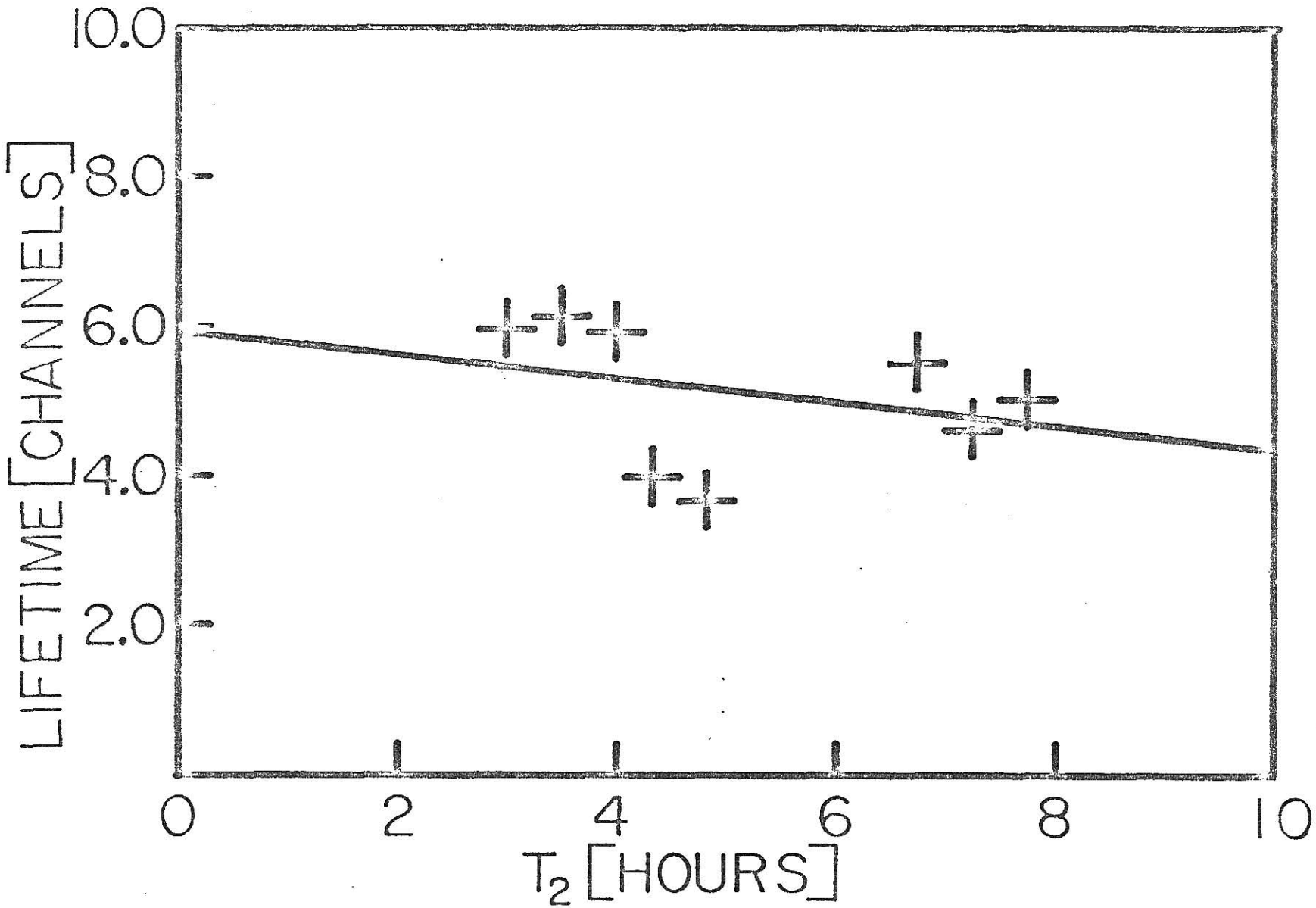
Instrument Function: Spectrum H-2A

.657 nsec/channel

PLATE XLIII

Linear least squares fit of lifetime vs. T_2 for cell/FDA background fluorescence. Refer to Table XXI.

T_2 = mixing time of cells and FDA.


10.0
8.0
6.0
4.0
2.0
LIFETIME [CHANNELS]
0
2
4
6
8
10
T2 [HOURS]

V. SUMMARY OF CONCLUSIONS

In summation the intention of this thesis has been to construct a pulsed laser system capable of measuring short lifetimes of fluorescing dyes in single cells and to verify the possible existance of variations in fluorescence decay lifetimes of hydrolyzed fluorescein diacetate. These variations are assumed to have their basis in the differences between the cell interior and exterior. Preliminary experiments performed have given results that indicate the existence of the conditions that (1) sample preparation must be carried out in a definite manner, such as given in Appendix I, (2) intracellular fluorescein concentrations appear to be in the regime where concentration lifetime quenching is dominant and (3) that there is a definite possibility of significant difference in decay lifetimes between intracellular fluorescein and the background fluorescence caused by cell leakage of fluorescein, the latter indicating a possible gradual increase in concentration lifetime quenching in the background.

The instrumentation has shown itself capable of reasonable precision, although the results clearly indicate the needed improvements. In particular, the conclusions reached above are in excellent agreement with expectations and lie well outside the estimated instrumental and statistical uncertainties. Therefore, the final conclusion reached by the author is that the assumption of no variation between intracellular and exterior fluorescence decay lifetimes is an unfounded statement, in need of much further investigation.

APPENDIX I

SAMPLE PREP-PROCEDURE

Time	
0:00 hours	1) Began cultures at 10^6 cells/mℓ in synthetic complete media. 2) Made new base solution of FDA in acetone as follows: (a) 0.416 grams of FDA in 10 mℓ acetone = 10^5 μM FDA (b) 1:10 dilution in acetone = 10^4 μM FDA.
6:50 hours	1) Mixed XL67B-3a cells into various FDA concentrations at a ratio of .2 mℓ: .2 mℓ. 2) Viewed samples under microscope for fluorescence at 10 minute intervals for 30 minutes with no results using old and new FDA concentrations of (a) 10 μM (b) 25 μM (c) 50 μM
10:43 hours	1) New sample of X2180-1B cells taken from the culture at 4.85×10^7 cells/mℓ in sc and diluted 1:10 in sterile water. 2) Sample was then sonicated and counted as stated in cell count table.
10:45 hours	Dilutions prepared from cold FDA using both the old 10^4 μM and new 10^4 μM FDA solutions with dilutions as previously noted.

10:55 hours — Cells were mixed with the 6 different FDA solutions at 24°C in ratios of 1 mℓ: 1 mℓ.

11:05 hours — Each of six samples checked and scored for fluorescence as according to Table XXII.

11:55 hours — New samples mixed from cells and FDA which had been standing at room temperature for approximately 1 hour and 10 minutes to see if activity had been lost during that time. Cells/FDA ratio was 1:1 solution using 25 µM and 100 µM FDA concentrations.

12:00 hours — New 25 µM cells/FDA solution showed fluorescence but wide variation in intensity from cell to cell.

12:30 hours — Results of 11:55 samples scored for fluorescence:

	25 µM	100 µM
New FDA @ R.T.	None	None

12:40 hours — Viewed same slide of 100 µM new FDA/cells solution from 11:35 sample and observed cells to fluoresce brightly but also with high background.

12:50 hours — New samples taken from cultures:

(a) X2180-1B @ 7.7×10^7 cells/mℓ diluted 1:50

(b) XL67B-3a @ 1.5×10^7 cells/mℓ diluted 1:10

13:15 hours — New dilutions of FDA were made from 10^4 µM to 10^2 µM, which had been kept at 0°C. To test the effect of old cells,

1) cells from the 10:43 sample were mixed with the new 10^2 µM FDA solution. Simultaneously,

2) fresh cells were mixed with the old 10^2 µM FDA made at 10:45 hours.

13:45 hours — Results of 13:15 mixtures are scored in Table XXIII.

TABLE XXII

Qualitative scoring of fluorescence for various solutions of FDA.

Time		10 µM	25 µM	100 µM
11:05 hours				
	New FDA Solution:	None	None	None
	Old FDA Solution:	None	None	1 Budded Cell
11:20 hours				
	New FDA Solution:	None	None	Yes
	Old FDA Solution:	None	Yes	Yes
11:35 hours				
	New FDA Solution:	Weak	Weak	Strong
	Old FDA Solution:	Weak	Weak	Strong

TABLE XXIII

Qualitative scoring of fluorescence for various cell/FDA solutions.

Time		Strain	FDA	Fluorescence
13:45	1)	X2180-1B	10^2 µM FDA (fresh)	strong-no background
	2)	XL67B-3a	10^2 µM FDA (fresh)	strong-no background
	3)	X2180-1B in H_2O for 3 hours	10^2 µM FDA (fresh)	strong in cells - high background
	4)	X2180-1B	10^2 µM FDA @ R.T. for 3 hours	None

At this point the J, k. L and M series spectra were run consecutively and the specifics of each spectrum are included with the data.

APPENDIX II

To provide a more efficient procedure in data analysis, the PDP-15/30 computer of the Nuclear Science Laboratories was chosen in preference to the IBM 370. The choice was made on the basis of user contact/control at all times during programming and calculating which resulted in considerable time saving. Since there is computer-user communication via teletype, computer command responses and user commands will be included in addition to the necessary programs and documentaries.

A. Program Functions

Consider the signals recorded by the PHA. These discrete signals represent a given time interval between correlated start-stop pulses received by the TAC. The time of start for the TAC is determined by the photodiode pulse amplitude because the trigger point of the level crossing discriminator is dependent upon the pulse amplitude. Since this amplitude varies from experiment to experiment because of the necessary laser power adjustments it is clear that this effect merely acts as a variable delay between the start-stop TAC channels. This variable delay effect manifests itself, not in the spectrum shape, but only in the relative position; an additional constant delay merely contributes a constant voltage and hence a constant spectral shift. Although the shift is random from spectrum to spectrum, proper consideration must be given to this effect for a proper deconvolution since laser pulse and resultant fluorescence timing spectrum generally do not have their peaks common to the same position. Treatment of this concept will be provided shortly.

Initially the raw data is transferred from the PHA to paper tape for computer analysis. However, the computer must receive all data from magnetic tape, properly formatted. Hence, data must be transferred from the paper tape onto magnetic tape. Computer program "OMPARE"[36] performs this operation and consists of a main program "READER" with subroutines "PAPER(ISEG)", "LPOUT(ISEG)","VPOUT(ISEG)", "READ3", "WRITE3", and "PAPERTEST". In essence, the program takes paper tape output from a 1024 channel analyzer and puts it into a 4096 area in computer core and then to magnetic tape. The core is separated into (4) X 1024 segments which are then divided into (4) quadrants. Thus, each tape file is capable of 16×256 channel storage areas. In addition, the program provides for a visual scope plot of the recorded data as well as line print output, which is recommended for use in order to guarantee proper data entry. Assuming proper operation, all data is now transferred to magnetic tape. The data is not as yet ready for computer analysis.

As mentioned earlier, the spectra are randomly shifted in channel position from one another and therefore must be corrected for at this time. There is no definitive technique for determining the proper corrections to be made other than comparing the individual spectra (data plots were done on the Hewlett-Packard calculator-plotter directly from data paper tape) and the necessary channels shift for the data was decided by inspection. The technique which follows has been found to be quite satisfactory in determining this correction. A good instrument spectrum whose position is as far left as possible without eliminating any data channels is obtained. This may be done by delaying the start pulse slightly, yielding a smaller time interval and, hence, a smaller

voltage pulse. The decay spectra to be analyzed are now compared with the instrument function. A number of channels are deleted from the beginning of the decay spectrum one by one until only the first low-count channels of both peaks are close to superposition. Generally this will result in the decay spectrum peak being situated to the right of the laser peak by a few channels. The reason for superimposing only the initial channels is because for each channel there are contributions from preceeding channels, described in Chapter III. Therefore the first channels only of the decay spectrum are essentially those of the laser pulse. Each estimated channel delection is recorded, as well as the instrument function to which the spectra are compared. A simple program has been written for this purpose and is titled "FIX"[37]. Operationally the program provides teletype output asking for a particular data file and spectrum and how many channels to delete from that spectrum. Channel deletions are entered consecutively upon computer messages and when input is terminated the computer automatically corrects all spectra, retaining original data files and creating new corrected data files on magnetic tape. The data are now ready for subsequent deconvolution. The point should be made that the computer plot output of the decay spectra and corresponding fitted spectra will reveal whether or not the correct channel shift correction had been made. The effect will show up as a erroneous shift between data and fitted curve. Therefore, the new corrections can be obtained if necessary and deconvolution redone. Preliminary to deconvolution, as a check to ensure that the data had been corrected as initially specified, it is beneficial to obtain a line printer output of the new data files. Computer program "LPP"[37] performs a line printer plot and lists the content of each channel for

easy comparison with original PHA teletype output. "LPP" consists of a main program "MPLPG" and subroutine "LPG".

The main data deconvolution and fitting program is "CONFIT"[64], consisting of subroutines "MATINV", "READ", "DATA", "DCON", and "FUNCT(N)". This program will fit a set of 256 data points with an arbitrary empirical 256 channel instrument function and an arbitrary decay function. Although the included program provides for individual variation of 5 parameters, provision can be made to accommodate up to 30 parameters.

The particular function that is being fit to the NDAT equally spaced data points is expressed in computer notation as

$$YC(I)=YC(I)+\sum_{K=1}^{LIM} FD(K)*\left[EXP\left[-FLOAT(LIM-K)*(1.\emptyset\emptyset/B(1))\right]*\left[1.\emptyset-EXP\left[-1.\emptyset\emptyset/B(I)\right]\right]\right] \qquad \text{Eq. II-1}$$

where

YC(I) = calculated value in channel I

FD(K) = value of instrument function in channel K

LIM = number of channels to be summed over

K = summation variable

B(1) = parameter value corresponding to (1) parameter, expressed in channels

EXP = usual exponential function

FLOAT = computer command designating real arithmetic operation.

Other computer names necessary to define are:

NPV = number of parameters to vary

NDAT = number of data points

YO(I) = observed data value in channel I

I(PAR) = number of parameter being varied

ITMAX = maximum number of fitting iterations, user stated.

NPRT = number of parameters to print

NLOES = number of singular points in matrix

DEG = NDAT - NPV, value indicating degrees of freedom for calculating reduced χ^2

ITER = iteration number being performed

TMP = total error in fit

G(I) = statistical error in fit.

Equation II-1 is merely a restatement of Equation (15) in Chapter III, presented in a form suitable for computer computation. Suitable qualification has already been given for this equation.

In obtaining the best fit the expression minimized by the program is called CHISQ, where

$$CHISQ = \sum_{I=1}^{NDAT} \frac{(YO(I) - YB(I))^2}{(YB(I)+1.0)} \quad , \qquad \text{Eq. II-2}$$

the 1.0 being included so as to eliminate division by zero. Inclusion of this number is of no consequence due to its relative smallness compared to YC(I). The best fit is obtained for which

$$\frac{\partial CHISQ}{\partial B(K)} = 0 \quad , \qquad \text{Eq. II-3}$$

for each K. The resulting set of equations is then solved by an iterative search technique to calculate successive corrections to B(K) which improve the fit. The set of equations is best solved as a matrix equation, using

standard techniques such as those presented by Bevington[33], Draper and Smith[39], and Simonis[40], represented as

$$\tilde{A} = \tilde{D}\,\tilde{B}\,\tilde{\tilde{S}} \quad , \qquad \text{Eq. II-4a}$$

where

A(K) = the sum of the deviations, weighted by the effect that B(K) has on the fit and is of the form

$$\sum_{I=1}^{NDAT} [YO(I) - YB(I)\ Z(I,K)] \quad , \qquad \text{Eq. II-4b}$$

DB(K) = a change in the parameter B(K) which improves the fit,

S(L,K)= sum of the second cross partial derivatives and of the form

$$\sum_{I=1}^{NDAT} Z(I,L)\ Z(I,K) \quad , \qquad \text{Eq. II-4c}$$

$Z(I,K) = \frac{\partial YB(I)}{\partial B(K)}$, the effect of the fitting parameter on the fit itself.

The equation which must be solved is II-4. Multiplying by $\tilde{\tilde{S}}^{-1}$, one obtains

$$\tilde{DB} = \tilde{A}\,\tilde{\tilde{S}}^{-1} \quad . \qquad \text{Eq. II-5}$$

The matrices $\tilde{S}$ and $\tilde{S}^{-1}$ are traditionally known as the curvature matrix and error matrix, respectively, and for a full explanation one should consult the previously stated references. $\tilde{S}^{-1}$ is designated as such because it contains most of the information needed in determining parameter errors:

$$\tilde{S}^{-1}_{jj} = \sigma^2_{B(J)} \quad . \qquad \text{Eq. II-6}$$

Equation II-5 is the basis for determining successive corrections to the fitting parameters and computation is continued until the computer can no longer improve the fit, the criteria being one of the following conditions.

(A) ITER > ITMAX.

This condition limits the number of iterations performed. When this condition is met the calculation is stopped, "ITER OUT" is printed and final output is initiated.

(B) IF(ABS(TMP) - Ø.ØØ1).

This condition determines the precision by which χ^2 must change. If χ^2 does not change by a value greater than Ø.ØØ1 on a given iteration then the calculation is stopped, "OK EXIT" is printed and final output is begun.

(C) IF(ITER-6).

This condition limits the total number of iterations performed to 6 (or a different value if desired). Should the χ^2 value change by more than Ø.ØØ1 on the sixth iteration, then the calculation is stopped "CHI UP" is printed and final output is begun.

Using the Poisson distribution appropriate for photon counting the goodness of the fit is determined by the reduced χ^2 value of the form

$$\chi^2 = \sum_{I=1}^{NDAT} \frac{[YO(I) - YC(I)]^2}{[\sigma(I)]^2\ [NDAT-NPV]} = \sum_{I=1}^{NDAT} \frac{[YO(I) - YC(I)]^2}{YO(I)\ DEG}\ , \quad \text{Eq. II-7}$$

where

$\sigma(I)$ is the standard deviation of the data point YO(I), approximated as $\sqrt{YO(I)}$ for the Poisson distribution.

Using this criterion for the goodness of fit, the computer-calculated errors are

$$G(I) = \frac{\sqrt{NDAT}}{\sqrt{\sum \frac{1}{\sigma^2(I)}}} \quad \text{Eq. II-8}$$

for the statistical error, and

$$TMP = G(I) * CHISQ \quad \text{Eq. II-9}$$

total error, where

$G^2(I)$ = weighted average of the individual variances,

TMP^2 = the variance of the fit which is an estimate of the variance of the data $\sum \sigma^2(I)$.

TMP includes a weighting factor for each data point which is the inverse of the variance $\sigma^2(I)$ describing the uncertainty of the data point, normalized to the average of all the weighting factors. By definition,

$$\chi^2 = \frac{TMP^2}{G^2(I)} \quad \text{Eq. II-10}$$

and one may note that this value is not only a measure of goodness of fit

but also of the spread of the data[41]. If the fitting function is a good representation of the data, χ^2 values on the order of unity are to be expected. However, due to statistical considerations, χ^2 values less than a perfect fit (<1.0) are frequently obtained and do not indicate necessarily an improvement in fit.

In order to estimate the confidence interval of the final parameter, use is made of the error matrix. Computationally,

$$G(I) = SQRT(ABS(S^{-1}(I,I))) \quad . \qquad \text{Eq. II-11}$$

But the matrix element $S^{-1}(I,I)$ is equivalent to the variance in the fitting parameter[42], B(I), and the computer output of statistical error, G(I), is merely the confidence interval of the parameter. However, the statistical uncertainties quoted through the text are on the order of magnitude smaller than the estimated instrumental uncertainties and, therefore, are not to be considered the limiting circumstances.

B. Program Execution

In order to be brief only the necessary command-response statements will be included. All information regarding proper program loading and data file labeling is assumed to be understood. The entire program is not compiled into one execute program. Rather, it is segmented and must be performed in four distinct operations:

	Program Function	Program Title
1)	Data Transfer	"OMPARE"
2)	Data Correction	"FIX"

3) Data Plot (corrected) "LPP"

4) Deconvolution "CONFIT".

"OMPARE" Execution

Load main program and subroutines via magnetic tape.

C: "You have just entered the land of the omnipotent paper tape reader. If you do not know your way around please set all sense switches to the zero state."

"Enter file name (A9)"

(Response)

C: "Load paper reader. Control P to start reading."

"Pause ØØØØ37"

(Response = control P)

C: "This program takes paper tape output from a 1Ø24 channel analyzer (in particular the ND1ØØ and stuffs it into a 4Ø96 area core and from there to dectape. Core is separated into 4 1Ø24 segments which are divided into quadrants. To ignore further output of this message set sense switch 1Ø".

"What segment do you want"?

(Response)

C: "Quadrant = _____ Starting channel = _____"

"If you want to change quadrant or starting channel put in new values".

"zeroes = default".

(Response), one value to a line.

C: "Assuming "ALL" made used for analyzer output"

"Flick sense switch 1 for VP plot"

"Flick sense switch 2 for line printer output"

"Flick sense switch 3 for same file name more paper"

"Flick sense switch 4 for new file name more paper".

"FIX" Execution

Load "FIX" via magnetic tape

C: "Type file name, ext".

(Response)

C: "Which spectrum (1-16), zero to quit"

(Response)

C: "Number of channels to chop"

(Response)

Continue in this manner until all corrections are made in the file.

(Response) Type Ø

C: "Output file name, ext".

(Response)

Data is now corrected and stored on magnetic tape.

"LPP" Execution

Load "LPP" via magnetic tape

C: "**** 88 LPA"

(Response) Carriage return

C: "Type file name and ext (A9)"

(Response)

C: "Type record number, default = 1"

(Response)

C: "Minimum channel number? default = 1"

(Response)

C: "Maximum channel number? default = 313Ø"

(Response)

C: "Desired compression? default = 1"

(Response)

C: "Type full scale for graph default = _____"

(Response)

C: "Type 2, 1, or Ø for log, linear, or both"

(Response)

C: "Type file name and ext (A9)"

Continue in this format after plot is finished until all desired correction plots are made.

"CONFIT" Execution

Load "CONFIT" main program and subprograms via magnetic tape.

C: Type NPAR, CR, NPRT, CR"

(Response) 1
1

C: "Type file name for instrument function"

(Response)

C: "Which spectrum of _____ do you want? 1-16"

(Response)

C: "Type file name for data spectrum"

(Response)

C: "Which spectrum of _____ do you want? 1-16"

(Response)

C: "Initial parameters, one to a line"

(Response) value of parameter

C: "New controls"

"IFUN, ITMAX, NPV, IPAR(I), I = 1, NPV/One to a line"

(Responses)

IFUN = -1 = return to "initial parameters" step

IFUN = Ø = return to beginning of "CONFIT"

IFUN = 1 = return to "new controls" step

Computer will now perform calculations and will respond with

C: "Output file name, ext"

Typing a file name will result in the transfer of the instrument function data, fluorescence data and calculated data to magnetic tape. Otherwise, program will return to point designated by the value of IFUN and waits for further command. Immediately following the computer program is a sample output of final analysis.

```
C       READER
        DIMENSION IDAT(4096),FN(2),ISTAT(4,4)
        COMMON IDAT,FN,ISTAT
        WRITE(1,100)
100     FORMAT(' YOU HAVE JUST ENTERED THE LAND OF THE'/
       1' UNIMPORTANT PAPER TAPE READER'/
       2' IF YOU DO NOT KNOW YOUR WAY AROUND PLESE SET'/
       3' ALL SENSE SWITCHES TO THE ZERO STATE')
1       DO 10 I=1,4
        DO 11 J=1,4
11      ISTAT(I,J)=0
10      CONTINUE
        DO 12 I=1,4096
12      IDAT(I)=0
        WRITE(1,101)
101     FORMAT(' ENTER FILE NAME (A9)')
        READ(1,102) FN(1),FN(2)
102     FORMAT(A5,A4)
        CALL FSTAT(3,FN,ICHK)
        IF(ICHK.NE.-1) GO TO 2
        WRITE(1,103) FN(1),FN(2)
103     FORMAT(' FILE ',A5,A4,' EXISTS,  TYPE -1 TO ALTER')
        READ(1,104) ICHK
104     FORMAT(I6)
        IF(ICHK.NE.-1) GO TO 1
        CALL READ3
2       CALL PAPER(ISEG)
        CALL WRITE3
        CALL READ3
        WRITE(1,105)
105     FORMAT(' FLICK SENSE SWITCH 1 FOR VP PLOT'/
       1' FLICK SENSE SWITCH 2 FOR LINE PRINTER OUTPUT'/
       3' FLICK SENSE SWITCH 3 FOR SAME FILE NAME MORE PAPER'/
       4' FLICK SENSE SWITCH 4 FOR NEW FILE NAME MORE PAPER')
3       IF(ISENSW(1).NE.0) GO TO 4
        IF(ISENSW(2).NE.0) GO TO 5
        IF(ISENSW(3).NE.0) GO TO 2
        IF(ISENSW(4).NE.0) GO TO 1
        GO TO 3
4       CALL VPOUT(ISEG)
        GO TO 3
5       CALL LPOUT(ISEG)
        GO TO 3
        END
```

```
C
C
C
      SUBROUTINE PAPER(ISEG)
      DIMENSION IDAT(4096),FN(2),ISTAT(4,4),IBUFF(10),ATCHK(10)
      COMMON IDAT,FN,ISTAT
      DATA BLNK,AT/1H ,1H@/
1     IMODE=0
      WRITE(1,101)
101   FORMAT(' LOAD PAPER READER.  AP TO START READING')
      PAUSE 07
      READ(6,102,END=1,ERR=1) ITIME
102   FORMAT(I6)
      READ(6,103,END=1,ERR=1) CHK,IQUAD,ISTART
103   FORMAT(A1,I1,I4)
      IF(CHK.EQ.AT) IMODE=-1
      IF(CHK.EQ.BLNK) IMODE=1
      IF(IQUAD.EQ.0) GO TO 107
2     IF(ISEG.GT.0.AND.ISEG.LT.5) WRITE(1,104)
104   FORMAT(' THIS PROGRAM TAKES PAPER TAPE OUTPUT FROM A 1024!/
     1' CHANNEL ANALYZER( IN PARTICULAR THE ND100 )!/
     2' AND STUFFS IT INTO A 4096 AREA IN CORE AND FROM THERE TO !/
     3' DECTAPE.  CORE IS SEPARATED INTO 4 1024 SEGMENTS WHICH ARE '/
     4' DIVIDED INTO QUADRANTS.  TO IGNORE FURTHER OUTPUT OF '/
     5' THIS MESSAGE SET SENSE SWITCH 1@')
      WRITE(1,105)
105   FORMAT(' WHAT SEGMENT DO YOU WANT?')
      READ(1,106) ISEG
      WRITE(1,107) IQUAD,ISTART
107   FORMAT(' QUADRANT = ',I2,1PX,' STARTING CHANNEL=',I6)
      WRITE(1,108)
108   FORMAT(' IF YOU WANT TO CHANGE QUADRANT OR STARTING CHANNEL!/
     1' PUT IN NEW VALUES.  ZEROES=DEFAULT!')
      READ(1,102) IQ,IS
      IF(IQ.NE.0) IQUAD=IQ
      IF(IS.NE.0) ISTART=IS
      IF(ISTAT(ISEG,IQUAD).NE.-1) GO TO 3
      WRITE(1,109)
109   FORMAT(' THIS SEGMENT AND QUADRANT USED.!/
     1' TYPE -1 TO USE AGAIN OR FOR NEW VALUES!')
      READ(1,102) ICHK
      IF(ICHK.NE.-1) GO TO 2
3     ISTAT(ISEG,IQUAD)= -1
      JSTART=ISTART + 1024*(ISEG-1) + 256*(IQUAD-1)
      IEND=JSTART + 1023
      IF(IMODE.EQ.-1) GO TO 6
      WRITE(1,110)
110   FORMAT(' ASSUMING "ALL" MODE USED FOR ANALYZER OUTPUT!')
      IENDF=1
      ICHK=ISTART
      J=JSTART
      I=ISTART
502   CONTINUE
      JCHK=(I/100)*100 - I
      IF(JCHK.EQ.0.AND.ICHK.NE.0) GO TO 510
      ICHK=1
511   READ(5,601,END=5,ERR=5) (IBUFF(IN),IN=1,10)
```

```
601     FORMAT(I6,917)
        GO TO 20
5       IENDR=-1
20      DO 502 IJK=1,10
        IF(J.GT.IFIN) GO TO 15
        IF(I.LT.1.OR.J.GT.4096) GO TO 503
        IDAT(J)=IBUFF(IJK)
503     CONTINUE
        J=J+1
        I=I+1
502     IBUFF(IJK)=0
        IF(IENDR.NE.-1) GO TO 500
15      RETURN
6       WRITE(1,111)
111     FORMAT(' ASSUMING "MARKERS" OR "REGIONS" MODE FOR ANALYZER'
       1' OUTPUT')
        IENDR= +1
        ICHK=ISTART
        J=JSTART
        I=ISTART
        N=10 -(ISTART-10*(ISTART/10))
10      CONTINUE
        JCHK= (I/10)*10 - I
        IF(JCHK.EQ.0.AND.ICHK.NE.0) GO TO 521
        ICHK=1
522     READ(6,605,END=9,ERR=6) (ATCHK(IN),IBUFF(IN),IN=1,N)
605     FORMAT(A1,I5,9(1X,A1,I5))
        GO TO 40
9       IENDR=-1
40      DO 532 IJK=1,N
        IF(J.GT.IFIN) GO TO 25
        IF(I.LT.1.OR.J.GT.4096) GO TO 26
        IF(ATCHK(IJK).EQ.AT) GO TO 27
        IDAT(J)=IBUFF(IJK)
26      CONTINUE
        I=I+1
        J=J+1
532     IBUFF(IJK)=0
        N=10
        IF(IENDR.NE.-1) GO TO 10
25      RETURN
27      READ(6,103,END=525,ERR=525) CHK,IQ,ISTART
        IF(CHK.NE.AT) GO TO 525
        JSTART=ISTART + 1024*(ISEG-1) + 256*(IQUAD-1)
        GO TO 6
1000    WRITE(1,1001)
1001    FORMAT(' MODE MIXUP STARTING OVER')
        GO TO 1
510     READ(6,602,END=5,ERR=5)  IQ,ICHK
602     FORMAT(I2,I4)
        IF(ICHK.EQ.1) GO TO 511
        WRITE(1,610)
610     FORMAT(' CHANNEL MIXUP')
        RETURN
521     READ(6,103,END=523,ERR=523) CHK,IQ,ICHK
        IF(CHK.NE.AT) GO TO 523
        IF(ICHK.EQ.1) GO TO 522
```

```
523     WRITE (1,610)
        RETURN
525     WRITE(1,606)
606     FORMAT(' END OR AT NOT FOLLOWED BY AT')
        RETURN
        END
```

```
C
C
C
      SUBROUTINE LPOUT(ISEG)
      DIMENSION IDAT(4096),FN(2),ISTAT(4,4)
      COMMON IDAT,FN,ISTAT
      WRITE(1,101) ISEG
101   FORMAT(' SEGMENT ',I2,' TO CHANGE ENTER NEW VALUE')
      READ(1,102) I
102   FORMAT(I6)
      IF(I.NE.0) ISEG=I
      WRITE(2,103) ISEG,FN(1),FN(2)
103   FORMAT('1SEGMENT ',I2,10X,' OF FILE ',A5,A4)
      I=1 + (ISEG-1)*1024
      J=I + 1023
      WRITE(2,104) (IDAT(K),K=I,J)
104   FORMAT(' ',10I10)
      RETURN
      END
```

```
C
C
C
      SUBROUTINE VFOUT(ISEG)
      DIMENSION IDAT(4096),FN(2),ISTAT(4,4)
      COMMON IDAT,FN,ISTAT
      WRITE(1,101) ISEG
101   FORMAT(' SEGMENT ',I2,'  TO CHANGE ENTER NEW VALUE')
      READ(1,102) I
102   FORMAT(I6)
      IF(I.GT.0.AND.I.LE.4) ISEG=I
      CALL INIT
      IF(ISEG.LE.0.OR.ISEG.GT.4) ISEG=1
      IYMAX=1
      DO 1 IX=1,1023,2
      I=IX +(ISEG-1)*1024
      IY=IDAT(I)/2 + IDAT(I+1)/2
      IYMAX=MAX0(IYMAX,IY)
1     CONTINUE
      SCALE= 360./FLOAT(IYMAX)
      IX=0
      DO 2 I=1,1023,2
      J=I + (ISEG-1)*1024
      IX= IX + 1
      IY=IFIX(SCALE*FLOAT(IDAT(J)+IDAT(J+1))/2.0)
      IPT=NUVAL(0,IX,IY)
      CALL POINT(1,0,IPT)
2     CONTINUE
      RETURN
      END
```

```
      SUBROUTINE READ3
      DIMENSION IDAT(4096),FN(2),ISTAT(4,4)
      COMMON IDAT,FN,ISTAT
      CALL SEEK (3,FN)
      IB=0
      DO 3 I=1,64
      IA=IB + 1
      IB=IB + 64
      READ(3) (IDAT(J),J=IA,IB)
3     CONTINUE
      DO 4 I=1,4
      DO 5 J=1,4
      IJK= 1 + (I-1)*1024 + (J-1)*256
      IJJ= IJK + 255
      ISUM=0
      DO 6 K=IJK,IJJ
6     ISUM=ISUM + IDAT(K)
      IF(ISUM.NE.0) ISTAT(I,J)=-1
5     CONTINUE
4     CONTINUE
      RETURN
      END
```

```
C
C
C
      SUBROUTINE WRITE3
      DIMENSION IDAT(4096),FN(2),ISTAT(4,4)
      COMMON IDAT,FN,ISTAT
      CALL ENTER(3,FN)
      IB=0
      DO 1 I=1,64
      IA=IB + 1
      IB=IB + 64
      WRITE (3) (IDAT(J),J=IA,IB)
1     CONTINUE
      CALL CLOSE(3,FN)
      RETURN
      END
```

```
C
C
C       PROGRAM TO TEST PAPER READER
C
C
        DIMENSION IDAT(1024)
1       WRITE(3,101)
101     FORMAT(' LOAD PAPER TAPE,  AP TO START READING!')
        PAUSE
        READ(5,102,END=1,ERR=1) ITIME
102     FORMAT(I5)
        READ(5,103,END=1,ERR=1) CHK,IQUAD,ISTART
103     FORMAT(3I1,I4)
        WRITE(1,104) IQUAD,ISTART
104     FORMAT(' LOAD #',I2,10X,'START =',I5)
        IF(ISTART.EQ.0) READ(5,102,END=1,ERR=1) I
        IF(ISTART.EQ.0) ISTART=ISTART + 1
        JSTART= ISTART + 255*(IQUAD-1)
        JFISTART = 1
        DO 2 I=JSTART,1024
        J=J + 1
        JCHK=(J/10)*10 -J
        IF(JCHK.NE.0) GO TO 3
        READ(5,105,END=4,ERR=4) IDAT(I)
105     FORMAT(I6)
3       READ(5,106,END=4,ERR=4) IDAT(I)
106     FORMAT(I7)
2       CONTINUE
4       CONTINUE
        WRITE(2,107) (IDAT(I),I=1,1024)
107     FORMAT(1H ,10I12)
        GO TO 1
        END
```

```
   FIX
      DIMENSION FILE(2),FOUT(2)
      COMMON IDAT(4096)
1     WRITE(1,10)
      READ(1,11)FILE
      CALL FSTAT(3,FILE,NF)
      IF (NF.EQ.-1) GO TO 2
      WRITE(1,12) FILE
      GO TO 1
2     CALL SEEK(3,FILE)
      DO 3 J=1,4096,64
      JX=J+63
      READ(3) (IDAT(I), I=J,JX)
3     CONTINUE
4     WRITE(1,13)
      READ(1,14) NS
      IF (NS.EQ.0) GO TO 20
      WRITE(1,15)
      READ(1,14)  NC
      IS=(NS-1)*256
      L=256-NC
      DO 5 I=1,L
      IX= IS+I
      IDAT(IX)=IDAT(IX+NC)
      IF(IDAT(IX).GT.2000)  IDAT(IX)=0
5     CONTINUE
      GO TO 4
20    WRITE (1,16)
      READ (1,11) FOUT
      CALL ENTER (3,FOUT)
      DO 21  J=1,4096,64
      JX=J+63
      WRITE(3) (IDAT (I), I=J,JX)
21    CONTINUE
      CALL CLOSE(3,FOUT)
      GO TO 1
10    FORMAT (' TYPE FILENAME,EXT')
11    FORMAT (A5,A4)
12    FORMAT (' FILE ',A5,A4,' CANNOT BE FOUND')
13    FORMAT ('WHICH SPECTRUM (1-16), ZERO TO QUIT')
14    FORMAT (I6)
15    FORMAT (' NUMBER OF CHANNELS TO CHOP')
16    FORMAT (' OUTPUT FILE NAME, EXT')
      END
```

```
C
C  MAIN PROGRAM FOR LINE PRINTER GRAPHING
C
      IMPLICIT DOUBLE INTEGER (J)
      LOGICAL PT
      COMMON IDAT(3000),FI(2),MN,MX,JFS,INC,IOR
      DATA MN,LN,LM /0,-99,2/
      LP=2
      WRITE(LP) 88,88
    1 WRITE(1,20)
      READ(1,21) FI(1),FI(2)
      CALL OPDAT(3,FI,,PT)
      IF(PT) GO TO 2
      WRITE(1,22) FI(1),FI(2)
      GO TO 1
    2 CALL SEEK(3,FI)
      WRITE(1,23)
      READ(1,24) NN
      IF(NN.LE.0) NN=1
      DO 3 K=1,NN
      DO 3 L=1,4096,84
      KC=L+83
      READ(3)(IDAT(I),I=L,KC)
    3 CONTINUE
      DO 4 I=4096,1,-1
      IF((I.GE.3721).AND.(I.LE.3720)) GO TO 4
      IF((IDAT(I).NE.0).AND.(IDAT(I-1).NE.0).AND.(IDAT(I-2).NE.0))GOTO5
    4 CONTINUE
    5 I=(I/10)*10
      WRITE(1,25)
      READ(1,24)MN
      IF(MN.LE.0)MN=1
      WRITE(1,26)I
      READ(1,24)MX
      IF(MX.LE.0)MX=1
      WRITE(1,27)
      READ(1,24)INC
      IF(INC.LE.0) INC=1
      IF(INC.EQ.0) GO TO 7
      MX=MX/INC
      IF(MX.GT.0) MX=1
      MX=MX/INC
      IS=4096/INC
      DO 6 I=1,IS
      IDAT(I)=0
      IA=I+INC
      IE=IA-I+1
      DO 6 L=IA,IE
    6 IDAT(I)=IDAT(I)+IDAT(L)
    7 IS=MX-1
      JS1=0
      DO 8 I=NN,IS
      JS=JUMBLE(IDAT(I))
      IF(JS.LT.0) JS=JS+80777777
      IF(JS.GT.JS1) JS1=JS
    8 CONTINUE
```

```
      READ(1,24)JFS
      IF(JFS.EQ.0)JFS=JS1
      WRITE(1,2*)
      READ(1,24)IC
      CALL LPS
      GO TO 1
20    FORMAT(' TYPE FILE NAME & EXT   (A9)')
21    FORMAT(A5,A4)
22    FORMAT(' FILE ',A5,A4,' WAS NOT FOUND ON DECTAPE 3')
23    FORMAT(' TYPE RECORD NUMBER  DEFAULT=1')
24    FORMAT(I6)
25    FORMAT(' TTY 3: CHANNEL NUMBER?     DEFAULT=1')
26    FORMAT(' MAGTAPE CHANNEL NUMBER?    DEFAULT=',I4)
27    FORMAT(' DESIRED COMPRESSION?      DEFAULT=1')
28    FORMAT(' TYPE FULL SCALE FOR GRAPH   DEFAULT=',I6)
29    FORMAT(' TYPE: 2, 1, OR 0  FOR LOG, LINEAR, OR BOTH')
      END
```

```
      SUBROUTINE TIME_LPS
      IMPLICIT DOUBLE INTEGER (J)
      COMMON IDA(4,200),FI(2),MN,MX,JFS,IMC,IOW
      DATA JC,C,R/ 7,7777,1H+,1H /
      F=1H/
      S=1H*
      IF(IOW.EQ.0) I=1
      IF(IOW.EQ.1) F=1H
      IF(IOW.EQ.2) S=1H
      WRITE(2,101)
101   FORMAT(1H1)
      DO 9 I=1,5
      WRITE(2,1) FI,IMC
1     FORMAT(12X,'*** ',A5,A4,'  LOG=X,LIN.=*   COMP=',I2)
2     CONTINUE
      WRITE(2,3)
3     FORMAT(//////' CHANNEL',3X,'DATA',7X,'AREA')
      X=FLOATJ(JFS)+1.
      LGNF=IFIX(ALOG10(X)+.999)
      JA=0
      DO 7 I=MN,MX
      JI=JMOL.(IDAT(I))
      IF(JI.LT.0) JI=JI+JC
      JA=JA+JI
      X=FLOATJ(JI)+1.
      IY=IFIX((ALOG10(X)-1.0)*100.0/FLOAT(LGNF-1))+1
      IX=IFIX((FLOATJ(JI)*100.0)/FLOATJ(JFS))+1
      IF(IY.GT.100) IY=100
      IF(IX.GT.100) IX=100
      IF(IY.LT.1) IY=1
      IF(IY.LT.1) IX=1
      IF(IY.GT.IX) GO TO 5
      IF(IX.GT.IY) GO TO 6
      WRITE(2,4) I,JI,JA,(M,M=1,IX),E
4     FORMAT(1X,I5,3X,I7,2X,I9,102A1)
      GO TO 7
5     IS=IY-IX
      WRITE(2,4) I,JI,JA,(F,M=1,IX),S,(F,N=1,IS),F
      GO TO 7
6     IS=IX-IY
      WRITE(2,4) I,JI,JA,(S,M=1,IY),F,(S,N=1,IS),S
7     CONTINUE
      RETURN
      END
```

```
      DIMENSION  Y0(256),YC(256),FD(256),IDAT(256),B(5),IPAR(5)
      DIMENSION  P(5),A(5,5),G(5),FINS(2),FDATA(2),PLOT(121),FOUT(2)
      COMMON  NDAT, NPAR, NPV, ITMAX, IFUN, NLOES, NPRT
      COMMON P,G,B,IPAR,Y0,YC,FD,IDAT,A,DUMMY(150)
      EQUIVALENCE(PLOT(1),DUMMY(1))
      CALL ERRSET(2)
      CHIMAX=1.E5
1     IFUN=0
2     CALL DATA
      ITER=1
      DEGFRDAT-NPV
      IF(DEG) 6,5,20
5     WRITE(2, 7)
7     FORMAT(1/H OVER SPEC)
      DEG=1.0
20    CHISQ=CHIMAX
      WRITE(2,3)
3       FORMAT(//9X16H INITIAL PARAMETER   )
      WRITE(2,4)(I,P(I),I=1,NPAR)
4      FORMAT ( 9X, I5, F10.3 )
      WRITE(2,5)(IPAR(I),,I=1,NPV)
5     FORMAT(5H VARY,1515)
        CALL TIME(MINUTE,ISECND,IOFF)
10    ITER=ITER+1
      CHIL=CHISQ
      CHISQ=0.
      DO 200 I=1,NDAT
      CALL FUNCT(I)
      TMP=Y0(I)-YC(I)
      CHISQ=CHISQ+TMP*TMP/(YC(I)+1.)
200   CONTINUE
      WRITE(2,201)CHISQ
201   FORMAT(1HX,8H CHISQ =,1PE13.5)
220   IF(ITER-ITMAX) 230,230,1100
230   TMP=CHISQ-CHIL
      IF(ABS(TMP)-0.001)  1000,1000,240
240   IF(TMP) 260,260,250
250   IF(ITER-6)  260,260,1200
260   DO 271 I=1,NPV
      G(I)=0.
      DO 270 J=1,NPV
      A(I,J)=0.
270   CONTINUE
271     CONTINUE
      DO 120 I=1,NDAT
      TMP=YC(I)
      DO 110 III=1,NPV
      J=IPAR(III)
      PTMP=B(J)
      DELP=PTMP*0.001
      IF(DELP) 102,101,102
101   DELP=0.001
102   B(J)=PTMP+DELP
      CALL FUNCT(I)
      B(J)=PTMP
      P(III)=(YC(I)-TMP)/DELP
110   CONTINUE
      YC(I)=TMP
```

```
      TMP=YG(I)-TMP
      DO 121 JJ=1,NPV
      PTMP=P(JJ)/(YG(I)+1.)
      G(JJ)=G(JJ)+TMP*PTMP
      DO 120  II=JJ,NPV
      A(II,JJ)=A(II,JJ)+P(II)*PTMP
      A(JJ,II)=A(II,JJ)
  120 CONTINUE
  121   CONTINUE
  100 CONTINUE
      CALL MATINV
      IF(NLOOS) 1300,300,1300
  300 DO 310 I=1,NPV
      J=IPAR(I)
      B(J)=B(J)+G(I)
  310 CONTINUE
      GO TO 10
 1100 WRITE(2,1101)
 1101 FORMAT(24H ITER OUT)
      GO TO 1010
 1000 WRITE(2,1001)
 1001 FORMAT(8H OK EXIT)
 1010 CHISQ=CHISQ/DEG
      WRITE(2,1012)CHISQ
 1012 FORMAT(6X,11HCHISQ/DEG =,1PE13.5)
      WRITE(2,1011)
 1011 FORMAT(13H FINAL PARAMS,10X,5HVALUE,5X,25HSTAT ERROR    TOTAL ERRO
     1R)
        CHISQ=SQRT(CHISQ)
        DO 1020 I=1,NPAR
        G(I)=0.0
 1020 CONTINUE
        DO 1030 I=1,NPV
      J=IPAR(I)
      G(J)=SQRT(ABS(A(I,I)))
 1030 CONTINUE
      DO 1040 I=1,NPAR
      TMP=G(I)*CHISQ
      WRITE(2,1013) I,B(I),G(I),TMP
 1013 FORMAT(1PX,I5,3(1PE15.5))
 1040 CONTINUE
        WRITE(2,1014)
 1014 FORMAT(6H AREAS)
      DO 1302 I=4,NPAR,4
      SPI=1.2506141
      DELP=SPI      *(B(I)*G(I+2)+B(I+2)*G(I))
      TMP= SPI      *B(I)*B(I+2)
      WRITE(2,1303)B(I+1),TMP,DELP
 1303 FORMAT(14X,3(1PE15.5))
 1302 CONTINUE
        IOFF=1
        WRITE(2,4000)MINUTE,ISECND
 4000   FORMAT(8 ELAPSED TIME= 8I38MINUTES,I38SECONDS8)
      IF(NPRT)401,400,401
  401 WRITE(2,211)
  211 FORMAT(14x,1HX,11X,4HDATA,10X,5H  FIT,9X,6HBACKGD)
        DO 213 I=1,NDAT
        XII=I
```

```
        YOII=YO(I)
        YCII=YC(I)
        YBII=B(1)+B(2)*FLOAT(I)
213     WRITE(2,212)II,YOII,YCII,YBII
 212  FORMAT(5(1PE15.5))
  400 WRITE(2,1400)INAME
1400    FORMAT(1H1,10A8,///)
      BIG=0.0
      DO 9100 I=1,NDAT
      IF(BIG-YO(I)) 9110,9120,9120
9110  BIG=YO(I)
9120  IF(BIG-YC(I)) 9130,9100,9100
9130  BIG=YC(I)
9100  CONTINUE
      BIG=120./BIG
      DO 9900 I=1,NDAT
      DO 9900 J=1,121
      PLOT(J)=1H
9900  CONTINUE
        J=(B(1)+B(2)*FLOAT(I))*BIG
      PLOT(J)=1HX
      J=YC(I)*BIG
      PLOT(J)=1H*
      J=YO(I)*BIG
      PLOT(J)=1H0
        WRITE(2,800)I,PLOT
9800    CONTINUE
 800  FORMAT(1X,I3,2H A,121A1)
        WRITE (1,21)
        READ (1,22) FOUT
        IF (FOUT(1).EQ. 5H    ) GO TO 2
        CALL ENTER (3,FOUT)
        DO 23 J=1,100,10
        JX=J+9
        WRITE(3) (YO(I),FO(I),YC(I), I=J,JX)
23      CONTINUE
        CALL CLOSE(3,FOUT)
21      FORMAT(' OUTPUT FILENAME,EXT')
22      FORMAT(A5,A4)
      GO TO 2
 1200 WRITE(2,1201)
 1201 FORMAT(7H CHI UP)
      DO 1210 I=1,NPV
      J=IPAR(I)
      B(J)=B(J)-G(I)
 1210 CONTINUE
      ITER=ITMAX
      GO TO 10
 1300 WRITE(2,1301)
 1301 FORMAT(9H SINGULAR)
      IF(ITER-1) 2,2,1010
      END
```

```
      SUBROUTINE DATA
        DIMENSION YO(256),YC(256),FO(256),IDAT(256),B(5),IPAR(5)
        DIMENSION P(5),A(5,5),G(5)
        COMMON NDAT,NPAR,NPV,ITMAX,IFUN,NLOES,NPRT
        COMMON P,G,B,IPAR,YO,YC,FO,IDAT,A,DUMMY(150)
      IF(IFUN) 200,100,300
  100   WRITE(1,1001)
 1001   FORMAT(' TYPE  NPAR, CR, NPRT, CR   ')
        READ(1,203) NPAR,NPRT
  203   FORMAT(I3)
  204   FORMAT(F10.3)
 2005   FORMAT(I4)
        CALL READ
        IF (NPRT.LT.3)GO TO 5000
  200   WRITE(1,3000)
 3000   FORMAT(34H INITIAL PARAMETERS, ONE TO A LINE)
        READ(1,204)(B(I),I=1,NPAR)
  300   WRITE(1,4000)
 4000   FORMAT(13H NEW CONTROLS /34H IFUN,ITMAX,NPV,IPAR(I),I=1,NPV  /
        1 14H ONE TO A LINE   )
        READ(1,203)IFUN,ITMAX,NPV,(IPAR(I),I=1,NPV)
 5000   CONTINUE
      RETURN
      END
```

```
      SUBROUTINE READ
      DIMENSION  YO(256),YC(256),FO(256),IDAT(256),B(5),IPAR(5)
      DIMENSION  P(5),A(5,5),G(5),FINS(2),FDATA(2)
      COMMON      NDAT,NPAR,NPV,ITMAX,IFUN,NLOES,NPRT
      COMMON       P,C,H,IPAR,YO,YC,FO,IDAT,A,DUMMY(150)
1     WRITE (1,20)
      READ (1,21) FINS
      WRITE (2,26)FINS
26    FORMAT(30X' FILE ',10X  A5,A4  )
      CALL FSTAT(3,FINS,NF)
      IF(NF.EQ.-1)  GO TO 2
      WRITE(1,22) FINS
      GO TO 1
2     WRITE(1,23) FINS
      READ(1,24) NB
      WRITE (2,27)NB
27    FORMAT(30X ' SPECTRUM ',6XI6)
      CALL SEEK(3,FINS)
      DO 4  J=1,NB
      DO 3  I=1,256,64
      IX=I+63
      READ(3)(IDAT(K),K=I,IX)
3     CONTINUE
4     CONTINUE
      SUM=0.0
      DO 5  I=1,256
      FO(I)= FLOAT(IDAT(I))
5     SUM=SUM+FO(I)
6     WRITE(1,25)
      READ(1,21) FDATA
      WRITE(2,26)FDATA
      CALL FSTAT(3,FDATA,NF)
      IF(NF.EQ.-1)  GO TO 7
      WRITE(1,22) FDATA
      GO TO 6
7     WRITE(1,23) FDATA
      READ(1,24) NB
      WRITE(2,27)NB
      CALL SEEK(3,FDATA)
      DO 9  J=1,NB
      DO 8  I= 1,256,64
      IX=I+63
      READ(3) (IDAT(K), K=I, IX)
8     CONTINUE
9     CONTINUE
      DSUM=0.0
      DO 10  I=1,256
      YO(I)=FLOAT(IDAT(I))
10    DSUM=DSUM+YO(I)
      R=SUM/DSUM
      DO 11  I=1,256
      YO(I)=YO(I)*R
11    CONTINUE
      NDAT=100
20    FORMAT(' TYPE FILENAME FOR INSTRUMENT FUNCTION!)
21    FORMAT(A5,A4)
22    FORMAT(' FILE ',A5,A4,' WAS NOT FOUND!)
23    FORMAT(' WHICH SPECTRUM OF ',A5,A4,' DO YOU WANT?  1-16!)
```

```
24      FORMAT(I5)
25      FORMAT(' TYPE FILENAME FOR DATA SPECTRUM')
        RETURN
        END
```

```
      SUBROUTINE MATINV
        DIMENSION YC(256),YC(256),FD(256),IDAT(256),B(5),IPAR(5)
        DIMENSION P(5),A(5,5),G(5),IPIVOT(8),INDEX(8,2),PIVOT(8)
        COMMON NDAT,MPAR,NPV,ITMAX,IFUN,NLOOS,NPRT
        COMMON P,G,B,IPAR,YO,YC,FD,IDAT,A,DUMMY(150)
      EQUIVALENCE (IROW,JROW),(ICOLUM,JCOLUM),(AMAX,T,SWAP)
      NLOOS=0
      DO 20 J=1,NPV
   20 IPIVOT(J)=0
      DO 550 I=1,NPV
      AMAX=1.0E-30
      IANZ=0
      DO 105 J=1,NPV
      IF(IPIVOT(J)-1) 60,105,60
   60 DO 100 K=1,NPV
      IF(IPIVOT(K)-1) 80,99,71
   71 NLOOS=1
      RETURN
   80 IF(ABS(AMAX)-ABS(A(J,K))) 84,99,99
   84 IANZ=IANZ+1
      IROW=J
      ICOLUM=K
      AMAX=A(J,K)
   99   CONTINUE
  100 CONTINUE
  105   CONTINUE
  105 CONTINUE
      IF(IANZ) 71,71,110
  110 IPIVOT(ICOLUM)=IPIVOT(ICOLUM)+1
      IF(IROW-ICOLUM) 150,200,150
  150 DO 200 L=1,NPV
      SWAP=A(IROW,L)
      A(IROW,L)=A(ICOLUM,L)
  200 A(ICOLUM,L)=SWAP
      SWAP=G(IROW)
      G(IROW)=G(ICOLUM)
      G(ICOLUM)=SWAP
  250 INDEX(I,1)=IROW
      INDEX(I,2)=ICOLUM
      PIVOT(I)=A(ICOLUM,ICOLUM)
      A(ICOLUM,ICOLUM)=1.0
      DO 350 L=1,NPV
  350 A(ICOLUM,L)=A(ICOLUM,L)/PIVOT(I)
      G(ICOLUM)=G(ICOLUM)/PIVOT(I)
      DO 551 L1=1,NPV
      IF(L1-ICOLUM) 400,552,400
  400 T=A(L1,ICOLUM)
      A(L1,ICOLUM)=0.0
      DO 450 L=1,NPV
  450 A(L1,L)=A(L1,L)-A(ICOLUM,L)*T
      G(L1)=G(L1)-G(ICOLUM)*T
  552   CONTINUE
  551   CONTINUE
  550 CONTINUE
      DO 710 I=1,NPV
      L=NPV+1-I
      IF(INDEX(L,1)-INDEX(L,2)) 630,709,630
  630 JROW=INDEX(L,1)
```

```
      JCOLUM=INDEX(L,2)
      DO 705 K=1,NPV
      SWAP=A(K,JROW)
      A(K,JROW)=A(K,JCOLU
      A(K,JCOLUM)=SWAP
  705 CONTINUE
  709   CONTINUE
  710 CONTINUE
      RETURN
      END
```

```
      SUBROUTINE FUNCT(N)
      DIMENSION YO(256),YC(256),FD(256),IDAT(256),B(5),IPAR(5)
      DIMENSION P(5),A(5,5),G(5)
      COMMON NDAT,NPAR,NPV,ITMAX,IFUN,NLOES,NPRT
      COMMON P,G,B,IPAR,YO,YC,FD,IDAT,A,DUMMY(150)
      YC(N)=0.0
      T=1.00/B(1)
      LIM=N
      C=1.0-EXP(-T)
      DO 5 K=1,LIM
      IF (FD(K).EQ.0.0)  GO TO 5
      E=FLOAT(LIM-K)*T
      YC(N)=YC(N)+FD(K)*EXP(-E)*C
    5 CONTINUE
      RETURN
      END
```

```
                                        FILE            BLASERBIN
                                        SPECTRUM           10
                                        FILE            BYFDA28IN
                                        SPECTRUM            5

        INITIAL PARAMETER
           1      3.000
VARY  1
          CHISQ =  1.42028E+02
          CHISQ =  1.39401E+02
ITER OUT
     CHISQ/DEG =  1.43[illegible]E+00
FINAL PARAMS          VALUE       STAT ERROR     TOTAL ERROR
           1      3.67752E+00     8.34315E-02    9.85277E-02
AREAS
ELAPSED TIME:   1MINUTE  8SECONDS
              X              DATA              FIT           BACKGD
   1.[illegible]E+00     8.29723E+00     3.33321E+00     3.67752E+00
   2.[illegible]E+00     1.65114E+01     1.89576E+01     3.67752E+00
   3.[illegible]E+00     3.35945E+01     4.79695E+01     3.67752E+00
   4.[illegible]E+00     7.74731E+01     8.68134E+01     3.67752E+00
   5.[illegible]E+00     1.43391E+02     1.47806E+02     3.67752E+00
   6.[illegible]E+00     2.[illegible]64E+02     2.13489E+02     3.67752E+00
   7.[illegible]E+00     3.11949E+02     2.93541E+02     3.67752E+00
   8.[illegible]E+00     4.18217E+02     3.80172E+02     3.67752E+00
   9.[illegible]E+00     4.80892E+02     4.37552E+02     3.67752E+00
   1.[illegible]E+01     5.91224E+02     4.93923E+02     3.67752E+00
   1.[illegible]E+01     5.[illegible]23E+02     5.24178E+02     3.67752E+00
   1.20[illegible]E+01     5.64539E+02     5.42421E+02     3.67752E+00
   1.36[illegible]E+01     5.39[illegible]9E+02     5.49035E+02     3.67752E+00
   1.48[illegible]E+01     4.84721E+02     5.37361E+02     3.67752E+00
   1.5[illegible]E+01     4.12[illegible]47E+02     5.16561E+02     3.67752E+00
   1.60[illegible]E+01     4.39[illegible]5E+02     4.98[illegible]0E+02     3.67752E+00
   1.7[illegible]E+01     4.37414E+02     4.56573E+02     3.67752E+00
   1.8[illegible]E+01     3.79138E+02     4.32[illegible]9E+02     3.67752E+00
   1.9[illegible]E+01     3.71[illegible]5E+02     3.96436E+02     3.67752E+00
   2.[illegible]E+01     3.3[illegible]6E+02     3.71985E+02     3.67752E+00
   2.1[illegible]E+01     3.41439E+02     3.48736E+02     3.67752E+00
   2.2[illegible]E+01     3.[illegible]E+02     3.10987E+02     3.67752E+00
   2.3[illegible]E+01     2.87267E+02     2.76401E+02     3.67752E+00
   2.40[illegible]E+01     2.56415E+02     2.46164E+02     3.67752E+00
   2.5[illegible]E+01     2.[illegible]1E+02     2.17[illegible]E+02     3.67752E+00
   2.6[illegible]E+01     2.15279E+02     1.8[illegible]E+02     3.67752E+00
   2.7[illegible]E+01     1.[illegible]E+02     1.[illegible]E+02     3.67752E+00
   2.8[illegible]E+01     1.41[illegible]E+02     1.45[illegible]E+02     3.67752E+00
   2.9[illegible]E+01     1.3[illegible]E+02     1.24[illegible]E+02     3.67752E+00
   3.[illegible]E+01     1.16[illegible]E+02     1.08111E+02     3.67752E+00
   3.1[illegible]E+01     9.94123E+01     9.45134E+01     3.67752E+00
   3.2[illegible]E+01     9.39275E+01     7.96298E+01     3.67752E+00
   3.3[illegible]E+01     [illegible].45[illegible]E+01     6.7[illegible]E+01     3.67752E+00
   3.4[illegible]E+01     5.3477[illegible]E+01     5.56475E+01     3.67752E+00
   3.5[illegible]E+01     4.29[illegible]E+01     4.69223E+01     3.67752E+00
   3.6[illegible]E+01     3.9[illegible]E+01     3.86077E+01     3.67752E+00
   3.7[illegible]E+01     2.74241E+01     3.29871E+01     3.67752E+00
   3.8[illegible]E+01     2.12537E+01     2.67999E+01     3.67752E+00
   3.9[illegible]E+01     1.98625E+01     2.20858E+01     3.67752E+00
   4.[illegible]E+01     1.91969E+01     1.80179E+01     3.67752E+00
```

4.1[illegible]E+01	1.43976E+01	1.49185E+01	3.67752E+00
4.2[illegible]E+01	1.85113E+01	1.24809E+01	3.67752E+00
4.3[illegible]E+01	8.81263E+00	9.44206E+00	3.67752E+00
4.4[illegible]E+01	1.78257E+01	7.07[illegible]8E+00	3.67752E+00
4.5[illegible]E+01	9.59[illegible]43E+00	5.84439E+00	3.67752E+00
4.6[illegible]E+01	6.85502E+00	4.45292E+00	3.67752E+00
4.7[illegible]E+01	6.63[illegible]2E+00	3.63983E+00	3.67752E+00
4.8[illegible]E+01	3.42[illegible]1E+00	2.76636E+00	3.67752E+00
4.9[illegible]E+01	4.11[illegible]1E+00	2.10774E+00	3.67752E+00
5.0[illegible]E+01	2.75[illegible]1E+00	1.60592E+00	3.67752E+00
5.1[illegible]E+01	2.69[illegible]1E+00	1.46166E+00	3.67752E+00
5.2[illegible]E+01	4.79[illegible]2E+00	1.11366E+00	3.67752E+00
5.3[illegible]E+01	3.12[illegible]1E+00	1.08604E+00	3.67752E+00
5.4[illegible]E+01	2.74241E+00	8.27892E-01	3.67752E+00
5.5[illegible]E+01	1.37129E+00	6.30782E-01	3.67752E+00
5.6[illegible]E+01	8.35[illegible]2E-01	4.60502E-01	3.67752E+00
5.7[illegible]E+01	0.[illegible]3E-01	3.66177E-01	3.67752E+00
5.8[illegible]E+01	2.05[illegible]1E+00	2.75995E-01	3.67752E+00
5.9[illegible]E+01	1.37[illegible]2E+00	2.12573E-01	3.67752E+00
6.0[illegible]E+01	6.85[illegible]2E-01	4.[illegible]47E-01	3.67752E+00
6.1[illegible]E+01	5.85[illegible]2E-01	3.24[illegible]1E-01	3.67752E+00
6.2[illegible]E+01	0.[illegible]3E-01	2.32232E-01	3.67752E+00
6.3[illegible]E+01	1.37128E+00	1.76941E-01	3.67752E+00
6.4[illegible]E+01	6.85[illegible]2E-01	1.34814E-01	3.67752E+00
6.5[illegible]E+01	6.85[illegible]2E-01	1.02716E-01	3.67752E+00
6.6[illegible]E+01	0.[illegible]7E-01	7.82[illegible]9E-02	3.67752E+00
6.7[illegible]E+01	0.[illegible]3E-01	5.96[illegible]1E-02	3.67752E+00
6.8[illegible]E+01	0.[illegible]3E-01	2.83518E-01	3.67752E+00
6.9[illegible]E+01	0.[illegible]3E-01	2.16[illegible]6E-01	3.67752E+00
7.0[illegible]E+01	0.[illegible]3E-01	1.64586E-01	3.67752E+00
7.1[illegible]E+01	0.[illegible]5E-01	1.25[illegible]8E-01	3.67752E+00
7.2[illegible]E+01	0.[illegible]5E-01	9.5544[illegible]E-02	3.67752E+00
7.3[illegible]E+01	0.[illegible]3E-01	7.27963E-02	3.67752E+00
7.4[illegible]E+01	0.[illegible]3E-01	5.54645E-02	3.67752E+00
7.5[illegible]E+01	0.[illegible]0E-01	4.22591E-02	3.67752E+00
7.6[illegible]E+01	0.[illegible]3E-01	3.21978E-02	3.67752E+00
7.7[illegible]E+01	0.[illegible]7E-01	2.45319E-02	3.67752E+00
7.8[illegible]E+01	6.85[illegible]2E-01	1.86912E-02	3.67752E+00
7.9[illegible]E+01	2.[illegible]7E-01	1.42411E-02	3.67752E+00
8.0[illegible]E+01	0.[illegible]5E-01	1.08585E-02	3.67752E+00
8.1[illegible]E+01	0.[illegible]3E-01	8.23713E-03	3.67752E+00
8.2[illegible]E+01	0.[illegible]2E-01	6.29[illegible]2E-03	3.67752E+00
8.3[illegible]E+01	0.[illegible]3E-01	4.79917E-03	3.67752E+00
8.4[illegible]E+01	0.[illegible]0E-01	3.65[illegible]E-03	3.67752E+00
8.5[illegible]E+01	0.[illegible]1E-01	2.78[illegible]E-03	3.67752E+00
8.6[illegible]E+01	0.[illegible]1E-01	2.12[illegible]E-03	3.67752E+00
8.7[illegible]E+01	0.[illegible]0E-01	1.61738E-03	3.67752E+00
8.8[illegible]E+01	0.[illegible]3E-01	1.23224E-03	3.67752E+00
8.9[illegible]E+01	0.[illegible]0E-01	9.39867E-04	3.67752E+00
9.0[illegible]E+01	0.[illegible]9E-01	7.15[illegible]E-04	3.67752E+00
9.1[illegible]E+01	0.[illegible]2E-01	5.45[illegible]E-04	3.67752E+00
9.2[illegible]E+01	0.[illegible]9E-01	4.15256E-04	3.67752E+00
9.3[illegible]E+01	0.[illegible]4E-01	3.15391E-04	3.67752E+00
9.4[illegible]E+01	0.[illegible]4E-01	2.41[illegible]E-04	3.67752E+00
9.5[illegible]E+01	0.[illegible]3E-01	1.83[illegible]E-04	3.67752E+00
9.6[illegible]E+01	0.[illegible]8E-01	1.3994[illegible]E-04	3.67752E+00
9.7[illegible]E+01	0.[illegible]3E-01	1.06622E-04	3.67752E+00
9.8[illegible]E+01	0.[illegible]6E-01	8.12367E-05	3.67752E+00

APPENDIX III

EQUIPMENT AND SPECIFICATIONS

Optical

1. Molectron Model UV1000 Pulsed Nitrogen Laser.

2. Molectron DL-200 Tunable Dye Laser.

3. Coherent Radiation Model 52 Argon Ion Laser.

4. Jobin-Yvon Model H-20 concave holographic grating monochromator.

   Aperture: f/3.5

   Accuracy: ± .2 nm

   Resolution: 2 nm.

5. Pellin-Broca prism; quartz

   Brewster Angle: .54 microns

6. Leitz Ortholux Microscope

   Accessories:

   a. Trinocular Head

   b. Dry darkfield condenser (transmitted light).

      DO.80 - 0.95.

   c. Ploem fluorescence vertical illuminator

   d. 150 W xenon lamp (X130)

   e.

10X N.A. = 0.25	objective 170/-
22X N.A. = 0.65	objective ks 0_{el}
25X N.A. = 0.50	objective 170/0.17
40X N.A. = 0.65	objective 170/0.17

   f. Dry/oil brightfield condenser.

7. EMI 9502S 13-stage photomultiplier tube

   Anode pulse FWHM: 15 nsec.

   Transit time: 55 nsec.

   Anode pulse rise time: 10 nsec.

Quantum efficiency: 8% @ .520 microns

Electronics

1. Ortec 454 Timing filter amplifier, rise time $\leq$ 4.5 nsec, nonlinearity $\leq \pm$ 1%.
2. EG & G/Ortec T105/N dual discriminator. Voltage instability of pulse width < 60 psec. Maximum timing deviation $\leq$ 0.8 nsec.
3. Ortec 467 time-to-pulse-height converter. Time resolution < 10 psec FWHM on 100 nsec range.
4. Keithley 417 high speed picoammeter W/4170 input head.
5. Fluke Model 413C H.V.D.C. power supply.
6. Hewlett-Packard photodiode.

REFERENCES

1. A. H. Coons, J. H. Creech and R. N. Jones, Proc. Soc. Exp. Biol. 47, 200 (1941).
2. A. H. Coons, H. J. Creech and R. N. Jones, J. Immunol. 45, 159 (1942).
3. A. H. Coons and M. H. Kaplan, J. Exp. Med. 91, 1 (1950).
4. J. L. Riggs, R. J. Seiwald, J. H. Bruckhalter, C. M. Downs and T. G. Metcalf, J. Path. 34, 1081 (1958).
5. R. C. Nairn, Fluorescent Protein Tracing (E. & S. Livingstone LTD., Edinburgh and London, 1962).
6. A. A. Thaer and M. Sernetz, Ed., Fluorescence Techniques in Cell Biology (Springer-Verlag, Berlin, 1973).
7. C. S. Chadwick, M. G. McEntegart and R. C. Nairn, Immunology 1, 315 (1958).
8. M. Sernetz, Fluorescence Techniques in Cell Biology, A. A. Thaer and M. Sernetz, Ed. (Springer-Verlag, Berlin, 1973) p. 243.
9. G. Weber, Biochem. J. 51, 155 (1952).
10. C. S. Chadwick, M. C. McEntegart and R. C. Nairn, Lancet. 1, 412 (1958).
11. A. G. E. Pearse, Histochemistry - Theoretical and Applied (Churchill, London, 1960) 2nd Ed., pp. 137, 722.
12. L. Cercek, B. Cercek and C. H. Ockey, Biophysik 10, 187 (1973).
13. L. Cercek, B. Cercek and C. I. V. Franklin, Br. J. Cancer 29, 345 (1974).
14. L. Cercek and B. Cercek, Biophysik 9, 109 (1973).
15. S. S. Kasatiya, N. G. Lambert and R. A. Laurence, App. Microbio. 27, 11, 838 (1974).

16. C. Lewis, W. R. Ware, L. J. Doemeny and T. L. Nemzek, Rev. Sci. Inst. 44, 2, 107 (1973).

17. R. Schuyler and I. Isenberg, Rev. Sci. Inst. 42, 6, 813 (1971).

18. G. I. Kaufman, J. F. Nester and D. E. Wasserman, J. Histochem. and Cytochem. 19, 8, 469 (1971).

19. Molectron Corporation, manufacturer.

20. A. Lamolla, Ed., Creation and Detection of the Excited State (Marcel Dekkar Inc., New York, 1971).

21. J. I. Steinfeld, Molecules and Radiation (Harper and Row, New York, 1974).

22. B. Rotman and B. W. Papermaster, Biochem. 55, 134 (1966).

23. L. Cercek and B. Cercek, Biophysik 9, 105 (1973).

24. M. Fox, T. Manney and C. E. Hathaway, Kansas State University, Private Communication.

25. R. Rigler and M. Ehrenberg, Quarterly Rev. of Biophysics 6, 2, 139 (1973).

26. J. Yguerabide, Fluorescence Techniques in Cell Biology, A. A. Thaer and M. Sernetz, Ed. (Springer-Verlag, Berlin, 1973) p. 311.

27. W. R. Ware, Fluorescence Techniques in Cell Biology, A. A. Thaer and M. Sernetz, Ed. (Springer-Verlag, Berlin, 1973). p. 15.

28. C. C. Davis and T. A. King, J. Phys. (A) 3, 101 (1970).

29. Eastman Kodak, manufacturer.

30. J. S. Ploem, Annals N. Y. Acad. Sci. 177, 414 (1971).

31. I. Isenberg and R. D. Dyson, Biophysical J. 9, 1337 (1969).

32. W. R. Ware, L. J. Doemeny and T. L. Nemzek, J. Phys. Chem. 77, 17, 2038 (1973).

33. P. R. Bevington, Data Reduction and Error Analysis for the Physical Sciences (McGraw-Hill, Inc., New York, 1969) p. 18.

34. P. R. Bevington, Data Reduction and Error Analysis for the Physical Sciences (McGraw-Hill, Inc., New York, 1969) pp. 104, 114.

35. G. Weber, Fluorescence Techniques in Cell Biology, A. A. Thaer and M. Sernetz, Ed. (Springer-Berlag, Berlin, 1973) p. 5.

36. C. Woods, Kansas State University, Nucl. Sci. Lab.

37. K. Jamison, Kansas State University, Nucl. Sci. Lab.

38. K. Jamison, R. Kauffman and D. Elliott, Kansas State University, Nucl. Sci. Lab.

39. N. R. Draper and H. Smith, Applied Regression Analysis (Wiley, New York, 1960).

40. G. Simonis, Ph.D. Dissertation, Kansas State University, 1973.

41. P. R. Bevington, Data Reduction and Error Analysis for the Physical Sciences (McGraw-Hill, Inc., New York, 1969) p. 188.

42. P. R. Bevington, Data Reduction and Error Analysis for the Physical Sciences (McGraw-Hill, Inc., New York, 1969) p. 154.

ACKNOWLEDGEMENTS

The author wishes to express his sincere gratitude and apprecation to his major professor, C. E. Hathaway, for providing me with the professional motivations necessary to this thesis and for his helpful endeavors in so many other ways, and to his committee members, Assistant Professor A. C. Compaan and Associate Professor T. R. Manney, for their assistance in professional and academic achievement. In addition, the author wishes to acknowledge Mr. Michael Fox for his willingness to involve many hours for sample preparation, lengthy discussions and guidance through biological consideration; to Mr. Keith Jamison, without his much needed assistance with computer programming the task of data analysis would surely have been formidable; to Mrs. Gail Buckner, my typist, for her patience throughout times of seemingly complete unorganization; and to all of my many friends and colleagues, to whom I shall always be greatful.

FLUORESCENCE LIFETIMES OF FREE AND INTRACELLULAR FLUORESCEIN AS MEASURED AT THE CELLULAR LEVEL IN SACCHAROMYCES CEREVISIAE

by

Steven Joseph Page

B.S., Southwest Missouri State College, 1972

AN ABSTRACT OF A MASTER'S THESIS

submitted in partial fulfillment of the

requirements for the degree

Master of Science

Department of Physics
Kansas State University
Manhattan, Kansas

1975

ABSTRACT

An experimental apparatus suitable for measuring decay lifetimes on the order of nanoseconds has been constructed with the primary intention of observing the different states of interaction which occur between fluorescent fluorescein molecules interior and exterior to the cell. In order to provide possible correlation with work performed by other researchers, samples of Saccharomyces cerevisiae, using two different strains, were used. Sample preparation could not be effectively carried through using methods previously used. Therefore, a detailed procedure is described which allowed the author to effectively produce satisfactory samples.

Emphasis has been placed on the instrumentation needed to measure and remove instrumental effects from these variations. In particular, instrumental reproducibility is of prime consideration and reasonable estimates of uncertainties are given, including the effect of these uncertainties on all data used in the analysis. Examination of this effect shows that the instrumental precision is such that significant preliminary results could be obtained. These preliminary results suggest that the dominant mechanism involved is concentration lifetime quenching. This phenomena gives rise to intracellular and exterior decay lifetimes which differ by amounts adequate to account for fluorescence emission polarization characteristics previously attributed to changes in the "structuredness of the cytoplasmic matrix".